THE EFFECT OF CRYSTAL FORM ON THE CATALYTIC AND MECHANICAL STABILITY OF CROSS-LINKED ENZYME CRYSTALS (CLECs)

A thesis submitted to the University of London
for the degree of Doctor of Philosophy

by

Timothy Shan Wei Lee

October 1999

Advanced Centre for Biochemical Engineering
Department of Biochemical Engineering
University College London
Torrington Place
London WC1E 7JE

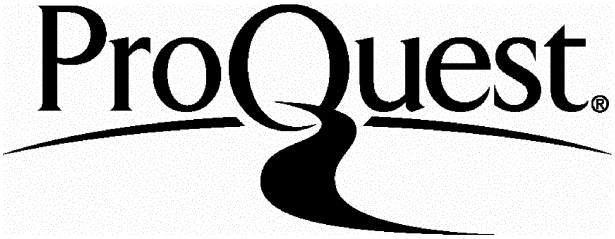

ABSTRACT

Cross-linked enzyme crystals (CLECs) are a novel form of immobilised biocatalyst which exhibit higher catalytic stability than conventional immobilised enzyme preparations. This makes them suitable for application in industrial biotransformation processes and for the synthesis of chiral pharmaceuticals. In this work, a new and generic screening technique for protein crystallisation is first described which allows the effect of three factors, e.g. protein concentration, precipitant concentration and pH, to be varied simultaneously. The results are presented as a simple two-dimensional triangular diagram where a 'window of crystallisation' describing activity recovery, crystal size etc. can be immediately visualised.

The approach is illustrated with yeast alcohol dehydrogenase I (YADH I). The formation of two crystal habits (rod and hexagonal) could be controlled as a function of pH (6.5-10) and temperature (4-25 °C). At pH 7, in 10-16 % (w/v) polyethylene glycol (PEG) 4000, only rod-shaped crystals (4.6 μm) formed while at pH 8, in 10-14 % (w/v) PEG, only hexagonal crystals (10 μm) existed. Catalyst recovery was greatest (87 %) at high crystallisation agent concentrations and low protein concentration. YADH I crystallisation was successfully scaled up from 0.5 to 500 mL (1, 000 fold) with reproducible results, in terms of crystal size, shape and recovery being obtained at both scales. Both crystal forms of YADH I were cross-linked with glutaraldehyde to form CLECs. Catalytic studies showed that hexagonal CLECs maintained a more constant specific activity at higher temperatures (50 °C) and within a broader pH range of 5-11 than rod CLECs. Hexagonal CLECs also maintained a constant activity up to 24 hours in the presence of proteases as opposed to rod CLECs which lost activity after 6 hours. Rod CLECs however were catalytically more stable than hexagonal CLECs in aqueous-organic solvents (log P values from -0.76 to 3), maintaining greater than 80 % of their initial activity.

Small-scale experiments using a rotating-disc shear device were performed as a function of speed and duration of disc rotation and over a range of CLEC concentrations

(0.26-2.5 mg.mL^{-1}) and energy dissipation rates (2.2x10^{3}-6.8x10^{5} W.kg^{-1}). Owing to their small size, no breakage occurred for rod CLECs. Breakage of the larger hexagonal-shaped CLECs did occur at energy dissipation rates, ε_{max}, above 1.0x10^{5} W.kg^{-1} where the length scale of turbulence was less than 2.0 μm. Based on visual observation of the sheared CLEC suspensions and models of crystal breakage, it was concluded that breakage of the hexagonal CLECs occurred due to shear-induced attrition. Small-scale filtration studies showed that rod-shaped CLECs had a greater flux and hence lower cake resistance (3-9x10^{12} m.kg^{-1}) than the flat hexagonal CLECs
(1-2x10^{14} m.kg^{-1}). The specific cake resistances of rod and hexagonal CLECs remained constant during several filtration cycles at 50-100 kPa. Size measurements indicated that no breakage of crystal forms occurred as a result of pressure.

The rotating-disc shear device was shown to be a useful scale-down tool to predict the breakage of CLECs by comparing the maximum shear rate, G_{max}, of 3.4x10^{5} s^{-1} to that found in a standard Rushton turbine reactor. It was predicted that no breakage of CLECs would occur at impeller speeds (200 rpm) sufficient to disperse the crystals. Breakage of CLECs occurred at G_{max} values above 1.5x10^{4} s^{-1} corresponding to rotational speed above 1, 000 rpm. Breakage of CLECs reduced the recovery of the catalyst due to possible membrane clogging by fines generated by shear-induced attrition.

ACKNOWLEDGMENTS

I wish to thank Professor Mike Turner and Dr. Gary Lye for their support, direction and encouragement throughout my PhD. They have been extremely kind and helpful to me.

I would also like to thank Dr. Parvis Shamlou, Jeetendra Vaghjiani, Dr. Carsten Jacobsen, the Biotranformation and Shear groups for their useful criticisms and suggestions in this project.

I want to thank especially my mother, father and Claire for their love and confidence in me to complete my PhD. Thank you always for your support and encouragement.

Finally, I want to thank my Lord Jesus for His love and abundant blessings.

The King sent for his wise men all
To find a rhyme for W;
When they had thought a good long time,
But could not think of a single rhyme,
'I'm sorry', said he, 'to trouble you'.

James Reeves

(In appreciation of Prof. Mike Turner's fine sense of humour)

CONTENTS PAGE NO.

LIST OF FIGURES

LIST OF TABLES

LIST OF GELS

NOMENCLATURE

A	total cross-sectional area of the filter cake (m^2)
ADH	alcohol dehydrogenase
c	solids concentration ($kg.m^{-3}$)
D_i	impeller diameter
D_T	tank diameter
d_{50}	dimensionless ratio comparing the median diameter after shearing with the median diameter of the unsheared sample
d_i	impeller diameter (m)
E	turbulent energy component (J)
e	energy required to generate an attrition particle (J)
f	intensity, frequency (s^{-1})
G_{max}	maximum shear rate (s^{-1})
ΔG_g	activation free energy (J)
H_T	Tank height
J_n	nucleation rate (s^{-1})
K_2	constant in crystal-crystal attrition rate equation
k_b	Boltzmann constant
k_{cat}	turnover number of the enzyme
k_m	substrate concentration at which the reaction rate is half of its maximal value
k_v	volumetric shape factor
l	cake thickness (m)
L_o	mean crystal size (m)
M_i	molal (g salt/1000 g water) or molar (mole salt/litre water) salt concentration
m	material properties
n	number of particles (m^{-3})
N	rotational speed (revs s^{-1})
NAD	nicotinamide adenine dinucleotide
P	power (W)
PEG	polyethylene glycol

PF	purification factor
P_o	Power number [$= \rho N^3 d_i^5/P$]
ΔP	applied pressure difference (kPa)
Q_0	volumetric flow number
R	disk diameter (m)
Re_{disk}	disk Reynolds number [$= \omega R^2/\nu$]
Re_i	impeller Reynolds number [$=\rho N d_i^2/\mu$]
R_m	membrane resistance (m^{-1})
S	Specific particle surface (m^2)
T	torque (N)
TK	transketolase
TTN	total turnover number
t	time (s)
t_c	temperature (°C)
v_∞	tip velocity ($m.s^{-1}$)
V	volume (m^3)
V_m	packing density
x	distance from the rotating-disc edge (m)
Y	Young's modulus
YADH I	yeast alcohol dehydrogenase I
Z_i	valency of ions present in the solution

Greek symbols

α	cake resistance ($m.kg^{-1}$)
β	solubility product
e	voidage
γ	shear rate (s^{-1})
ε	energy dissipation rate ($W.kg^{-1}$)
μ	dynamic viscosity (Pa.s)
μ_c	superficial velocity of the filtrate (s^{-1})
η_T	target efficiency

ν	kinematic viscosity ($m^2.s^{-1}$)
ρ	density ($kg.m^{-3}$)
$\Delta\rho$	density difference [$= \rho_c - \rho_f$] ($kg.m^{-3}$)
σ	Poisson's ratio
τ	stress ($N.m^{-2}$)
v	volume of cake deposited by unit volume of filtrate
ω	angular velocity ($rad.s^{-1}$)
λ	length scale of turbulence (m)

Subscripts/superscripts

c	crystal (parent)
cc	crystal-crystal
ci	crystal-impeller
d	drag
e	fine, eddy
f	fluid
i	impeller
imp	impact
s	shear
ss	steady-state
st	stirring, stirrer
tot	total
turb	turbulent

1 INTRODUCTION

The industrial enzyme business is receiving increased attention as their potential uses for novel chemistry is more widely recognized. This has come about as a result of recombinant DNA technology, which has led to improvements in enzyme production in a variety of host organisms, giving the biochemical engineer a greater choice of catalyst options. The ability to express enzymes in a variety of forms (isolated enzymes, cells, immobilised enzymes and cells) has allowed for the development of commercial biotransformation processes which were previously economically non-viable.

The industrial usefulness of biotransformations has been increased via awareness of the role biocatalysis can play in the synthesis of enantiomerically pure products (Hodgson, 1992) and in the development of more environmentally-compatible processes. Worldwide sales of industrial enzymes total about $ 1.6 billion which will double in sales by the year 2008 according to Stroh (1998). Major customer groups can be broken down into the following groups: food (45%), detergents (34 %), textiles (11 %), leather (2.8 %), pulp and paper (1.2 %) and others (5.6 %) which excludes diagnostic and therapeutic enzymes.

An equally important achievement in the development of enzymology was the demonstration that enzymes could be immobilised onto macroscopic particles with the retention of activity. This method of enzyme immobilisation has allowed for its recovery and reuse by scaleable methods such as filtration (Navia *et al.*, 1993). Some general approaches to enzyme immobilisation might include encapsulation, absorption on solid supports, covalent attachments to supports, entrapment in polymeric gels and the precipitation of soluble proteins by cross-linking them with bi-functional reagents in a random manner. Current immobilisation procedures can have significant disadvantages both in mild aqueous and harsh environments where serious loss of activity can occur over time periods of operational commercial interest (Roda *et al.*, 1988). Enzyme crystals can be employed as a novel form of immobilised enzyme through a process of crystallisation and cross-linking to form Cross-Linked Enzyme Crystals (CLECs). Owing to their catalytic stability, CLEC catalysts may prove an alternative source of enzyme immobilisation, useful in their application to

industrial biocatalytic processes. For such applications, protein crystals need not be large or perfect, thereby relaxing those time requirements required for crystal growth. Nonetheless, to produce enzyme crystals commercially viable as CLECs, three serious issues have to be addressed and resolved. These are:

1) The technique of growing crystals reliably and economically
2) The catalytic rates essentially free from diffusional limitations and stable under process conditions.
3) The fragility of these crystalline particles and their application to process equipment.

1.1 Process aims

Chapter 2 reviews the different approaches to enzyme immobilisation and advantages of using CLECs as a novel form of an immobilised biocatalyst. It explores the different crystallisation techniques that have been used in the past to crystallise proteins. Chapter 3 deals with the different crystallisation parameters such as pH, salt, organic and protein concentrations which are important in driving the system to a state close to the phase boundary that initiates crystallisation. An efficient approach in Chapter 5 has been devised where three parameters are varied simultaneously in a triangular format so that a window of crystallisation can be visualized. This technique optimises crystallisation conditions with respect to yield, crystal size and habit for subsequent production of CLECs as large-scale biocatalysts. Chapter 5 addresses question 1 above where this technique has been used successfully to produce different forms of crystals on a large-scale.

Chapter 6 introduces a series of catalytic and mechanical experiments that are useful to test the CLECs stability under certain process conditions. Chapter 7 investigates the catalytic stability of the two different crystal forms and whether the morphology has an important role in the stability of CLECs in different pHs, temperatures, proteases and in organic and aqueous-organic mixtures. Chapter 7 addresses question 2 above where catalytic rates and stability studies were carried out for two different forms to see if the morphology was important in the catalytic activity of the CLECs.

Chapters 8, 9 and 10 deal with question 3 above concerning the mechanical stability of the CLEC forms under conditions of shear-induced attrition, filtration and

their performance in a standard Rushton turbine stirred-tank reactor. Small-scale experimental tools such as the rotating shear device and the pressurised filtration unit were used in Chapters 8 and 9 to study the mechanical stability and the recovery of CLECs. After formulating the small-scale experiments to study shear and recovery of CLECs, these experiments were then used to test the performance of the CLECs in a standard Rushton stirred-tank reactor. Chapter 12 identifies some of the initial work and difficulties associated with the crystallisation of *Escherichia coli* (*E. coli*) transketolase. Chapter 11 concludes the work done in the PhD and future work that could arise from the current work done in this thesis.

2 LITERATURE SURVEY

2.1 The importance of enzyme immobilisation

In the 1960s, immobilisation was developed to allow the re-use of expensive biological catalysts such as enzymes. Large-scale processes for the isolation and purification of intracellular enzymes were available at that time but the cost of these isolated water-soluble enzymes could not compete economically with large-scale chemical processes. In speciality areas such as in the production of pharmaceuticals and expensive chemicals, the desirable enzymes were generally too expensive or, more important, too scarce to be of commercial importance (Turner, 1998).

The interest in biotransformations arises from the properties of biological catalysts such as their selectivity and specificity. Biological catalysts may be used to perform reactions that may be difficult to be accomplished by chemical methods (Turner, 1998). An early example was the introduction of a hydroxyl group at position 11 on the steroid nucleus to produce a range of anti-inflammatory corticosteroids. In recent years, there has been a growing demand for food and pharmaceutical products to be a single enantiomer rather than a racemic mixture. Such optically pure drugs are more selective in their mode of action and show less side effects (Turner, 1998).

The objective of immobilisation was to convert the enzyme into a water-insoluble form which could be recovered from or retained in a reactor. Immobilisation facilitates the recovery of enzyme or separation of the product from the catalyst. The choice between the use of soluble free enzyme and immobilized enzyme also depends on the nature of the conversion process and the relative operational stabilities of the two forms. If the enzyme can be stabilized by modification or immobilization, then reuse of the enzyme may be worthwhile (Lilly and Dunnill, 1976).

2.2 Conventional techniques of enzyme immobilisation

The first category is the immobilisation of enzymes using the method of entrapment. This involves creating a porous barrier, such as in the form of a gel or membrane, through which substrate and product molecules can pass freely but is impermeable to the biocatalyst. The entrapment technique is a preferred approach for

delicate biocatalysts such as cells. Where multistep processing with cofactor requiring enzymes is involved, it is preferable to use whole cells which have an inbuilt system of cofactor recycling (Rosevear, 1993).

The second category is the binding of the biocatalysts directly to a solid support through, for an example, an ionic or covalent interaction. In addition, the method of cross-linking enzymes with a bi-functional reagent in a random manner after precipitation may be used to immobilise enzymes. The binding of biocatalyst directly to a solid support exploits the chemical characteristics of the enzyme. Most ion exchanges have been successful as immobilised enzyme supports (Bar *et al.*, 1986).

2.2.1 Entrapment in polymeric gels

The method involves using a matrix such as acrylamide/bis-acrylamide to entrap cells or enzymes (Rosevear, 1993). It involves the gelation of an aqueous suspension of enzyme so that the biocatalyst is distributed throughout the solid mass. The most successfully done technique was the production of calcium alginate beads. A suspension of cells in sodium alginate is added dropwise to calcium chloride solution. Gelation at the surface of the droplets is instantaneous and spherical beads can be obtained. The gel can be stabilized by the polymerization of small amount of acrylamide within the sodium alginate solution (Rosevear, 1993).

2.2.2 Encapsulation in membranes

The technique traps the enzymes through an impermeable membrane but permits diffusion of reactants and products. Encapsulation may be with dialysis membranes, hollow fibers, liposomes and microcapsules (Rosevear, 1993). In the last example, microcapsules contain a mixture of water, organic solvents and detergent. They are structured into aqueous and oil microdomains separated by a surfactant-rich film. Enzymes can be dissolved in the aqueous domain with high retention of catalytic activity. The large interfacial area minimizes mass transfer limitations (Rosevear, 1993).

2.2.3 Absorption on solid supports

The binding of amino acid acylase to ion exchange resins is the first example of the industrial use of immobilised enzymes. This simple approach involves adding the enzyme solution to the support, stirring and washing away the unattached enzyme. Inorganic materials, like titanium (IV) hydrated oxides, form stable conjugates with enzymes and cells. Cells absorb more strongly than enzymes due to the production of extracellular polysaccharides that may help them bind more efficiently to the surface (Rosevear, 1993).

2.2.4 Covalent attachment to supports

Desorption of enzymes from a support can be prevented by the formation of a stable covalent link between the biocatalyst and a support. Many different supports can be used, such as cellulose, cross-linked dextran and agarose, to provide a suitable hydrophilic environment for the enzyme. The most widely used bi-functional reagent is glutaraldehyde, which forms a stable Schiff's base with amine groups on the protein. To reduce the potential for inactivation of the active site by chemical reagents, the binding of substrate or ligand to the active site during immobilisation is employed (Hon, 1979).

2.2.5 Cross-linking of enzymes with bi-functional reagents

This approach may be useful in the formation of agglomerations of enzymes (or enzymes and other proteins) that precipitate from solution or in the incorporation of the enzymes chemically into a polymer. These cross-linked bridges may be covalent i.e. disulfide bonds or non-covalent such as salt bridges involving bivalent metal ions. The most commonly used reagents are glutaraldehyde and di-imido esters. This technique produces very stable systems but the attachment can destroy catalytic activity through chemical modification of the active site. Also the reactants may have problems reaching the catalyst (Rosevear, 1993).

2.2.6 Disadvantages of Immobilisation

The different approaches to enzyme immobilisation such as adsorption on solid supports, covalent attachments to supports, entrapment in polymeric gels, encapsulation and the precipitation of soluble proteins by cross-linking them randomly with bi-functional reagents have significant disadvantages. In harsh conditions, one can experience loss of activity over time. Immobilised enzymes are prone to digestion and diffusional limitation of reaction rates (Navia *et al.*, 1993).

Diffusional or mass-transfer effects arise from diffusional resistances to the translocation of substrate, product or effector to or from the site of the enzymatic reactions (Bedell *et al.*, 1998). An immobilised enzyme functioning under conditions of diffusional restrictions would be exposed to local concentrations of substrate, product or effector different from those in the bulk solution.

2.3 Cross-Linked Enzyme Crystals (CLECs)

Protein crystals can be employed as an immobilised form quite distinct from the rest. Crystal growth is the result of a controlled precipitation of a concentrated protein solution driven thermodynamically by the interaction of factors such as temperature, pH, type and concentration of precipitant and the presence of counter-ions. Chemical cross-linking of enzyme crystals serves to stabilize the crystalline lattice and its constituent enzyme components, forming Cross-Linked Enzyme Crystals (CLECs) (Byrne and Stites, 1995).

A commonly used approach for the production of CLECs involves batch crystallisation of enzymes and chemical cross-linking of crystals. Batch crystallisation, used in the production of the CLEC form of thermolysin (rods) (Persichetti *et al.*, 1995) and subtilisin (needles) (Wang *et al.*, 1996), yielded uniform microparticles of less than 100 μm in length and minimum thickness of less than 5μm (Margolin, 1996). The CLECs gave high activity due to the lack of mass-transfer limitations (Borman, 1992). The size of the particle can be altered by changing the crystallisation conditions, such as precipitant concentration, while retaining uniformity (Lalonde, 1995).

While many bi-functional agents have been used for cross-linking, glutaraldehyde has been the most popular. The mechanism of action of glutaraldehyde is uncertain but the cross-linking is known to be irreversible and the

protein components participating in the reaction are the primary amino groups of lysine residues and the N-terminus of the protein (Margolin, 1996).

The CLECs are microporous materials that do not require inert carriers or support structures to achieve separation by filtration, centrifugation or other protocols applied to conventional immobilised enzymes (Lalonde, 1997). CLEC particles can be lyophilized and stored at room temperature, retaining their catalytic activity and mechanical integrity (Lalonde, 1997) under harsh conditions of temperature, pH extremes, exogenous proteases and exposure to organic, aqueous and aqueous-organic solvent mixtures (Zelinski and Waldmann, 1997; Sobolov *et al.*, 1994).

The stability of CLECs may be the result of increased polar and hydrophobic interactions among the protein molecules in the crystal lattice preventing unfolding due to heat and denaturants (St. Clair and Navia, 1992). In addition, stability of CLEC catalysts against proteolysis may be explained by restricted protein-protein interaction in the lattice and exclusion of protease from solvent crystalline channels. 30-65% of protein crystal weight is attributed to solvent. The uniform solvent-filled channels, 20-55 Å in diameter, traversing the crystal body facilitates the transport of substrates and products into and out of the crystals (Navia *et al.*, 1993).

The major applications of crystalline catalysts have been in organic synthesis (Khalaf *et al.*, 1996) such as in the production of high fructose corn syrup, the formation of carbon-carbon bonds and the resolution of chiral compounds (Wang *et al.*, 1996). Dry CLECs-CRL (*Candida rugosa* lipase) in organic solvents have shown high entioselectivity in esterification and transesterification (Lalonde *et al.*, 1995). The application of CLECs in the manufacture of homochiral products could prove to be useful in the production and marketing of pharmaceuticals (Persichetti *et al.*, 1996). The high productivity of low molecular weight synthetic catalysts i.e. 1 mg of LPS-CLEC can resolve 4.6 g of sec-phenethylalcohol using vinyl acetate in toluene giving a volumetric productivity of 30 g/L (Margolin, 1996) and its high mechanical stability under high-shear conditions make CLECs very useful over other forms of immoblised catalysts.

2.4 Crystallisation techniques

Protein crystals form in supersaturated solutions which are thermodynamically metastable. Equilibrium can be restored by reducing the protein

concentration through precipitation or formation of nuclei and subsequent crystal growth. During nucleation, molecules associate in three dimensions to form a thermodynamically stable aggregate. These nuclei provide surfaces suitable for crystal growth. Proteins are induced to crystallise by adding agents that would perturb the interactions between the protein and bulk solvent water to promote associations that lead to crystallisation (Weber, 1991).

Enzyme crystals are grown by the controlled precipitation of protein out of an aqueous solution. In general, crystals are produced by combining the protein to be crystallised with an appropriate aqueous solvent or aqueous solvent containing appropriate precipitating agents, such as salts or organics. The solvent is combined with the protein at a temperature determined experimentally to be appropriate for crystallisation and maintenance of protein stability and activity. The solvent can optionally include co-solutes, such as divalent cations, cofactors or chaotropes, as well as buffer species to control pH. The objective of this section is to review the protein crystallisation methods that achieve and maintain the supersaturation state.

2.4.1 Batch crystallisation

This is a classical technique for early enzyme crystallisation. The protein is dissolved at low ionic strength to give a solution of high concentration. The precipitating agent (salt (NaCl) or organic solvent) is added to bring the solution to a state of supersaturation. The vessel is sealed and set aside until crystals appear. Frequently, the supersaturation point required to introduce nucleation is determined by adding the precipitant progressively until a turbidity in the solution has occurred. This technique is useful for the production of large crystals of lysozyme, ribonuclease and enzymes of the trypsin family (King, 1964).

2.4.2 Equilibrium dialysis

In this method, the protein solution is retained by a semipermeable dialysis membrane which maintains the solution at a constant concentration while allowing equilibrium with a surrounding solution. The formation of crystals can be achieved within the dialysis bag by using salts (ammonium sulfate) or small organic molecules (DMS) in the surrounding solution to reduce the protein's solubility.

Further crystal growth may be achieved by increasing the salt concentration or moving the pH nearer to the isoelectric point (pI) to reduce the protein's solubility. This method is suitable for pH variation, the use of organic solvents and for studying the effect of ions on crystallisation (Ries-Kautt and Ducruix, 1992).

2.4.3 Temperature Shift

Jakoby, (1968) developed a technique for microcrystallisation of proteins. The method depends on the decrease in solubility of proteins in ammonium sulphate solution with increase in temperature. The protein is precipitated with salt and is then extracted with ammonium sulphate solutions of decreasing concentrations at 0 °C. Thus, contaminating proteins soluble at high concentrations of ammonium sulphate are extracted first and removed. Extracts obtained in this manner are warmed to room temperature (25 °C) to allow crystallisation to occur.

2.4.4 Vapour Diffusion

This method uses the vapour phase to bring about equilibration and is very well suited to screening a large number of conditions when only a small quantity of material is available. With this approach, a microdroplet (as small as 5 μL) of protein solution plus precipitant at subsaturating concentrations of protein, is suspended from the underside of a microscope cover slip and placed over a larger reservoir (approximately 1 mL) of precipitating solution to equilibrate. After sealing in a closed vessel, the solutions equilibrate to achieve supersaturing concentrations of protein and thereby induce crystallisation in the drop. The wells are supplied by disposable plastic tissue culture plates (Linbro model FB-16-24-TC) that have 24 wells (1 cm diameter x 2 cm deep) (Ducruix and Giege, 1992).

2.4.5 Free Interface Diffusion

This method involves achieving transient highly supersaturating conditions required for nucleation, followed by a relaxation to conditions of lower supersaturation required for crystal growth. A protein solution is layered over a precipitant solution. Initially, molecules at the liquid-liquid interface achieve high supersaturation, promoting nuclei formation. As the liquids diffuse, the high protein

supersaturation at the interface decreases. The lowering in supersaturation favours crystal growth. At equilibrium, when the precipitant and protein solutions are mixed completely, the entire protein solution is supersaturated. Ideally, crystal growth would initially occur at the interface and proceed progressively throughout the entire protein solution (Weber, 1991).

2.4.6 Seeding

Seeding provides a template for the assembly of molecules to form a crystal with the same characteristics as the crystal from which the seed has originated. It is used in situations when, after the first crystallisation event, subsequent batches of protein fail to yield any crystals under identical crystallisation conditions (Stura and Wilson, 1992).

Seeding can be either homogeneous or heterogeneous. The two most common methods of homogeneous seeding are microseeding and macroseeding (Stura and Wilson, 1992). Microseeding involves the transfer of microscopic crystals from a seed source to a non-nucleated protein solution. Seed stock is prepared by washing three or four small crystals in a 'mother liquor' solution (Stura and Wilson, 1992) to remove defects or precipitates from crystal surfaces. This solution prevents the crystals from redissolving. The resulting seeds are crushed by a glass tissue homogenizer, washed and stored in a test tube.

Macroseeding, on the other hand, is a process in which pre-grown crystals are washed and introduced individually into a pre-equilibrated protein solution to enlarge small crystals enabling them to be used for X-ray diffraction studies (Stura and Wilson, 1992).

Heterogeneous seeding can be divided into cross-seeding and epitaxial nucleation. Cross-seeding is a form of seeding in which seeds come from a different protein or protein complex than that being crystallised. Crystals of related macromolecules can be used to induce nucleation of proteins. The resulting crystals may maintain some of the lattice dimensions of the initial seeds (Stura and Wilson, 1992). Epitaxial nucleation is a process where a regular surface rather than a 3-dimensional lattice induces crystal growth. A common observed case is seen in the nucleation of protein crystals on cellulose fibre impurities which are accidentally present in protein-precipitant drop. These surfaces provide platforms suitable for

macromolecular nucleation and may possibly support 3-dimensional crystal growth (Stura and Wilson, 1992).

2.5 ENZYME CHARACTERISTICS

2.5.1 Alcohol Dehydrogenase

Alcohol dehydrogenase (ADH) catalyses the reversible oxidation of alcohols to aldehydes or ketones. The family of ADHs are prevalent in prokaryotes and eukaryotes. The ADHs are active as tetramers, as in the case of yeast ADHs, or dimers, as observed in plants and vertebrates (DeBolle *et al.*, 1995). Yeast ADH I (YADH I) oxidizes aliphatic primary alcohols, secondary alcohols of the L series [(S)-configuration] and D(S)-lactic acid. The most important use of YADH I is for the preparation of chiral alcohols (Branden *et al.*, 1995). The fastest rate of oxidation is oberved with ethanol but decreases for secondary alcohol, hydroxy acids and polyalcohols as the chain length increases.

YADH I is a tetrameric enzyme of 150 kDa possessing 4 or 5 tightly bound zinc atoms per enzyme molecule (Magonet *et al.*, 1992). Electron microscopy and low-angle X-ray scattering experiments have revealed that 4 subunits of diameter 4.3 nm are arranged tetrahedrally to form a hexagonal array (Kunkel *et al.*, 1980). There is a similarity in the catalytic mechanism in the active pocket of both horse liver and YADH I. The two domains of the horse liver ADH subunit are separated by a cleft containing a wide and deep pocket (Eklund *et al.*, 1976) The zinc atom is coordinated to three protein ligands in the catalytic domain: two sulphur atoms from Cys 46 and Cys 174 and one nitrogen atom from His 67. A water molecule or hydroxyl ion, depending on the pH completes the tetrahedral structure within the pocket (Figure 1).

This water molecule is involved in hydrogen bonding with residues Ser 48 and His 51. These hydrogen bonds may be important for proton release upon NAD^+ binding and substrate polarization in the catalytic mechanism (Eklund *et al.*, 1976). Residues 95 to 113 forms a lobe that binds the second zinc atom of the subunit and this zinc is chelated in a tetrahedral arrangement by four sulphur atoms from Cysteine

residues 97, 100, 103 and 111 (Figure 1). There are only two polar residues Ser 48 (Thr 48 in YADH I) and Thr 178 within the pocket. All other residues are non-polar, creating a hydrophobic environment for the NAD co-enzyme and the substrate. Substitutions involving tryptophan residues (positions 57 and 93) and threonine (position 48), together with the insertion of two proline residues narrow the substrate specificity in YADH I in comparison to horse liver ADH (Eklund *et al.*, 1976).

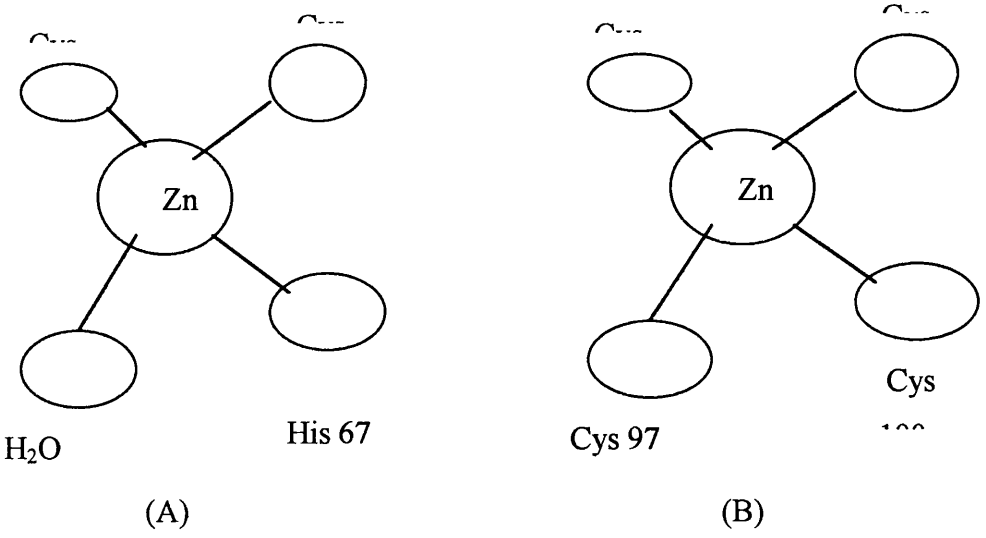

Figure 1: Schematic diagram showing the zinc ligands in horse liver ADH (Eklund *et al.*, 1976).

(A) Ligands to the catalytic zinc atom

(B) Ligands to the second zinc atom

2.5.2 Transketolase

Transketolase, a key enzyme in the pentose phosphate pathway, catalyzes the in vivo ketol transfer of the two carbon ketol donor group from D-xylulose-5-phosphate (D-xylulose-5-P) to two different aldose molecules : D-ribose-5-P, to produce D-sedoheptulose-7-P and D-erythrose-4-P, to generate D-fructose-6-P (Figure 2) (Lindqvist *et al.*, 1992). The products of these two reactions, fructose-6-P and glyceraldehyde 3-P, are subsequently the substrates of the glycolytic enzymes, phosphofructokinase and glyceraldehyde 3-phosphate dehydrogenase.

Thus, transketolase, together with transaldolase, creates a reversible link between a cell's two key metabolic pathways, the pentose pathway and glycolysis, allowing the adaptation of the cell to a variety of needs. Transketolase allows the cell to produce NADPH (reducing power) for biosynthesis and ribose-5-P for synthesis of DNA, glycolytic intermediates and the supply of ribulose-1,5-bisphosphate for photosynthetic production of carbohydrates during carbon dioxide fixation.

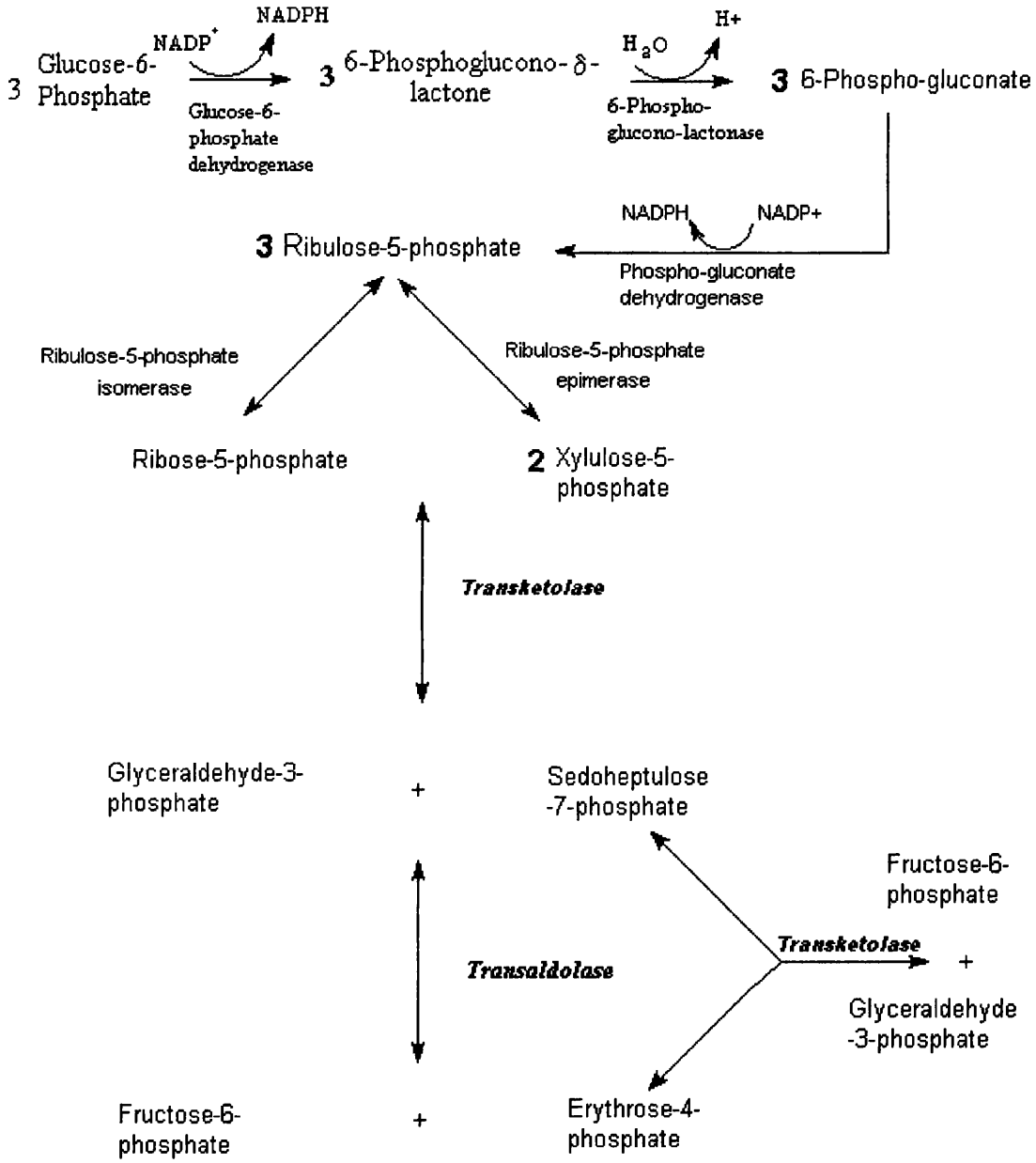

Figure 2 : The role of transketolase in pentose phosphate pathway.

Table 1: Physical and kinetic properties of the various sources of transketolase (Spender *et al.*, 1995; Harris, 1995).

Transketolase (TK) Source	Molecular Weight (kDa)	Subunits	Specific Activity (Units.mg^{-1} protein)
***E.Coli* K12**	145	Dimer 73 kD/subunit	50.4
Saccharomyces cerevisiae	150	Dimer 75 kD/subunit	20
Rat Liver	130	Dimer 65 kD/subunit	3
Spinach chloroplast	100	Monomer	40

Substrate affinities (k_m)(mM) for the different sugars

TK source	xylulose 5-P	Ribose 5-P	Erythrose 4-P	Li hydroxy pyruvate	Fructose 6-P
***E.Coli* K12**	0.16	1.4	0.09	18	1.1
Yeast	0.21	0.4	------	33	1.8
Rat Liver	0.022	0.066	0.044	----	----
Spinach chloroplast	-------	0.4	-------	----	3.2

The transketolase of baker's yeast, *Saccharomyces cerevisiae*, has two identical subunits, each with a molecular weight of 75 kDa (Lindqvist *et al.*, 1992). The enzyme contains the cofactor thiamine diphosphate (ThDP) and also Mg^{2+} ions for catalytic activity. Other metal ions like Ca^{2+}, Mn^{2+} and Co^{2+} can replace the Mg^{2+} ion. Transketolase has been isolated and purified from various sources such as yeast, spinach and *Escherichia coli* (*E. coli*). Their physical and kinetic properties have been elucidated (Table 1). For the enzyme from *E.coli* K12, the pH optimum is 8.5

and Michaelis constants (k_m) for the phosphorylated carbohydrate substrates are in the region of 90 μM to 18 mM with D-erythrose 4-P being the best acceptor.

In 1992, Lindqvist and co-workers (Figure 3) elucidated the 3-dimensional structure of the enzyme from yeast. The enzyme subunit is composed of three consecutive ∝/β domains. The cofactor, ThDP, binds in the deep cleft at the interface formed by the two subunits and residues from both domains contribute to cofactor binding. The diphosphate moiety of ThDP interacts with side chains of conserved residues Asp157 and Asn187 in the N-terminal domain of the enzyme through co-ordination with a bound Ca^{2+} ion. Further interactions to the enzyme are mediated through hydrogen bonding to histidine residues, His69 and His263.

The thiazolium ring forms mainly hydrophobic interactions with conserved residues Leu118 and Ile 191 which pack against the ring. The pyrimidine ring is bound in a hydrophobic pocket built by conserved residues of Phe442, Phe445 and Tyr448 from the carboxyl end of the β-sheet in the middle domain of the second subunit. Hence, there are many hydrogen and hydrophobic interactions responsible for the proper orientation of cofactor at the active site.

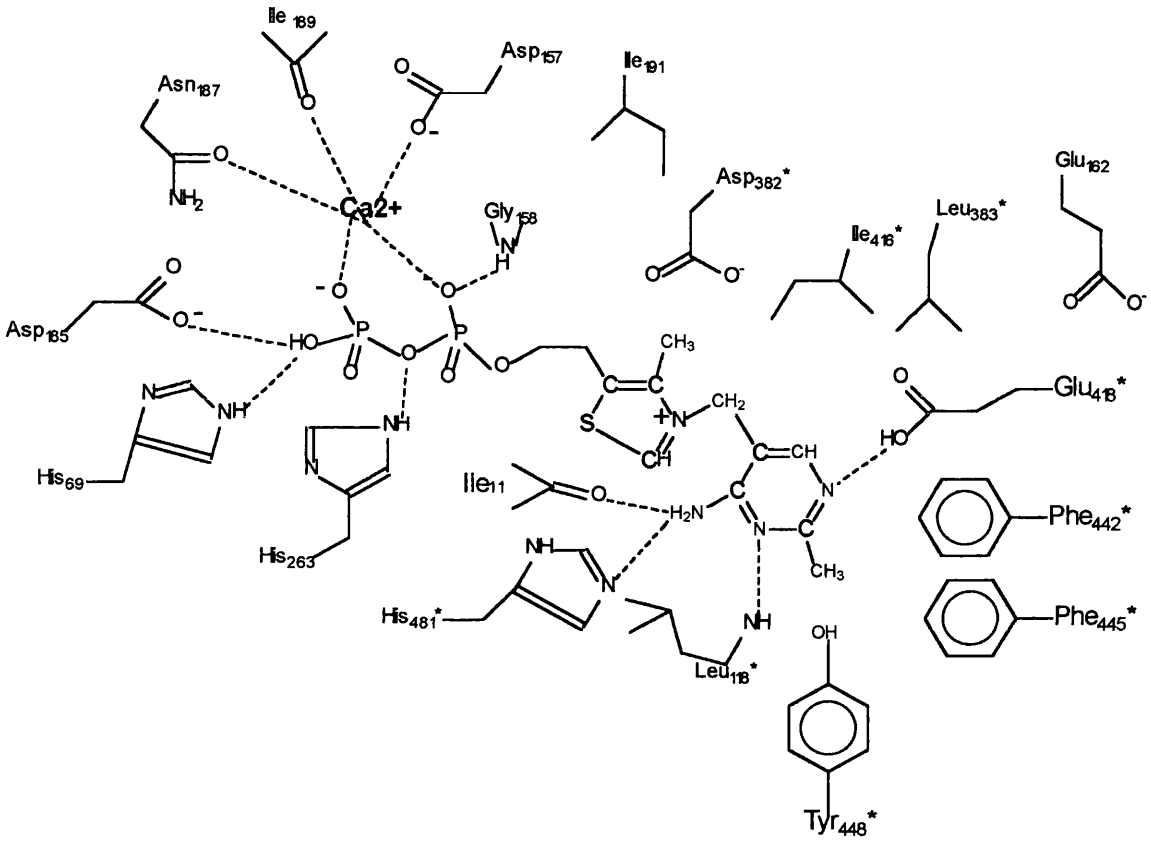

Figure 3: A diagram of the interactions of Thiamine Diphosphate at the cofactor binding site of transketolase. Residues coming from the second subunit are indicated by an asterisk after the residue number. Dashed lines indicate the possible hydrogen bonding occurring at the binding site (Zelinski and Waldmann, 1997).

2.6 Summary of the literature survey

The section introduces Cross-Linked Enzyme Crystals (CLECs) as a novel form of immobilised biocatalyst designed for application in industrial biotransformation processes. CLECs, with their increased stability, are more robust than other conventional forms of immobilised enzyme. Even though there are many crystallisation techniques available, there is no report of a convenient and reliable method for the batch production of CLECs. In this work, a 'windows' approach in the form of a triangular diagram has been used to vary three different crystallisation parameters to identify regions of crystallisation for the different forms of YADH I crystals (hexagonal and rods) and for their regions of optimum recovery (Section 5). YADH I is the choice of enzyme for study as it is readily available as an acetone extract and can be used without further purification. *E.coli* transketolase is also an additional enzyme for study.

Crystallisation parameters controlling crystal habit may allow for the selection of the crystal form most chemically stable for the process. A hierarchy of tests has been devised to systematically characterise the catalytic and mechanical properties of the different forms of the CLECs in comparison to free enzyme. Studying the stability of the different crystal forms under different experimental conditions such as in extreme pHs, temperatures, in organic solvents and exposure to proteases in Section 7 will allow for the evaluation of the crystal form most suitable for the process. Sections 8 and 9 explore in detail the effect of crystal form on the mechanical stability of CLECs and the recovery of CLECs in a pressurised system.

3 THEORETICAL CONSIDERATIONS:

3.1 Parameters influencing protein crystallisation

This section views the various effects on protein crystallisation and how to manipulate the crystallisation in general. The strategy employed to bring about crystallisation is to guide the system slowly to a state of reduced solubility by modifying the solvent's properties. This can be accomplished by increasing the concentration of precipitating agents or by altering physical properties, such as pH. For a specific protein, the precipitation points or solubility minima are dependent on the pH, temperature, the chemical composition of the precipitant, and the properties of both the protein and the solvent (McPherson, 1990).

3.1.1 pH

The optimal pH for crystallisation is given by the pI of the protein (McPherson, 1990). This is because at their pI, molecules have a minimum net charge and hence crystallisation units can more easily get in contact with each other. The influence of pH on crystallisation is as follows. The protein and salt ions present in solution compete for the water that keeps them solvated. When protein molecules are deprived of sufficient water by ionic competition, they are compelled to associate with other protein molecules. When the process proceeds in an orderly fashion to give 3-dimensional aggregates, then the nuclei of crystals will form and grow (McPherson, 1990).The advantage of pH as a control variable is the ease of its measurement and the short time it takes to adjust it.

3.1.2 Temperature

Crystals of α-amylase have been grown by raising the temperature of the solution above the solubility limit and then cooling it slowly until crystals appear (McPherson, 1990). An increased temperature will result in greater Brownian motion and therefore more protein-protein contacts increasing the rate of protein incorporation in the crystal. Temperature has also reported in determining the resulting crystal shape. Below 25°C, orthorhombic crystals grow while above 25°C, tetragonal crystals develop from a lysozyme solution (Feigelson, 1988). The

disadvantage of temperature as a control variable is that it is a slow process due to the limited transferring of energy to and from the solution.

3.1.3 Ionic strength

3.1.3.1 Salting-in

At low ionic strength, a phenomenon known as " salting-in" occurs in which the solubility of the protein decreases at very low ionic strength when the ions essential for satisfying the electrostatic requirements of the protein molecules decreases. As these ions are removed, the protein molecules seek to balance their electrostatic requirements through interactions amongst themselves. Thus, they aggregate and separate from the solution. The salting-in effect, can be used as a crystallisation tool through dialysis. One can dialyse a protein soluble at moderate ionic strength against distilled water. Many proteins like catalase, concanavalin B and immunoglobulins have been crystallised by this means (McPherson, 1990).

3.1.3.2 Salting-out

Salting out is a phenomenon in which salt ions and macromolecules compete for the solvent molecules, that is, water. Both ions and proteins require hydration layers to maintain solubility (McPherson, 1990). The increasing salt concentration favours interaction between hydrophobic and other residues which exclude water. Hence, they tend to associate with themselves and aggregate. Thus dehydration or the perturbation of solvent layers around the protein molecules, induces insolubility. The ionic strength, μ, takes into account the valency, Zi, of all ions present as well as the salt concentration (M_i) in the solution as indicated in Equation [1] (Ries-Kautt and Ducruix, 1992).

$$\mu = 1/2 \sum (M_i Zi^2) \qquad [1]$$

Classical salts such as ammonium sulphate as well as phosphates and citrates have been used to increase the ionic strength (McPherson, 1990).

3.1.3.3 Organic solvents and Polymers

The organic solvent can compete for water molecules and reduce their dielectric screening capacity. Reduction of the bulk dielectric increases the effective strength of the electrostatic forces allowing protein molecules to attract each other. Polymers such as poly (ethylene glycol) serve to dehydrate proteins in solution by altering the dielectric properties similar to organic solvents. They perturb the natural structure of the solvent and create a more complex network having both water and itself as structural elements. A consequence of this solvent restructuring is that macromolecules, particularly proteins, tend to be excluded and phase separation is promoted (McPherson, 1990).

3.1.3.4 Protein concentration

Proteins are kept in solution by a primary hydration sphere. This sphere of water becomes limiting when the protein concentration is increased beyond some point. The protein starts aggregating and at the solubility limit, the protein will crystallise or precipitate. The protein concentration is an important parameter in protein crystallisation in that it is difficult to define the optimal protein concentration. For crystallisation trials, protein concentration of 10 to 20 $mg.mL^{-1}$ is sufficient. Proteins in the Biological Macromolecule Crystallisation Database (BMCD) (Feigelson, 1988) have been crystallised from solutions containing less than 1.0 up to several hundred $mg.mL^{-1}$.

3.1.3.5 Purity

Crystal growth rates can be considered in terms of the transport of molecules to the growing nucleus and attachment of them to the growing surfaces. The capture of molecules by a growing crystal surface requires the molecules to be incorporated in the correct orientation and to be in a proper chemical state to form interactions with its neighbouring molecules (McPherson, 1990).

Crystal growth requires the population of molecules to be as chemically homogeneous as possible. This means that contaminating proteins should be eliminated. Because crystals have perfect symmetry and periodic translational

relationships between molecules in the lattice, non-uniform protein units cannot enter the crystal. Thus, contaminating impurities may serve as inhibitors of growth.

If they enter the lattice, they may introduce imperfections which produce defects, dislocations and probably termination of crystal growth. It has been recorded that the presence of foreign substrates may facilitate nucleation (Gilliland, 1988). Crystals of lipase from *Candida rugosa* have been crystallised from an impure solution by adjusting the pH to the pI of the protein (U.S Patent, 1992).

3.1.3.6 Description of a phase diagram

As the solubility of a biological macromolecule depends on the various parameters described, a two-dimensional solubility diagram is a representation of its solubility (mg.mL^{-1} or mM macromolecule in solution) as a function of one parameter, e.g. salt concentration, with all other parameters constant. The diagram comprises the following zones (Figure 4) (Ries-Kautt and Ducruix, 1992):

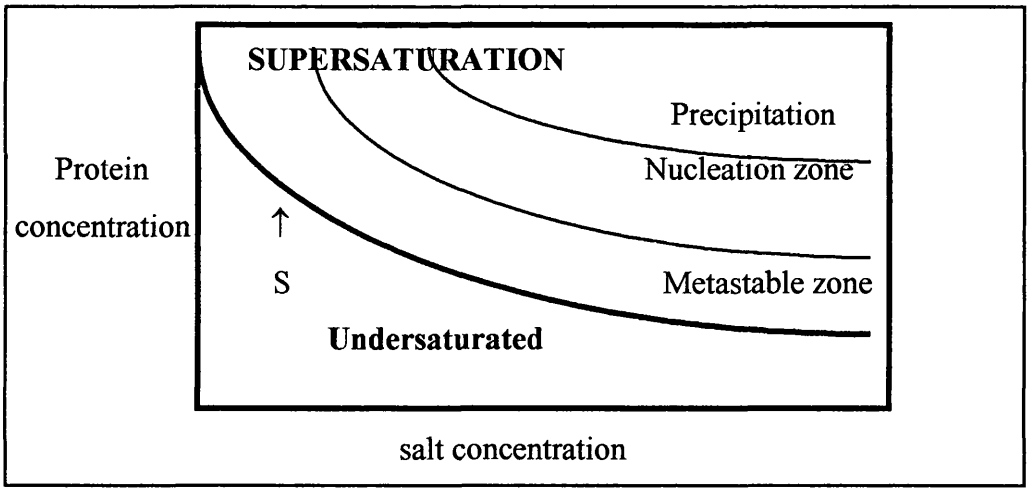

Figure 4: Schematic description of a two-dimensional solubility diagram, demonstrated by the change of protein concentration with crystallising agent concentration (Gilliland, 1988).

(a) The solubility curve S divides the unsaturated and supersaturated zones. In an experiment where crystallising agent and macromolecule concentration correspond to conditions of curve S, the saturated protein solution is in equilibrium with crystallised

protein. This corresponds to the situation at the end of the process of crystal growth from a supersaturated solution.

(b) Under the solubility curve (S), the solution is undersaturated and the protein will never crystallise.

(c) Above the solubility curve (S), the macromolecule concentration is higher than the concentration at equilibrium for a given salt concentration. This corresponds to the supersaturation zone and is subdivided into three regions. (I) The precipitation zone is where excess protein immediately separates from the solution in an amorphous state. (ii) The nucleation zone is where excess macromolecules separate under a crystalline form. Near the precipitation zone, crystallisation occurs as a shower of microcrystals which can be confused with precipitate. (iii) In a metastable zone, a supersaturated solution may not nucleate unless the solution is mechanically shocked or a seed crystal introduced. This region corresponds ideally to the growth of crystals with nucleation of new crystals.

3.2 THE PHYSICAL CHEMISTRY OF PROTEIN CRYSTALLISATION

3.2.1 Nucleation

The smallest stable unit of a crystal is the nucleus. Nuclei are formed by either homogeneous or heterogeneous nucleation. Homogeneous nucleation is the spontaneous formation of solute nuclei arising from energy fluctuations in a supersaturated solution. Heterogeneous nucleation is the formation of solute nuclei on foreign substrates such as dust particles or surface irregularities in the container. All nucleation is considered to be primary in systems without crystalline matter while secondary nucleation refers to nuclei growing out of a parent one (e.g. branching). Macroseeding (Stura and Wilson, 1992), described earlier, is an example of secondary nucleation.

The supersaturation zone is divided into three regions: (a) a metastable region where nucleation does not occur spontaneously, but crystals grow, (b) a labile region where stable nuclei form a crystal-like precipitate of microcrystals and (c) a precipitation region where amorphous precipitates result from non-specific Van der Waals attraction. Crystals will not grow out of all supersaturated solutions. Hence,

to create a new phase, the system must overcome an energy barrier called the activation free energy of germination ΔGg.

The nucleation rate (J_n) can be expressed as (Feher and Kam, 1985):

$$Jn = \beta s \exp(-\Delta Gg / k_b t_c) \quad [2]$$

where the kinetic coefficient βs is the solubility product, k_b, the Boltzmann constant and t_c, the temperature. It appears that as solubility and temperature increase, the greater amount of free molecules will occur in the solution and hence a faster nucleation rate. To favour nucleation, one must press the system as far as possible into the labile region of supersaturation thus favouring fast growth. And secondly, conditions must be chosen where protein solubility is as high as possible.

3.3 CRYSTAL HABIT

The crystal habit, or overall shape of the crystals, depends on internal factors, such as structure and bonds and external factors like supersaturation and solution composition (Gilliland, 1988). The degree of supersaturation, the composition of the solution, temperature and the presence of impurities will all affect crystal habit.

3.3.1 Supersaturation

Supersaturation variations can be used to change the crystal habit. This can be achieved, for example, by changing the solute concentration (Ries-Kautt and Ducruix, 1992). This was demonstrated on the crystallisation of carboxypeptidase where spherulites were grown at low supersaturation and large polyhedrons formed at higher supersaturation (Ries-Kautt and Ducruix, 1992). With high supersaturation, the growth unit incorporates rapidly into the faces of the crystal where their absorption energies are the greatest. Hence, when there is an important anisotropy in the bond, a needle will grow more needle-like and a thin plate will become thinner and wider (Ries-Kautt and Ducruix, 1992).

3.3.2 Impurity

An impurity is classified as anything in the solution other than the solvent or solute. An impurity such as the buffer or an additive may have a number of effects:
(a) It may act as a habit modifier without affecting the crystal lattice (e.g. needles becoming thicker). In this case, the impurity may not be incorporated into the lattice. A recent example demonstrated that the crystallisation of Tumor Necrosis Factor (Ries-Kautt and Ducruix, 1992) using β-octyl glucoside as an additive increased the diameter of the hexagonal prism-shaped crystals five-fold while not affecting their length. In this case, β-octyl glucoside may have some affinity for the face perpendicular to the six-fold axis hindering the attachment of molecules thus slowing down its growth rate. Therefore, long-chain impurities may anchor on crystal faces at several points and disturb crystal growth.

Additives can be sometimes affected by pH of the solution. This can be seen in the influence of glycine on sodium chloride. Glycine is a good habit modifier in the range of 3.5 to 8.5 due to its ionization as zwitterion NH_3^+-CH_2-COO^-. Outside this range, the positively or negatively charged monopolar ions are ineffective (Boistelle and Astier, 1988).
(b) Additives can affect crystal form. This is done by their specific interaction with the protein and so a new compound is crystallised composing of an additive and protein complex.
(c) Additives may decrease the protein's solubility and change the supersaturation in the solution.

3.3.3 Temperature

Temperature was used in a few cases as a habit modifier but it more likely changed the crystal lattice. In the case of lysozyme, a tetragonal form was obtained in the presence of NaCl at an acidic pH at a lower temperature than 25°C whereas an orthorhombic form was grown at higher temperatures (Ries-Kautt and Ducruix, 1992).

3.4 Summary of the parameters influencing protein crystallisation and their importance in the batch production of CLECs

In this section, many parameters, such as pH, temperature, protein concentration, the type and concentration of precipitant, that affect the protein crystallisation of a protein have been explored. The crystals which form may change their size and shape due to the composition of the protein solution. The screening of every parameter affecting crystallisation will require great quantities of protein which will be time consuming and will increase the number of experiments to be performed.

However, by screening more than two parameters at a time, the amount of protein and time needed for screening can be greatly minimised and the crystallisation conditions for the protein can be more efficiently determined and optimised with respect to yield, crystal size and habit. The screening of crystallisation conditions is further examined in Section 5.

4 MATERIALS AND METHODS

4.1 Materials

YADH I was purchased from Biozyme Laboratories Ltd. (Blaenavon, U.K.) and used without further purification. All other chemicals were purchased from Sigma Chemical Co. (Dorset, UK).

4.2 Assay for free yeast alcohol dehydrogenase I (YADH I) activity

YADH I catalyses the reaction:

$$\text{Ethanol} + NAD^+ \Leftrightarrow \text{Acetaldehyde} + NADH + H^+$$

which is monitored at 340 nm for 30 s. The change in absorbance with time is proportional to the amount of YADH I in the reaction mixture and is used to calculate YADH I activity (Bergmeyer, 1983). A 500 mL batch of YADH I assay mix was first prepared which contained 18 mL ethanol, 0.60 g NAD (β-nicotinamide adenine dinucleotide), 0.35 g semicarbazide and 0.15 g glutathione in 0.05 M Tris buffer, pH 8.8. The YADH I solution (1 $mg.mL^{-1}$) to be assayed was then diluted 100-fold in 0.1 M potassium phosphate buffer, pH 6.5. 50 μL of the diluted sample was added to a 3.5 mL acrylic cuvette before adding 3 mL of the assay mix. The progress of the reaction was then monitored at 340 nm using a DU 640 spectrophotometer (Beckman, USA). The measured linear rates ($\Delta A.min^{-1}$) were converted to $Units.mL^{-1}$ according to the equation below using a molar extinction coefficient of NADH (ε = 6.22 mL $\mu mole^{-1}$). One unit is defined as the formation of 1 μmole of NADH per minute. The coefficient of variance for this assay was 5%.

$$\text{YADH I activity} = (\text{Abs 340 nm}.min^{-1}) / 6.22 \times 3 / 0.05 \times 100$$

$$\text{Abs 340 nm}.min^{-1} = \text{change in absorbance}$$

min = time of reaction

6.22 = μM extinction coefficient of NADH

3 = volume of assay mix in cuvette

0.05 = volume of diluted YADH I sample added to cuvette

100 = sample dilution factor

4.3 Determination of protein concentration using the Bio-rad protein assay

Protein concentrations were determined according to the Bradford dye binding method using the Bio-rad assay reagent (Bio-Rad Laboratories GmbH). Protein concentration was calculated from a calibration curve using Bovine Serum Albumin (BSA) as a standard. To construct the calibration curve, standard solutions containing different BSA concentrations from 0.1-0.5 $mg.mL^{-1}$ in 0.1 M Tris-HCl buffer, pH 7.5 were prepared. A 100 μL aliquot of each standard solution was pipetted into separate 3.0 mL cuvettes. Subsequently, 2.5 mL of the Bio-rad protein assay reagent (diluted 1:4 with de-ionised water) was added to each of the standard solutions which were left for 5 minutes at room temperature before the absorbance was measured at 595 nm. The absorbance was linearly related to the concentration of protein in solution over the range investigated. The coefficient of variance for this assay was 2.7 %.

4.4 Analysing purity using an SDS-PAGE system

4.4.1 Preparation of the stacking gel buffer stock

The stacking buffer contained 0.5 M Tris-HCl and 0.4 % (w/v) sodium dodecylsulphate (SDS), adjusted to pH 6.8 in a final volume of 100 mL. The solution was stored at room temperature.

4.4.2 Preparation of the separating gel buffer stock

The separating buffer contained 1.5 M Tris-HCl and 0.4% (w/v) SDS adjusted to pH 8.8 in a final volume of 100 mL. The solution was stored at room temperature.

4.4.3 Preparation of the running buffer (10X)

The running buffer was made up using 50.3 g of Tris, 144.0 g of glycine and 10.0 g of SDS dissolved in 1 L of water. The pH was adjusted to 8.3. The final reservoir buffer contained 0.25 M Tris, 1.92 M glycine and 1 % (w/v) SDS at pH 8.3. The solution was stored at 4 °C.

4.4.4 Coomassie blue G-250 stain

The stain solution was made up to a total volume of 1 litre of water and contained 450 mL [45% (v/v)] methanol, 100 mL [10% (v/v)] acetic acid and 1 mL of a 0.2 % (w/v) G-250 Coomassie blue solution.

4.4.5 Preparation of the protein loading buffer (2X)

The load buffer contained 1% (w/v) SDS, 10 mM EDTA, 10 mM sodium phosphate (pH 7.0), 1% (v/v) β-mercaptoethanol, 15% (v/v) glycerol, 0.01% (w/v) bromophenol blue and 4 mM PMSF. The solution was stored at -20 °C.

4.4.6 SDS-Polyacrylamide gel electrophoresis

4.4.6.1 Resolving gel

The gel plates were cleaned with 70% ethanol and constructed according to Sambrook *et al* (1989). A 12.5 % separating gel containing 4.2 mL of a 30% (w/v) acrylamide/ bisacrylamide (Protogel) solution and 2.5 mL of separating gel buffer, pH 8.8 was made up to 10 mL with water. 140.1 µL of 10% (w/v) ammonium persulphate and 7.68 µL of N,N,N',N'- tetramethylethylenediamine (TEMED) were added to polymerize the gel. The gel solution was poured slowly into the plate cavity using a glass Pasteur pipette until the gel reached three-quarters of the height of the gel apparatus.

4.4.6.2 Stacking gel

A 3% stacking gel was made by adding 500 µL of the 30% (w/v) acrylamide/

bis-acrylamide (Protogel) solution and 1 mL of the stacking buffer, pH 6.8, made up to 5 mL with water. 56.25 μL of a 10% (w/v) ammonium persulphate and 5 μL of TEMED were added to the stacking gel and poured after the separating gel had polymerised. A 12 tooth comb was inserted into the surface and the gel was set aside to polymerise for 1 hr.

4.4.6.3 Running and staining the gel

10 μL of protein samples (8 $mg.mL^{-1}$) were mixed with 10 μL of the 2X protein load buffer and boiled for 10 min. before loading onto the lanes. The running buffer (10X) was diluted ten times and poured into the gel apparatus. The gel ran at 30 mA using a model 400 C (Gibco) power supply and was stained with coomassie blue G-250 staining solution for 1 hr. The gel was then destained in destaining solution for 2 hr. The destaining solution contains 30% (v/v) methanol, 10% (v/v) acetic acid in water.

4.5 Microscopy

Light microscopy using a Olympus E 2330 microscope fitted with an Olympus OM-2 camera was used to observe and photograph the size and shape of the crystals and cross-linked crystals. The sizes determined by the Elzone particle size analyser were initially confirmed using an eye-piece graticule. Given their small size, the rod-shaped crystals were also photographed using a Leica DMLB phase-contrast microscope fitted with an oil-emersion lens.

5 A RATIONAL APPROACH TO BATCH CRYSTALLISATION FOR THE PRODUCTION OF CROSS-LINKED ENZYME CRYSTALS FOR LARGE-SCALE BIOCATALYSIS

5.1 INTRODUCTION

5.1.1 Protein crystallisation and screening

Proteins form crystals during a slow precipitation process which occurs close to a phase boundary controlled by factors such as temperature, pH, the type and concentration of precipitant (salt or organic solvent) and the presence of counterions (McPherson, 1990). The crystals which form may change their size and shape with the conditions, so that their population is unlikely to be uniform. The result is that several conditions may need to be varied before a suitable operating window (i.e. set of conditions) for a large-scale crystallisation process is established. If the effects of all of the conditions throughout their range were to be varied independently the numerous experiments would require a large amount of both protein and time. Moreover much of the protein would be wasted in conditions where no crystals formed. Since proteins are often available in limited quantities, it is important, while optimising their crystallisation conditions, to test as few variations of the conditions as possible. A reduction in the number of experiments to be performed will also reduce the time required.

Efficient screening of the conditions based on factorial experiments (Betts *et al.*, 1979; Carter *et al.*, 1988; Abergel *et al.*, 1991; Carter, 1990) can identify the important variables and their effects, but a complete analysis of all of the interactions requires a full factorial design which is only practical where there is a limited number of variables. An incomplete factorial design (Carter and Carter, 1979) reduces the number of experiments but still examines a large number of crystallisation conditions. Instead of carrying out all possible combinations by varying only one condition at a time, incomplete factorials vary several conditions simultaneously. The experiments take place as if in a multidimensional space each of whose axes is associated with a given process condition, or factor (Abergel *et al.*, 1991). The actual values of the factors define the co-ordinates for each experiment in the space which the axes create.

The space is then filled randomly with experimental points such that the various factors and the conditions which they define are represented evenly. The results are then analysed statistically to determine the conditions which are critical for crystallisation.

The amount of protein and time needed for screening can be further minimised by the use of a sparse matrix in which the trial conditions are heavily biased towards a particular set of crystallisation conditions (Jancarik and Kim, 1991). The major variables explored are pH, buffer materials, additives and precipitating agents. The sparse matrix is formed from a set of about 50 conditions and its main advantage is that it needs only a small amount of protein to test a wide range of experimental conditions using the vapour diffusion method (section 2.4.4). This is now commercially available in kit form (Crystal Screen™ available from Hampton Research). Cudney *et al.*, (1994) have developed an alternative matrix which employs less traditional precipitating agents and this is also available as a commercial kit (Crystal Screen II™). These kits can be used to define the reagents which will drive the crystallisation and whose concentrations will be later optimised. If the initial screening protocols do not produce the required crystal habit or yield, ionic cross-linking agents and detergents may also be used as additives (Cudney *et al.*, 1994).

An alternative procedure known as reverse screening (Sura *et al.*, 1994), examines the solubility characteristics of the protein under study as a function of a particular precipitant (commonly poly (ethylene glycol) (PEG) and ammonium sulphate) and protein concentrations so as to define the conditions under which a solution of the protein is highly supersaturated. This favours the formation of the stable nucleus which is a prerequisite for crystal formation. The next stage in the reverse screen relates the solubility to changing pH and the introduction of additives. Finally, once crystals are obtained, these can be used to seed further experiments aimed at improving the crystallisation conditions. This systematic approach often uses the prior experience about the macromolecule from the BMCD crystallisation databank (Gilliland, 1988).

5.1.2 Biotechnological application of crystallisation

In the above studies on protein crystallisation and the screening of crystallisation conditions, the focus has usually been to produce single large crystals for structural determination studies. In recent years, however, a number of larger scale biotechnological applications of protein crystallisation has emerged such as the recovery of proteins from fermentation broths by direct crystallisation (Jacobsen *et al.*, 1998) and the use of Cross-Linked Enzyme Crystals, CLECs, as industrial biocatalysts (St. Clair and Navia, 1992; Margolin, 1996). When considering the production of protein crystals for the subsequent manufacture of CLECs, the aims of the crystallisation process are entirely different from those of structural studies. In this case, the production of a large number of crystals of uniform size and shape while maximising both protein yield and the retention of catalytic activity are the main objectives. Given the final application of the CLECs, a further requirement is to define a set of stable crystallisation conditions in order to facilitate a reliable scale-up of the process.

A simplified approach has been found to be an efficient way of optimising the crystallisation conditions where three factors are to be varied simultaneously. It has an advantage in that the experimental variation is presented as a simple two-dimensional diagram with a triangular format so that a window of crystallisation is immediately apparent. The approach is illustrated with YADH I, although it is a generic method which could be applied to a protein of interest. This "windows" approach (Woodley and Titchener-Hooker, 1996) is used rationally to optimise the crystallisation conditions with respect to yield, crystal size and habit for the subsequent production of CLECs as large-scale biocatalysts.

5.2 MATERIALS AND METHODS

5.2.1 Crystallisation of YADH I

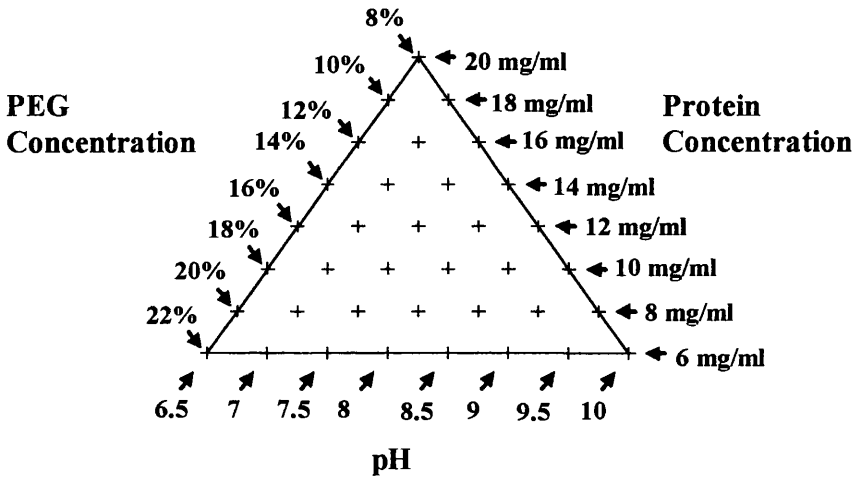

Figure 5: A crystallisation diagram for batch screening of YADH I crystallisation conditions.

The batch crystallisation of YADH I was performed by simultaneously varying three parameters, pH, protein concentration and PEG concentration in an anti-clockwise direction as shown in Figure 5. Protein concentration was varied from 8 to 20 $mg.mL^{-1}$, the precipitant concentration (PEG 4000) was varied from 8 to 22 % (w/v) and pH from 6.5 to 10. The arrows show the direction of the relevant gridlines for the diagram (Figure 5).

The crystallisation conditions investigated were based on previously published hanging-drop experiments as a starting point (Ramaswamy *et al.*, 1994), where YADH I concentration was 12 $mg.mL^{-1}$, PEG concentration was 10 % (w/v) and the pH was 8. By moving around the starting point, the screening for other crystallisation conditions, indicated by the crosses (+), for the crystallisation of YADH I could be accomplished (Figure 5). A 30 $mg.mL^{-1}$ stock protein solution, containing 2 mM NADH, 0.25 mM EDTA buffered with 0.1 M sodium phosphate at the appropriate pH was mixed with

50 % (w/v) PEG 4000 at the same pH to achieve the desired protein and PEG concentrations. The volume was made up to 0.2 mL with sodium phosphate again at the same pH. The crystallisation screening procedure was carried out at both 25 and 4 °C. The crystallisation mixture was set aside for a period of 4 days to ensure that crystallisation was complete. Samples (1 μL) were removed periodically and viewed under a light microscope. The number of microcrystals in the droplet and their approximate sizes were recorded, using an eye-piece graticule viewed at 400x magnification. To identify whether the crystals obtained were salt or protein, an organic dye (IZIT Crystal Dye, Hampton research) was applied to the crystals. The dye diffused through the channels colouring the crystals blue. Salt crystals, lacking these channels, were not coloured.

5.2.2 YADH I crystal activity and protein assay

The crystals produced were centrifuged down using the microcentaur bench centrifuge at 8, 000 rpm for 10 minutes. The supernatant was removed and the crystals were then redissolved back to 0.2 mL and assayed for YADH I activity (Units.mL^{-1}) according to section 4.2 and protein concentration (mg.mL^{-1}) according to section 4.3.

5.2.3 Cross-linking of crystals with glutaraldehyde

The rod crystals prepared under conditions of 14 mg.mL^{-1} protein concentration, 12 % (w/v) PEG, pH 7 and the hexagonal crystals crystallised under conditions of 10 mg.mL^{-1} protein concentration, 12 % (w/v) PEG, pH 8 were cross-linked using glutaraldehyde. Before the crystals were crosslinked, a cross-linking mother liquor was prepared. This contained 0.1 M sodium phosphate buffer, at the same pH the crystals were obtained, including 2 mM NADH, 0.25 mM EDTA and 10 % (w/v) PEG 4000. A 50 % (v/v) aqueous glutaraldehyde solution (Sigma, Inc.) was diluted in the mother liquor solution to achieve glutaraldehyde concentrations ranging from 0.01 to 15 % (v/v). These cross-linking mother liquors allowed the crystals to be cross-linked while preventing them from redissolving.

To perform the cross-linking, 1 mL of the crystal suspension was centrifuged at 8, 000 rpm for 10 minutes. The supernatant was removed and the crystals were

cross-linked in 1.5 mL of cross-linking mother liquor solution for 1.5 hours while agitating on a Vibrax vibrating platform (Janke & Kunkel GmbH, Germany) at 100 rpm at room temperature. After cross-linking, the cross-linked crystals were washed in 5 mL of buffer to remove any excess glutaraldehyde. The cross-linked crystals were stored in buffer at 4 °C.

5.3 RESULTS AND DISCUSSION

5.3.1 Effect of crystallisation conditions on YADH I crystal habit

For the final application of CLECs as large scale biocatalysts it is important to be able to control the size and shape of the initial enzyme crystals. This will determine both the mechanical stability of the CLECs and the limits on their catalytic activity, caused by mass transfer phenomena. Figure 6 shows that by varying the pH of the system at 25 °C, the crystal shape of the YADH I enzyme can be precisely controlled. For example, at pH 7, in 10 to 16 % (w/v) PEG 4000, only rod-shaped crystals of 5 μm in length and 1 μm in thickness were obtained. At pH 8 and PEG concentrations of 10 to 14 % (w/v), however, hexagonal crystals were formed as flat plates about 15 μm across and no more than 2 μm in thickness. Crystallisation of rod crystals took overnight while hexagonal crystals took a period of 4 days to ensure that crystallisation was complete. Finally at pH values above 8.5, both rod-shaped and hexagonal crystals were formed. From Figure 6, it can be seen that there are clear regions or "windows" in the triangular diagrams where it is possible to control the conditions to form either rod shaped or hexagonal crystals. The "windows" for each crystal form are reproducible although conditions for the formation of hexagonal crystals are considerably tighter than for the formation of the rods. This indicates that a conformational barrier dependent on pH must be overcome in order to create the hexagonal crystal phase which is dependent on the pH of the system (Ataka *et al.*, 1978).

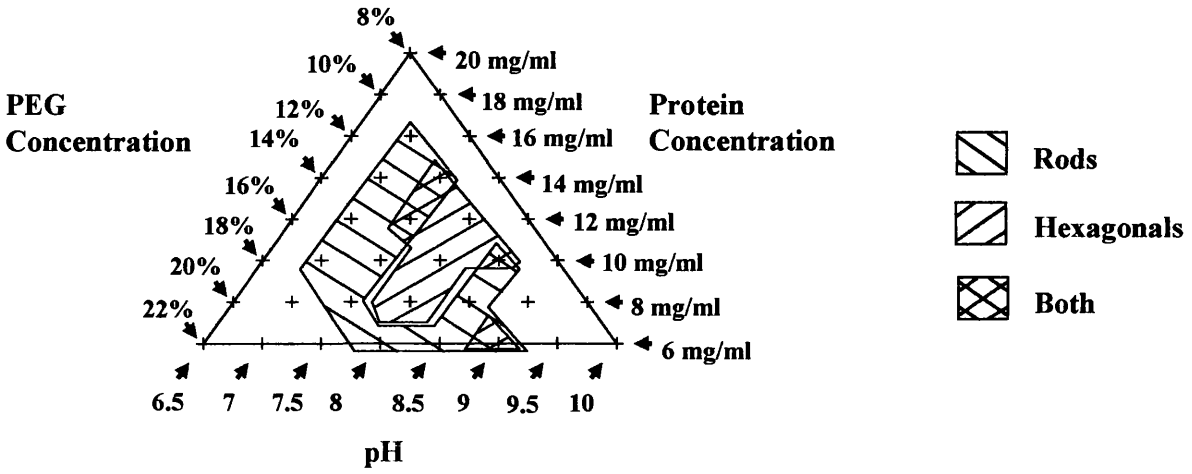

Figure 6: A crystallisation diagram showing the different crystal YADH I forms obtained at 25 °C.

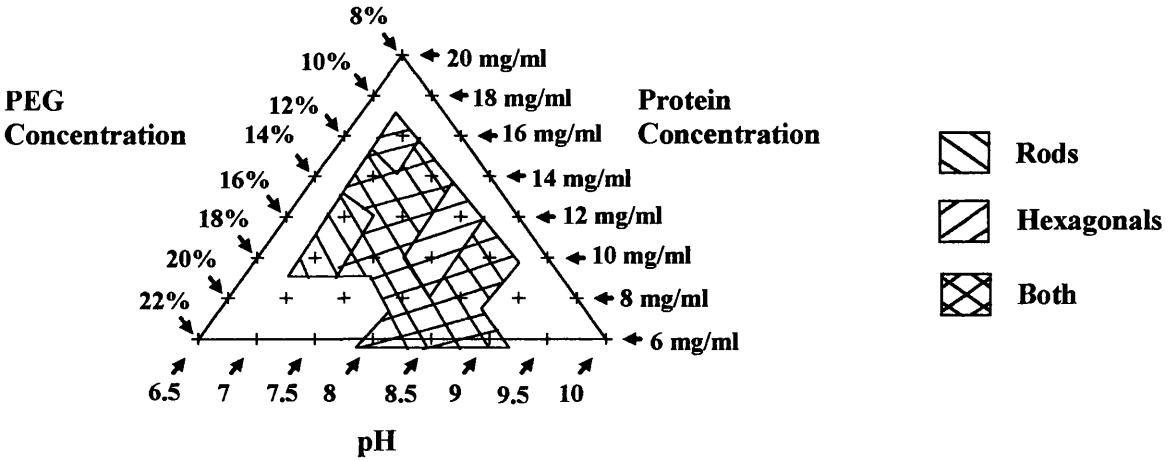

Figure 7: A crystallisation diagram showing the different crystal YADH I forms obtained at 4 °C.

Figure 7 shows results for the crystallisation of YADH I over the same pH, protein, and PEG 4000 concentration ranges but at 4°C rather than 25°C. Once again, two crystal shapes (rod and hexagonal) or a mixture of the two forms can exist. The

window shows that it is more difficult to select for a specific crystal form at 4°C since the majority of the crystallisation conditions favoured a mixture of both rod and hexagonal YADH I crystals. Control of the YADH I crystal shape is thus also dependent on the temperature as well as the pH of the system. In this case, the formation of a specific shape is also scattered across the triangle which makes it difficult to select for a specific form. This has obvious process implications for the control of large scale crystallisation processes.

According to McPherson, (1990), an advantage of using polyethylene glycol over other crystallisation agents is that most proteins can crystallise within a fairly narrow range of PEG concentration, 4-18% (w/v). It was found here that YADH I crystallised in the narrower range of 10-16% (w/v) throughout. In addition, the exact PEG concentration at which hexagonal YADH I crystals form is rather insensitive provided that the pH and temperature are fairly constant at around 8 and 25 °C respectively (Figure 6).

5.3.2 Effect of crystallisation conditions on YADH I crystal recovery

As shown in Figures 8 and 9, an activity recovery of crystals of 70 % or greater occurred in the lower left-hand corner of the crystallisation diagram at 25 and 4°C respectively under conditions of high PEG concentrations (14 to 16 % (w/v)) and low pH. Crystal recovery was found to be less than 50 % at lower PEG concentrations (10 % (w/v)). It is interesting to note that lower protein concentrations (6 to 12 $mg.mL^{-1}$) favour a crystallisation state which allows the greatest protein recovery in the crystalline form. As was shown in Figure 6, rod-shaped crystals are favoured in this area of the window. This trend of increased crystal recovery at higher crystallisation agent concentration and lower protein concentration is evident in the crystallisation of YADH I (Figure 8). It is difficult to conclude from the experiments performed here whether it is the decreased protein concentration or the increased precipitant concentration which is responsible for the increased yield as both components are being altered simultaneously. From the engineering standpoint, however, it is required to have the highest yield of crystals possible in order to make the most efficient, and economic, use of the biocatalyst. The advantage of

establishing windows within the triangular diagrams is that it shows where the crystal yield is highest and the sensitivity of this to the crystallisation conditions.

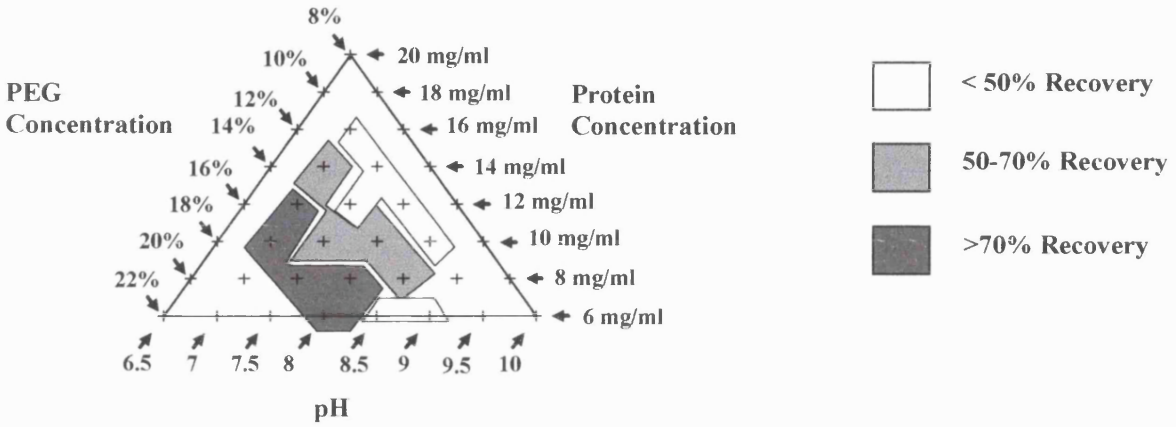

Figure 8: A crystallisation diagram showing the crystal activity recovery obtained at 25 °C. Percentage activity recovery was calculated by dividing the total units of the crystallised YADH I with the total units of soluble YADH I, before crystallisation.

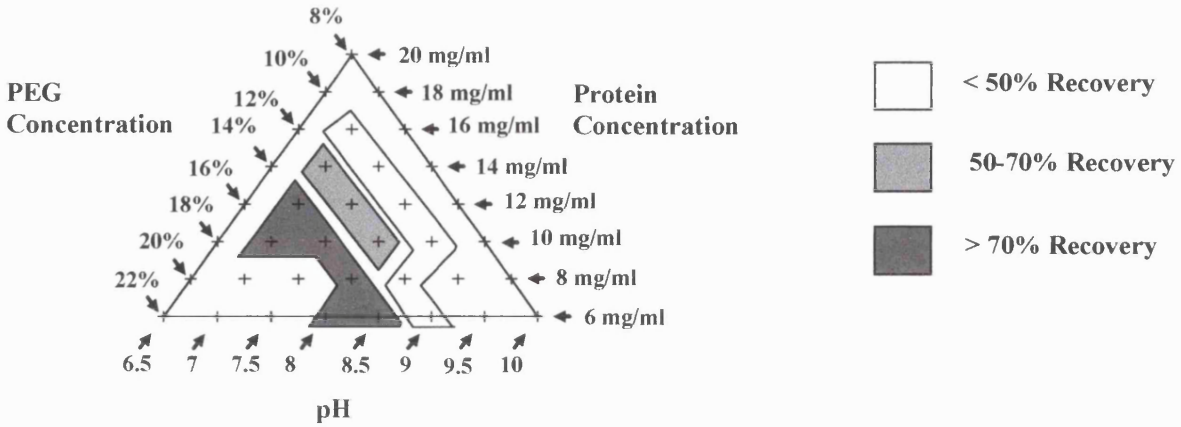

Figure 9. A crystallisation diagram showing the crystal activity recovery obtained at 4°C. Percentage activity recovery was calculated by dividing the total units of the crystallised YADH I with the total units of soluble YADH I, before crystallisation.

5.3.3 Effect of crystallisation conditions on YADH I purification

Figures 10 and 11 show that crystallisation of YADH I from the solution can be used as a purification process. The purification factor (PF) is determined by dividing the specific activity (Units.mg^{-1}) of the spun-down and redissolved YADH I crystals by the specific activity of the YADH I in the original sample. The PF is the degree to which YADH I is purified from the other impurities in the crude sample. The hexagonal crystals formed under conditions of 10 mg.mL^{-1} protein concentration, 12 % (w/v) PEG, pH 8, as shown in Figure 10, were redissolved and loaded onto an SDS-PAGE gel to assess their purity. Gel 1 shows that the removal of a majority of contaminants through crystallisation was accomplished. Crystallisation is thus an effective process on a rather crude extract from the yeast cells. Given that the PF is rather low (PF~3), the YADH I must be a major component of the extract.

By comparing Figures 6 and 10 at 25 °C, it is seen that the greatest purification, PF ≥ 3, occurred under crystallisation conditions which favoured the formation of only hexagonal YADH I crystals with 50 to 70 % crystal recovery. By comparing Figures 7 and 11 at 4 °C, the greatest purification, PF ≥ 3.0, occurred under crystallisation conditions which favoured a mixture of both hexagonal and rod crystals where the recovery of YADH I activity in the crystals is between 50 % and 70 %. It is interesting to note that the maximum PF shifts its position between 25 and 4 °C. At 25 °C, the maximum purification occurs in the hexagonal window whereas at 4 °C, it occurs in the window of mixed crystals. For both situations, the crystallisation diagrams at both 25 and 4 °C (Figures 10 and 11 respectively) demonstrated that the greatest PF is obtained more frequently at intermediate levels of crystal recovery.

Another SDS-PAGE gel was used to determine the level of purification that could be obtained from the rod YADH I crystals. Rod crystals that were formed at protein concentration of 14 mg.mL^{-1}, PEG concentration of 12 % (w/v) at pH 7 were redissolved, and ran on an SDS-PAGE gel (Gel 2). The rod crystals shown were obviously not as pure as the hexagonal YADH I crystals and are shown to contain lower molecular weight contaminants. This is a peculiar feature of the rod crystals which will be discussed in Section 9.4.4. The crystallisation of rod crystals did

remove contaminants of higher molecular weights, greater than 31 kD. The gels showed that the attainment of a pure crystalline product is a delicate process and is dependent strongly on the crystallisation conditions.

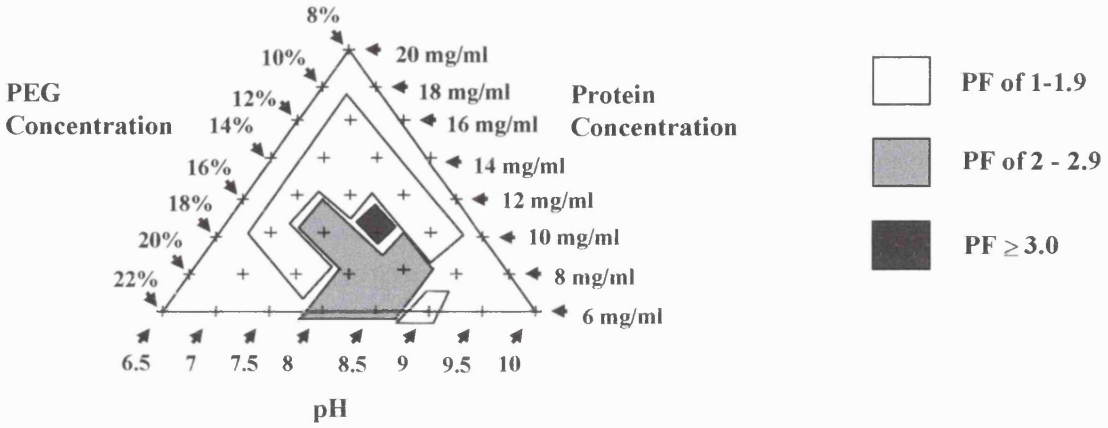

Figure: 10: A crystallisation diagram showing the different purification factors as a result of crystallisation at 25 °C. The Bradford protein assay was used to obtain these PF values.

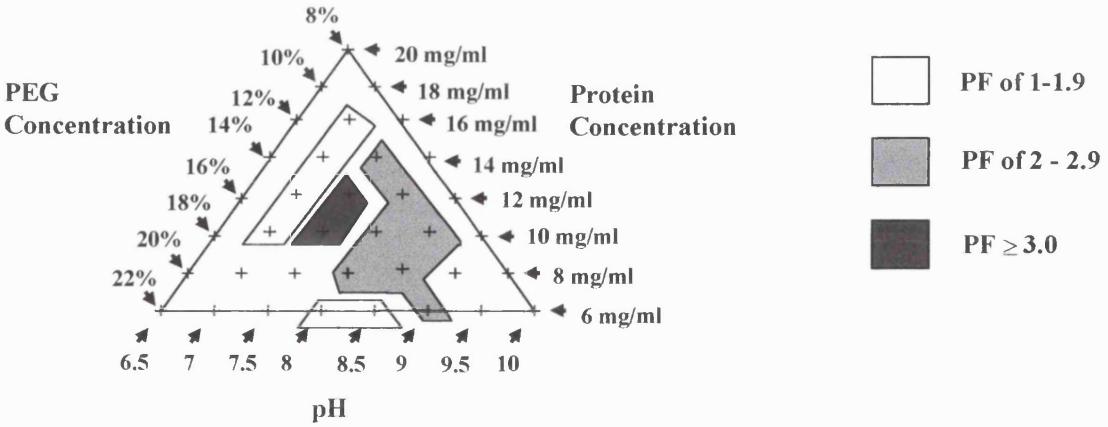

Figure 11: A crystallisation diagram showing the different purification factors as a result of crystallisation at 4 °C. The Bradford protein assay was used to obtain these PF values.

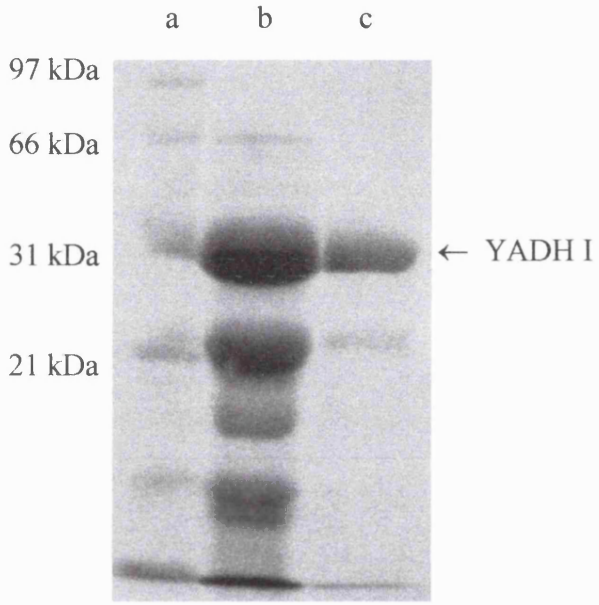

Gel 1: An SDS-PAGE gel showing the degree of purity as a result of crystallisation. Track (a) represents low molecular weight markers. Track (b) represents crude YADH I enzyme (10 $mg.mL^{-1}$) obtained from Biozyme, Inc. Track (c) represents redissolved hexagonal YADH I crystals.

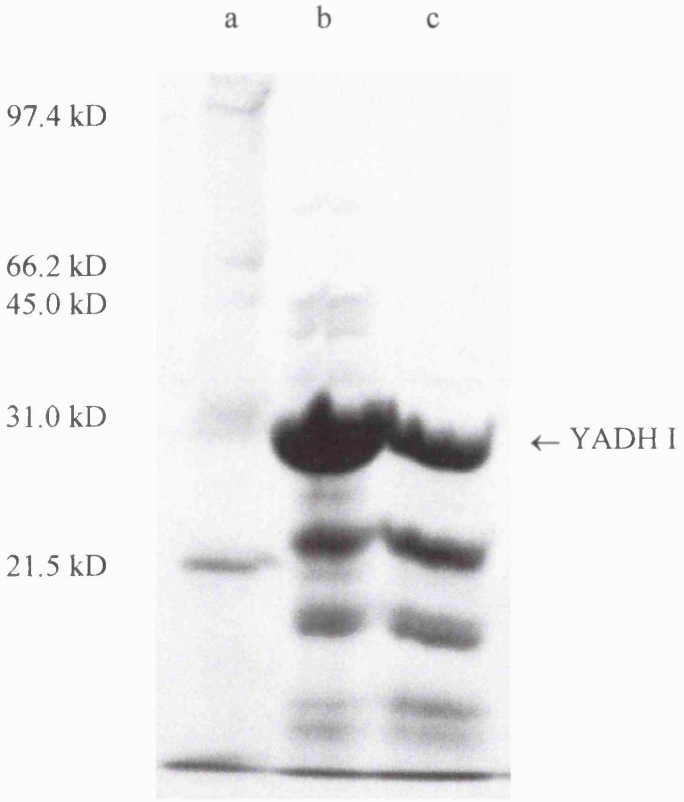

Gel 2: An SDS-PAGE gel showing the degree of purity as a result of crystallisation. Track (a) represents the low molecular weight markers. Track (b) represents crude YADH I enzyme (10 $mg.mL^{-1}$) from Biozyme, Inc. Track (c) represents the redissolved Rod YADH I crystals.

5.3.4 Comparison between sparse matrix screening and the crystallisation diagram approach

Sparse matrix screening is a technique that incorporates selected published crystallisation conditions for the crystallisation of proteins. The three main categories of parameters investigate pH and buffer materials, additives and precipitating agents (Jancarik and Kim, 1991). The authors chose five different pHs from 4.6 to 8.5 and to each pH value, buffer chemicals that were known to be successful in previous crystallisation were picked. Additives were chosen from past crystallisation experiences. Four types of precipitating agents were picked and categorized as volatile, for example 2-propanol, non-volatile, such as PEG, salting-out agents and mixtures. The multidimensional matrix was further simplified by deleting conditions that partially approximated other conditions. Once approximate conditions were deciphered, optimisation of conditions was carried out to achieve the point of obtaining single crystals for crystallographic studies.

Similar to the sparse matrix procedure, the crystallisation diagram was developed to screen for crystallisation conditions based on previous published conditions. The crystallisation diagram however is more specific for the optimisation of conditions to obtain enzyme microcrystals in batch for the purposes of manufacturing CLECs and not for growing single crystals for structural studies. The crystallisation diagram allows us, by starting with hanging drop volumes of 5 μL, to scale-up crystallisation conditions by a factor of 200-fold in 1 mL Eppendorf tubes. The diagram allows a rapid way of screening and optimisation of crystallisation conditions. The advantage is that the crystallisation diagram maps out regions of greatest activity yield and also of different crystal forms of the same enzyme.

By moving along any axis shown by the arrows in Figure 5, one can vary the other two parameters simultaneously. In the batch crystallisation of YADH I, the ionic strength and cofactor (NAD) concentration were kept constant at 0.1 M sodium phosphate and 2 mM respectively to reduce the number of variables investigating during crystallisation. It allowed the exploration of more crucial crystallisation parameters such as pH, precipitating agent and protein concentrations that have been known to affect crystallisation of YADH I (Ramaswamy *et al.*, 1994).

5.3.5 Comparison between incomplete factorial approach and the crystallisation diagram approach

The incomplete factorial (IF) approach to protein crystallisation was developed by Carter and Carter (1979), and it permits the assay of a large number of crystallisation conditions by varying more than one factor at a time in a given experiment. The different variables include pH of the solution, temperature, cofactors such as substrates and ligands and the presence of precipitating agents such as salts, alcohols and organic solvents.

The experiment is randomly arranged with individual crystallisation trials differing from each other with the various variables and their states represented with similar frequencies. A scoring scheme is employed to analyse the results where a score of 0 represents a soluble protein solution, 1 representing precipitates and 2 representing crystal formation. The effect of each variable can be identified by studying its influence on the score value in the experimental design with the influence of other variables. A cumulative merit value (CMV) for each variable of interest will be compared with other CMVs of other variables to extract those variables most critical for crystallisation (Chantal *et al.*, 1991).

The crystallisation diagram, in conjunction with the IF Approach, provides a useful tool of identifying and optimising the crystallisation conditions for the protein of interest. After scoring and assaying for the crystals of interest (i.e. YADH I), the crystallisation diagram offers a more schematic approach of creating a window of crystallisation of the protein and its various crystal form, while omitting any regions representing precipitation or soluble solution. To a greater extent, the diagram visually identifies the variables that influence the crystallisation of a specific crystal form of an enzyme.

The crystallisation diagram also shows the various purification factors one may achieve from crystallisation. The ability to crystallise the YADH I enzyme from a crude preparation is advantageous as it produces a purified enzyme with a good yield. Being able to crystallise YADH I from a crude preparation is useful in that no

chromatographic techniques have to be employed before crystallisation. By selecting a proper set of crystallisation conditions, one may produce a relatively pure and enzymatically active crystal form (i.e. hexagonal YADH I) for biocatalyst production.

5.3.6 Comparison between reverse screening and the crystallisation diagram approach

Reverse screening is a systematic approach to protein crystallisation by utilising prior experience or specific information about the macromolecule from the crystallisation database (BMCD; Gilliland, 1988). Reverse screening does not comprehensively screen all crystallisation conditions but focuses on precipitants such as ammonium sulfate and PEG 4000, that are effective precipitants used commonly in protein crystallisation (Stura *et al.*, 1994). The approach consists of determining the solubility characteristics of the macromolecule as a function of precipitant and also protein concentration to map the range of parameters that would yield crystals, establish conditions for seeding and maintain sufficient supersaturation for crystal growth. In addition, changes in solubility as a function of pH and with the addition of additives can also be evaluated. The reverse screening method employs using a 2-dimensional phase diagram of the macromolecule concentration ($mg.mL^{-1}$) as a function of precipitant concentration to map areas of crystallisation.

Like reverse screening, the crystallisation diagram optimises the crystallisation conditions for the macromolecule (i.e. YADH I) that were obtained from screening conditions in the BMCD. The crystallisation diagram however allows us to vary three conditions such as protein and precipitant concentration (i.e. PEG 4000) and pH all at once and to identify their combinatorial effect in the crystallisation of the two crystal forms of YADH I

The crystallisation diagram can also be used to investigate the effect any one variable has on solubility by varying the axis of one component, say PEG concentration, by shifting it to higher concentrations while keeping the other two axes constant. This shift would create a new window of screening of crystallisation conditions.

5.3.7 Representation of the triangular crystallisation diagram in 3-dimensional space

The triangular diagrams conveniently explore protein crystallisation where three factors are varied independently. If the three variables (e.g. A, B & C in Figure 12a) are set as the orthogonal axes of a three-dimensional space then the diagram represents a triangular fragment of a plane in the space which the axes create (Figure 12c). The position of the triangle depends on the order and direction of the variables along its sides. If a series of triangles is unfolded (see 1-4 in Figure 12b) without changing the ranges of the variables, but simply reflecting them where necessary along the sides of the parallelogram created, then the group together represents the four sides of a tetrahedron in the centre of the cube which the orthogonal axes define (Figure 12c). The conditions which the triangles define systematically cover the crystallisation behaviour throughout the cube except for the region at the centre of the tetrahedron. This can easily be explored by setting up just one experiment containing the three components at the mid-point of their respective concentration ranges.

The benefits of having the results displayed on the flat triangular diagrams are clear from a comparison of Figures 6 and 8. The results are simply displayed and the crystallisation conditions are easily optimised.

A ternary phase diagram (Mullin, 1993) could also be used to explore the influence of three components (A, B & C) on the crystallisation of proteins. Any point within this

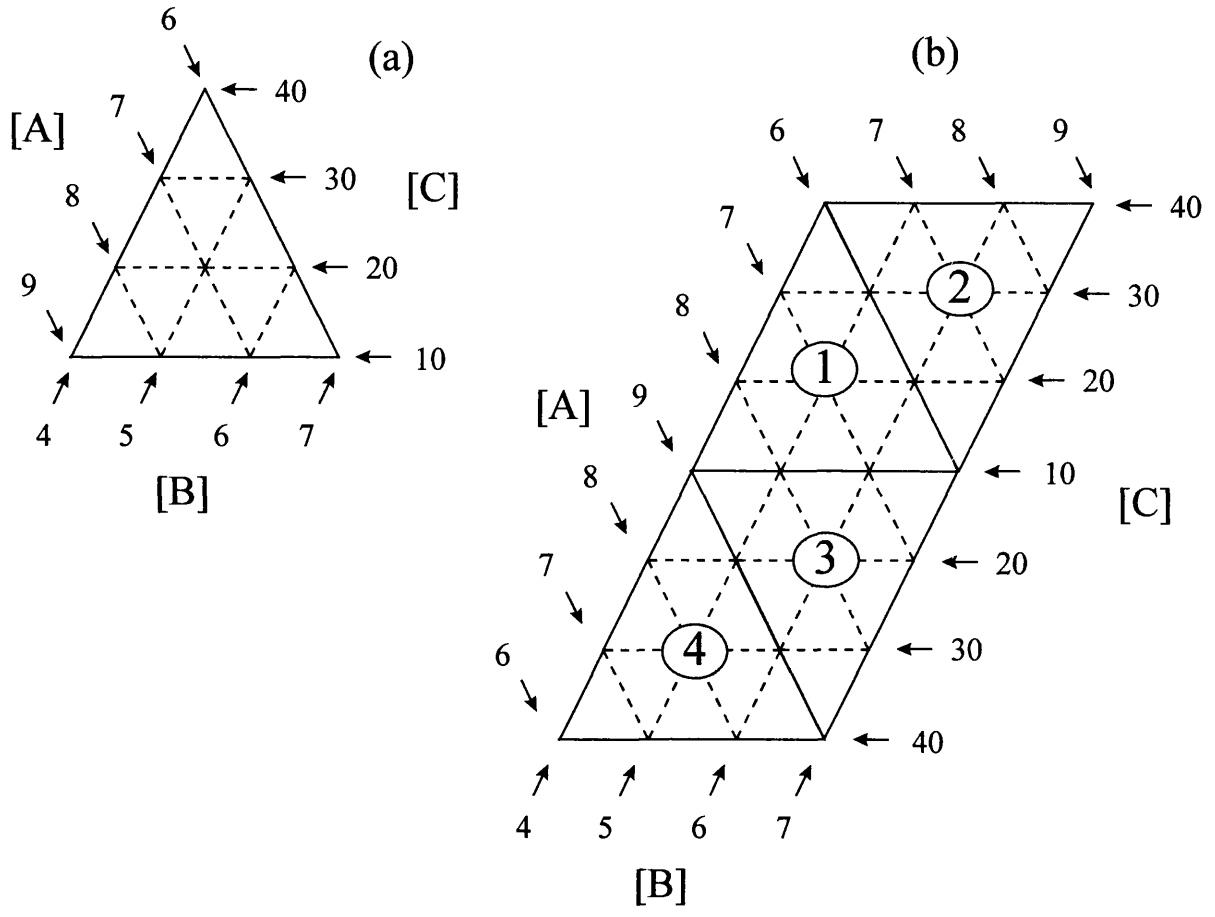

Figure 12(a) shows the co-ordinates of a typical crystallisation diagram (#1),
(b) shows the making of diagrams 2,3 and 4 using the method of reflection, starting with diagram #1.

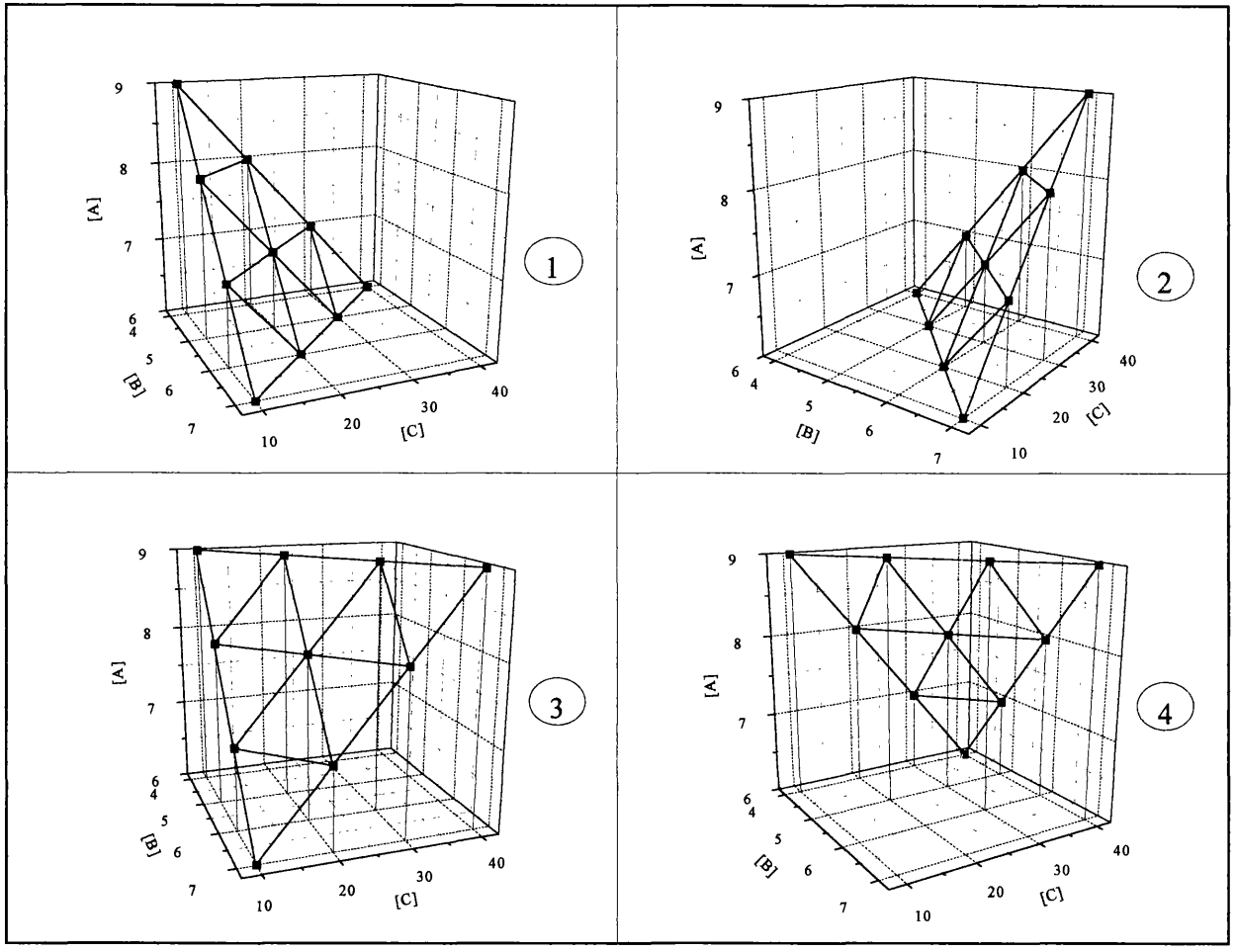

Fig. 12(c): Representation of the four crystallisation diagrams in 3-dimensional space.

diagram also represents a mixture of three components, but one which must now satisfy the equation A+B+C=1. In contrast to this ternary phase diagram, the three components of the triangular crystallisation diagrams do not satisfy this equation, and only two of the three components must be varied simultaneously. The diagrams are triangular fragments of planes in space, rather than a full two-dimensional representation of the ternary phase diagram. The triangles also have the advantage that they allow the effects of important variables such as pH to be explored independently of the concentration of any of the components. This allows conditions for the batch crystallisation of an enzyme to be rapidly and systematically screened.

5.3.8 Cross-linking of YADH I crystals with glutaraldehyde

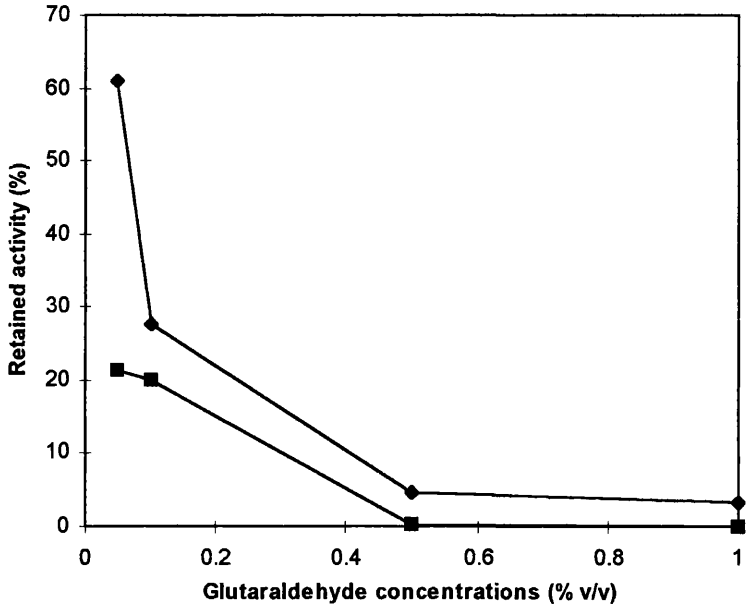

Figure 13: The percent retained activity of rod and hexagonal YADH I CLECs with increasing glutaraldehyde concentrations. ◆, rod CLECs, ■, hexagonal CLECs.

Rod and hexagonal YADH I crystals were subsequently cross-linked using increasing concentrations of glutaraldehyde for 1.5 hours. The purpose of these cross-linking experiments was to determine the glutaraldehyde percentage that gave the most retained activity after cross-linking. Uncross-linked crystals, when removed from their crystallising solution, could be dissolved. Both rod and hexagonal crystal forms of YADH I, after cross-linking with 0.05 % (v/v) glutaraldehyde, did not dissolve and retained 60 and 22 % respectively of their initial crystal activity of 250 and 363 Units.mg^{-1} respectively (Figure 13). This glutaraldehyde concentration was chosen for catalytic and mechanical studies since the activity greatly decreases as the glutaraldehyde concentration increases. Rod CLECs lost half of their activity as the glutaraldehyde concentration was increased to 0.1% (v/v) and almost all of their activity at 0.5 % (v/v) glutaraldehyde. Hexagonal CLECs lost all their activity at 0.5 % (v/v) glutaraldehyde.

5.3.9 Crystallisation of hexagonal YADH I using Tris buffer

Previously, hexagonal YADH I crystals have been obtained from a 0.1 M sodium phosphate buffer at pH 8 in the presence of NAD cofactor. Complete crystallisation needed 4 days. Scaling-up of hexagonal crystals beyond a 1 mL scale has been difficult because it takes a long time for hexagonal crystals to form and also the sodium phosphate buffer has been reported to increase the rate of decomposition of NAD in alkaline conditions (Chenault and Whitesides, 1987).

Tris buffer inhibits the action of phosphate (Chenault and Whitesides, 1987) and was picked for subsequent crystallisation work. Screening for the crystallisation of hexagonal YADH I crystals in Tris at pH 8 was performed by varying the protein and PEG concentrations at 25 °C. The starting conditions were 12 mg.mL^{-1}, 10 % (w/v) PEG at pH 8 similar to the conditions under which hexagonal crystals were obtained using phosphate as the buffer (Figure 6). By keeping the protein concentration at 12 mg.mL^{-1} and pH at 8, PEG concentrations were varied from 10 to 18 % (w/v). When the protein concentration was fixed at 12 mg.mL^{-1}, hexagonal crystals formed between PEG concentrations of 10 and 12 % (w/v) (Table 2). It can be seen from Table 2 that less than 50 % crystal recovery and a purification factor in the range of 1 to 1.9 occurred at lower PEG concentrations of 10 to 12 % (w/v). This

observation was similar to the hexagonal crystals formed in phosphate buffer at 25 °C as shown in Figures 8 and 10.

Similarly, protein concentration and pH were also fixed at 10 $mg.mL^{-1}$ and 8 respectively, while PEG concentrations were varied from 10 to 18 % (w/v) (Table 3). In this case, hexagonal crystals formed at higher PEG concentrations (i.e. 14 to 18 % (w/v)) and that there was a trend of greater crystal recovery as PEG concentrations were increased (Table 3).

Conditions	Total Units	Activity ($Units.mg^{-1}$)	Purification Factor	Activity recovery (%)
1) 12 $mg.mL^{-1}$ (control)	333	111	---	100
2) 12 $mg.mL^{-1}$ 10 % (w/v) PEG	41	127	1.2	12
3) 12$mg.mL^{-1}$ 12 % (w/v) PEG	123	182	1.6	37

Table 2: Row 1 shows the total units and specific activity ($Units.mg^{-1}$) of soluble YADH I at 12 $mg.mL^{-1}$ protein concentration in Tris buffer pH 8 with 2 mM NAD, before the addition of crystallising agent (PEG 4000). Rows 2 and 3 show the purification factor and activity recovery (%) of hexagonal crystals at PEG concentrations 10 and 12 % (w/v) respectively at 25 °C. The total volume of the crystallisation experiments was 0.3 mL.

Conditions	Total Units	Activity (Units.mg^{-1})	Purification Factor	Activity recovery (%)
1) 10 mg.mL^{-1} (control)	188	63	---	100
2) 10 mg.mL^{-1} 14 % (w/v) PEG	60	109	1.7	32
3) 10 mg.mL^{-1} 16 % (w/v) PEG	140	216	3.4	74
4) 10 mg.mL^{-1} 18 % (w/v) PEG	166	250	4.0	88

Table 3: Row 1 shows the total units and specific activity (Units.mg^{-1}) of soluble YADH I at 10 mg.mL^{-1} protein concentration in Tris buffer pH 8 with 2 mM NAD, before the addition of crystallising agent (PEG 4000). Rows 2 to 4 show the purification factor and activity recovery (%) of hexagonal crystals at PEG concentrations 14, 16 and 18 % (w/v) respectively at 25 °C. The total volume of the crystallisation experiments was 0.3 mL.

The hexagonal crystals obtained under crystallisation condition number 2 of Table 2 (12 mg.mL^{-1} YADH I, 10 % (w/v) PEG at pH 8) were used to seed a 40 mL batch (Table 4) of similar conditions to determine whether seeding can improve the recovery of the hexagonal crystals. After seeding, the 40 mL batch was mixed and put on a shaker at 100 rpm overnight at room temperature. Seeding resulted in the formation of hexagonal YADH I crystals with an activity recovery of 93 % after 2 days (Table 4). Seeding has been a very useful technique in scaling-up crystallisation. YADH I crystallisation in Tris buffer was successfully scaled up from 0.5 to 500 mL (1000 fold) with reproducible results in terms of crystal size and shape

with an increase in recovery. Also, Tris buffer, being a better system for NAD stabilisation, may have contributed to the ease of crystallisation of YADH I crystals (Chenault and Whitesides, 1987). This could result in a higher PF of 4 compared to phosphate buffer. Also, seeding may provide a fast and effective way to facilitate the optimisation of hexagonal YADH I crystals.

Conditions	Total Units	Activity (Units.mg^{-1})	Purification Factor	Activity recovery (%)
1) 12 mg.mL^{-1} (control)	44358	92.4	---	100
2) 12 mg.mL^{-1} 10 % (w/v) PEG	41093	368	4.0	93

Table 4: Scaling up of YADH I crystallisation (condition number 2 in Table 2, 12 mg.mL^{-1} protein, 10 % PEG (w/v) in Tris pH 8 in presence of 2 mM NAD) to 40 mL. The activity recovery (%) of hexagonal YADH I crystals is calculated after seeding with YADH I crystal seed stocks made from crystallisation conditions similar to condition number 2 at a 0.3 mL scale (Table 2).

5.4 Conclusions

The factors which together govern the solubility of a protein also influence its crystallisation behaviour. Temperature, pH, protein concentration, ionic strength, the nature of counterions and the presence of coenzymes are all important variables. The definition of an operational window for crystallisation as described here is a convenient technique with which to optimise the large-scale production of the crystals whether as an aid for protein purification or for the manufacture of CLECs as biocatalysts.

Starting with previously published conditions in the hanging drop at a 1 μL scale, the triangular crystallisation diagram allows us to explore systematically an appropriate range of conditions at a 1 mL scale in Eppendorf tubes. The diagram clearly shows how the combination of variables affects the crystallisation, and it allows a process window to be quickly identified with its regions of optimum recovery and of different crystal forms, while any regions of precipitation or high solubility are avoided. From this window the successful conditions can be increased to a scale of 0.5 L with little or no change in crystallisation behaviour, either of yield or habit.

Chemical cross-linking of the enzyme crystals (CLECs), serves to stabilise the crystals under harsh conditions such as high temperature, pH and in organic and organic-aqueous solvents. The retention of high activity under these conditions makes the CLECs very suitable as process catalysts. The next section examines the influences of crystallisation and cross-linking conditions on the catalytic and mechanical stability of YADH I CLECs as large-scale biocatalysts.

6 HIERARCHY OF CATALYTIC AND MECHANICAL TESTS FOR THE RATIONAL CHARACTERISATION OF CLECs

6.1 INTRODUCTION

The last chapter showed a novel and generic screening technique presented as a simple two-dimensional triangular diagram to identify the 'window of crystallisation' in which the activity recovery, crystal size etc.. can be immediately visualized. The crystallisation diagram has provided an efficient tool for the batch production of crystals of an enzyme for the purposes of CLEC production. By putting the enzyme catalyst in a crystalline form and then chemically cross-linking the crystalline catalyst with a bi-functional reagent such as glutaraldehyde, one can produce an immobilised, insoluble catalyst which can be studied both catalytically and mechanically. Although catalytic stability tests in high temperature, extreme pHs and solvents have been done previously with CLECs such as Thermolysin and *Candida rugosa* lipase (St. Clair *et al.*, 1992), the processing issues in the use of CLECs such as shear stability, ease of filtration and the ease of recovery of CLECs have not been thoroughly examined.

The Working Party on immobilised biocatalysts, appointed by the European Federation of Biotechnology, has proposed a number of questions for the investigations dealing with any form of immobilised biocatalysts (Working Party on immobilised biocatalysts, 1983). Some of the questions that may apply to the study of CLECs are as follows:

1) What quantity (g/L) of free enzyme (partially purified, crude extract) preparation is needed to prepare a unit volume of enzyme crystals?
2) What cross-linking conditions are needed to produce an insoluble crystalline product?
3) Are the observed reaction rates diffusion-limited in comparison to free enzyme?
4) In what ways are the reaction rates and stability of a CLEC affected by changes in reactant concentrations and reaction conditions in the range of interest and how do the rates and stability compare with those catalysed by the free catalyst?
5) What are the dimensions, shape and density of the wet particles?

6) Are the catalyst useful for the practical application in terms of its mechanical stability under conditions of its intended use?

According to the Working Party, there are no requirements on the absolute value of the characteristics, such as rate per unit catalyst volume, particle size or dimensional stability (Working Party on immobilised biocatalysts, 1983). These values are only meaningful in relation to each other and to the objective of the investigation.

6.2 The importance of a hierarachy of tests for the characterisation of CLECs

There are some of the initial characteristics such as the physical dimensions and activity of the wet crystalline particles which are important in the description of a CLEC because they define other essential quantities-such as reaction rates, stability under process conditions, such as in an agitated vessel and compression behaviour in a packed bed.

Little is known about the changes of catalytic and mechanical properties associated with the chemical modification of crystalline enzyme as a result of changing its crystallisation conditions. In this section, a hierarchy of tests has been developed to characterise the rod and hexagonal YADH I CLECs (Figure 14) at a catalytic and mechanical level in comparison to free YADH I. The hierarchy of tests is also used to characterise other batches of CLECs made from other enzyme sources. This list is a pragmatic way to obtain adequate information for sensible comparisons and process design purposes with a reasonable amount of effort. The hierarchy of tests reduces the number of experiments to be performed. However, this is no way of discouraging detailed studies on a particular system.

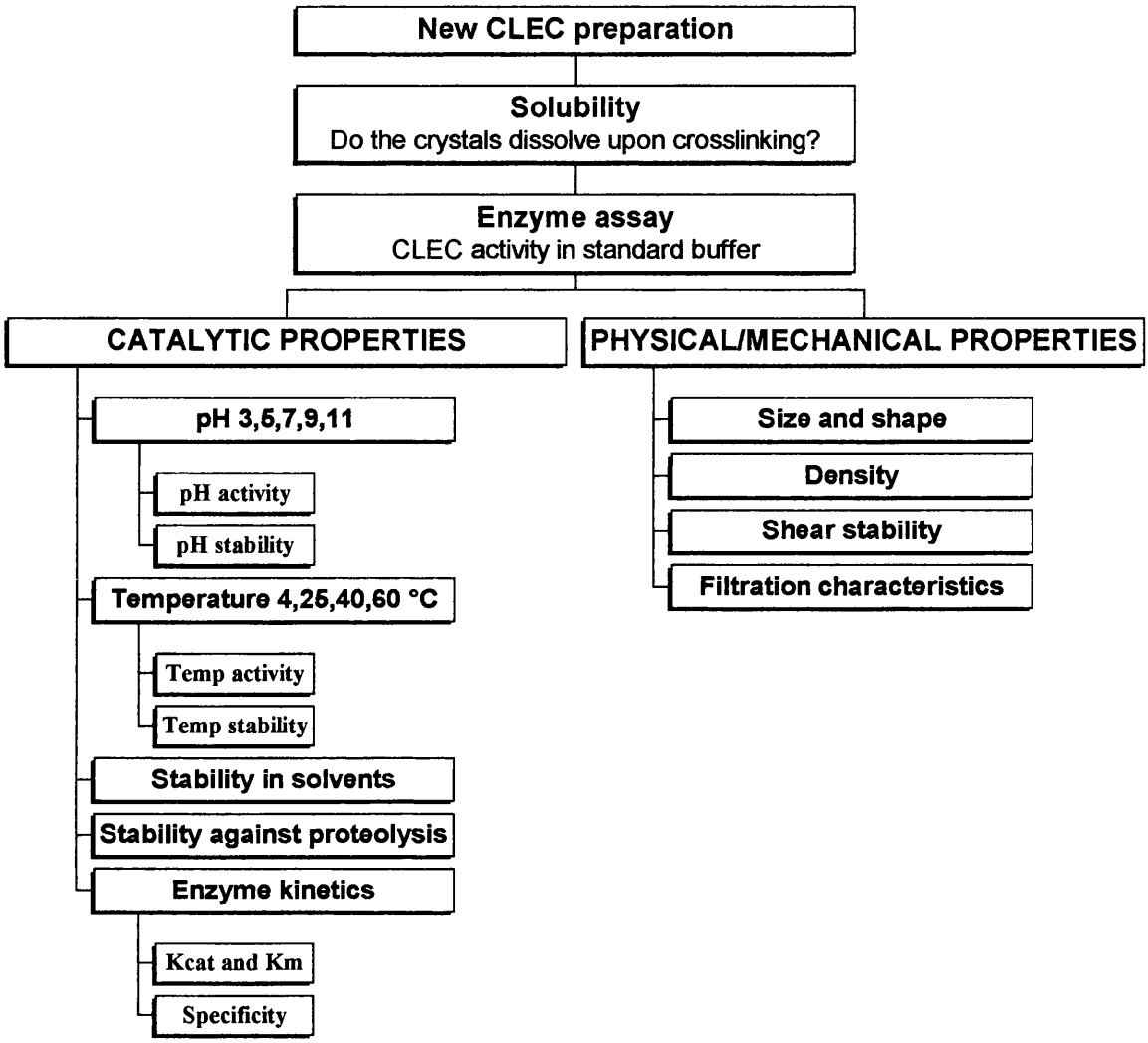

Figure 14: A hierarchy of tests for the characterisation of any batch of CLECs.

Before the CLECs are characterised, they must meet two important criteria. Firstly, the crystals must not dissolve upon cross-linking and secondly, they must have enzymatic activity. After they have met these two criteria, the catalytic and mechanical properties are then studied in more detail (Figure 14).

Firstly, the CLECs are tested for their catalytic activity and stability at different pHs and temperatures. Studying pH identifies the sensitivity of the CLECs to pH change and determines the operating pH range for each crystal form. The importance of studying the change in CLEC stability with temperature is to see if

reactions can be carried out at higher temperatures to increase the enzyme's productivity and whether CLECs can retain their stability at higher temperatures of 40 and 50 °C.

The study of catalytic stability in aqueous/organic mixtures is important since one and two phase mixtures create process options for handling substrate and products which are sparingly soluble in water (Persichetti *et al.*, 1995). These include synthetic reactions which are more favourable in organic mixtures which may otherwise not be thermodynamically feasible in an aqueous environment (Laane *et al.*, 1987). The study of CLEC stability in the presence of proteases in a process is important to see whether they may be applied to a crude preparation containing proteolytic enzymes. Lastly, kinetic properties for CLECs will be determined for both crystal forms to see if the catalytic velocities of CLECs are affected in an immobilised form.

After the batch of CLECs are known to be catalytically stable, the physical and mechanical properties of CLECs are studied to see if they can be applied in a mechanical process by studying its performance under mixing and filtration. At this stage of the hierarchy, the physical properties such as size, shape and density of the CLEC particles are investigated. Filtration studies investigate the filterability of CLECs and the ease of recovery of the particles after a number of cycles.

6.3 Catalytic characterisation of CLECs

After cross-linking the two forms of YADH I crystals- rod and hexagonal, their activities are determined using an enzymatic assay identical to the free enzyme. Before it is worthwhile to apply CLECs in a process, their kinetics have to be studied to show that they are robust catalysts. Some of the process conditions include studying the effects of pH, temperature, solvents and proteases on their activity and stability. The measurements performed on the biocatalyst preparations are in solution.

In each case, initial rates are obtained from the two different crystal forms and the free enzyme. Stability data is presented as CLEC activity (determined by initial rate measurements) versus time where the biocatalyst has been running under process conditions, at different pHs and temperatures, for an extended period of, say, 4 days.

6.4 Mechanical characterisation of CLECs

The physical characterisation of CLECs include the shape, mean size and density of the wet crystalline particle for the two CLEC forms. The physical properties are important when process issues such as abrasion in stirred vessels, the ability to reuse CLECs and the compression behaviour in column systems or filtration operation are studied. These studies show the mechanical stability and integrity of a CLEC in a stirred vessel and filtration device. For the study of CLECs in an agitated vessel, a rotating-disc shear device has been used to study the breakage mechanism of the CLEC biocatalyst. The mean size distribution and activity was measured at the start and after each stirrer speed for each CLEC form. By calculating the energy dissipation needed to break the CLECs in the small-scale device, the damage that may occur in other stirred vessels such as a 6-bladed Rushton turbine may be predicted.

The compression behaviour of CLECs in column systems may be studied using a filtration column device operated at different pressures of 50 to 100 kPa at constant protein concentration (1 $mg.mL^{-1}$) using a 0.2 μm membrane filter. By measuring the slope of t/V (time at constant pressure filtration (s)/ corresponding volume of filtrate obtained (g)) versus V (corresponding volume of filtrate obtained (g)), cake resistance can be calculated. Filtration studies were performed for 5 cycles on both YADH I crystal forms. For each cycle, the membrane resistance, the mean crystal size, activity and protein recovered in the retentate and permeate were calculated.

These experiments are to define the filtration conditions for CLECs as well as to determine their filterability characteristics. By determining the cake resistance (α) as a function of cycle, the time taken to recover the CLECs can be predicted. The cake resistance also shows whether the CLECs are likely to be compressed in a pressurised system. This may be important in the application of CLECs in a packed bed column.

7 CATALYTIC PROPERTIES OF THE TWO YADH I CLEC FORMS

7.1 INTRODUCTION

7.1.1 The importance of catalytic studies for characterisation of YADH I CLECs

Section 5 explored a rational 'windows' approach to the batch production of different forms of YADH I crystals. Cross-linking of the enzyme crystals to form CLECs served to stabilise the crystals under harsh conditions such as high temperatures, extremes of pH and in aqueous-organic mixtures. In this section, the effect of crystal morphology on the catalytic activity and stability of the CLECs was investigated. The catalytic activity and stability of the different crystal forms of the CLECs were also compared to that of the free enzyme. The proposed hierarchy which tested the catalytic properties of each CLEC preparation produced the benchmark data which allowed the various samples to be easily compared.

7.2 METHODS AND MATERIALS

7.2.1 CLEC-YADH I activity assay

The two different CLEC forms (rods and hexagonals) were assayed in the stirred vessel of a Radiometer SAM 90 autotitrator at a fixed impeller speed of 500 rpm. The YADH I assay solution was prepared as described in Section 4.2. The CLEC samples for assay were vortexed to achieve a homogeneous suspension and a 100 µL aliquot was pipetted into 9.9 mL of the YADH I assay solution present in the stirred vessel. 1 mL samples of the reaction mixture were removed after 1, 2, 4, 6, 8, 10 and 12 minutes and their absorbance was read at 340 nm using a DU 640 spectrophotometer (Beckman, USA). The increase in absorbance over time was recorded and used to calculate the YADH I activity expressed as Units.mg^{-1} where 1 unit is the amount in µmoles of NADH formed per minute. $\Delta\in_{340}$ for the reduction of NAD^+ to NADH is 6.22 x 10^{-6} $M^{-1}.cm^{-1}$. Owing to the low concentration of the CLECs present in the reaction mixture the scattering of light in the spectrophotometer cuvette was not significant. The coefficient of variance for this assay was 13%.

YADH I CLEC activity = (Abs 340 $nm.min^{-1}$) / 6.22 x 9.9 /0.1 x 100

Abs 340 $nm.min^{-1}$ = change in absorbance

min = time of reaction

6.22 = μM extinction coefficient of NADH

9.9 = volume in mL of assay mix in the stirred reactor

0.1 = volume in mL of CLEC mixture added to the stirred reactor

100 = dilution factor of CLEC sample in the reactor

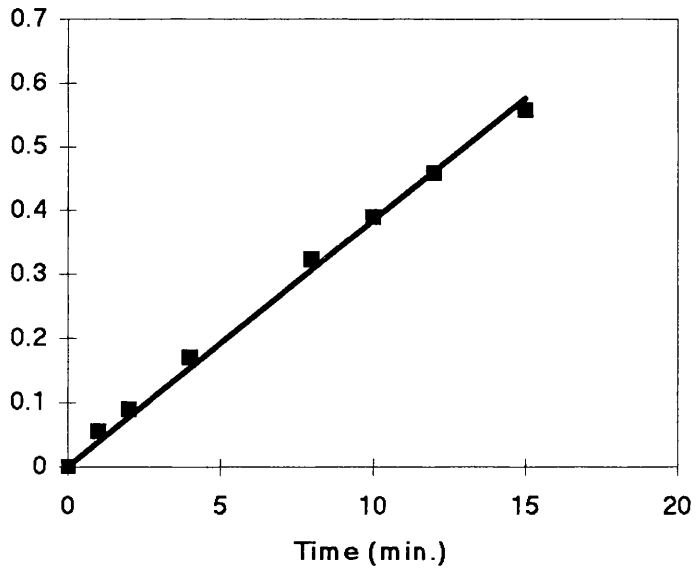

Figure 15: Typical activity assay showing the absorbance at 340 nm versus time for hexagonal YADH I crystals after cross-linking with 0.05 % (v/v) glutaraldehyde. The slope of the line indicates the average rate of change in absorbance.

7.2.2 YADH I crystals protein assay

To determine the concentration of protein present in the crystals before cross-linking, 200 μL of a homogeneous crystal suspension was removed and pipetted into a 1.5 mL Eppendorf tube. The 200 μL mixture was centrifuged down using a Microcentaur bench centrifuge at 8, 000 rpm for 10 minutes and the supernatant was removed. The crystal pellet was then redissolved in 200 μL of 0.1 M potassium phosphate buffer, pH 7.5. The redissolved mixture was diluted 1:10 in a final volume of 100 μL and the suspension was then assayed for protein concentration according to section 4.3. The measured protein concentration was taken to represent the amount of protein initially present in the crystal form and in the CLECs following cross-linking. After cross-linking and washing the crystals, the CLECs were centrifuged and the supernatant was assayed to make sure no residual protein was present. The protein concentration in the CLECs themselves could not be measured directly as they could not be redissolved following the cross-linking with glutaraldehyde.

7.2.3 Protein concentration determination of CLECs using the Lowry procedure

The Lowry method involves two steps of reaction (Lowry *et al.*, 1951). The first is the binding of copper (II) ions under alkaline conditions to the peptide nitrogen of proteins. The second is the copper-catalysed oxidation of aromatic amino acids by the reduction of Folin-Ciocalteau phosphomolybdicphosphotungstic acid to heteropolymolybdenum blue. The blue colour can be detected spectrophotometrically at 660 nm and is sensitive in the range of 0.05-0.5 $mg.mL^{-1}$ protein (Lowry *et al.*, 1951). This method of protein concentration determination was used directly for any batch of CLECs. The Bradford method could not be used for CLEC preparation because the CLEC particles interacted with the dissociated groups of the organic dye Coomassie blue to form coloured precipitates.

Alkaline copper sulphate solution was prepared by mixing 2.5 mL of 0.5 % (w/v) copper sulfate pentahydrate ($CuSO_4.5H_2O$) and 2.5 mL of 5 % (w/v) sodium potassium tartrate (KNa Tartrate). When mixed, the solution was diluted to 100 mL with 0.1 M sodium hydroxide (NaOH) in 2 % (w/v) sodium bicarbonate

(Na_2CO_3). This working reagent was prepared fresh before use. Diluted protein samples to be assayed (0.5 mL) were placed in acrylic test tubes to which the working reagent (2 mL) was added. These were mixed and left for 30 minutes. One part Folin-Ciocalteau phenol reagent was diluted with two parts water. 0.5 mL of diluted Folin-Ciocalteau phenol reagent was then added to each sample and immediately mixed. The colour was allowed to develop for 30 minutes at room temperature after which time the absorbance of the solutions were measured in a DU 640 spectrophotometer (Beckman, USA) at 660 nm. Solutions of known bovine serum albumin concentrations were used for preparation of a calibration curve (0.05-0.5 $mg.mL^{-1}$). The coefficient of variance for this assay was 5 %.

7.2.4 Studying the catalytic stability of YADH I CLECs and free YADH I

7.2.4.1 Variation of activity with pH

The YADH I assay mix was prepared according to section 4.2. and adjusted to pH values of 3, 5, 7, 9 and 11 as required. The activity assays were carried out according to section 7.2.1 for CLECs and section 4.2 for free YADH I respectively at each pH.

7.2.4.2 pH stability

After CLECs were prepared according to section 5.2.3, 500 μL volumes of CLEC suspension (0.5 $mg.mL^{-1}$) and free YADH I (1 $mg.mL^{-1}$) each suspended in 0.1 M Tris-HCl buffer at different pH values (5, 7, 9, 10, 11) were prepared. 100 μL aliquots of CLECs and free YADH I at those different pHs were taken after a time interval of 1 day and assayed using the standard assay conditions mentioned in Sections 7.2.1 and 4.2 respectively. Stability studies were carried out for a period of 4 days.

7.2.4.3 Variation of activity with temperature

Reactions were carried out at temperatures of 4, 25, 40, 50 and 60 °C in a temperature-regulated reaction vessel. A vessel temperature of ± 0.5 °C was maintained by the circulating of water from a temperature-regulated water bath (Grant Instruments, Inc.). Assays for both CLECs and free YADH I were performed under those temperatures.

7.2.4.4 Temperature stability

500 hundred μL volumes of CLEC slurry (0.5 $mg.mL^{-1}$) and free YADH I (1 $mg.mL^{-1}$) in 0.1 M Tris buffer, pH 7 were each incubated separately at temperatures of 25, 40, 50 and 60 °C in a temperature-regulated water bath. 100 μL aliquots of CLECs and free YADH I were taken after a time interval of 1 day and assayed using the standard assay conditions in Section 7.2.1. Stability studies were carried out for a period of 4 days.

7.2.4.5 Stability of YADH I CLECs and free YADH I upon exposure to solvents

7.2.4.5.1 Operation of freeze dryer

The Speed1Vac (Model 30P2) centrifugal freeze dryer (Edwards high vaccuum Ltd.) consisted of three main parts. The three units are the RT 100 refrigerated condensation trap, the speedvac SC100 centrifugal rotor and the VP100 pump. The condensation trap was switched on 45 mintues before use. The samples were placed in the rotor opposite to each other to ensure balance of the rotor. The rotor was then switched on at a medium temperature set at about 40 °C. The pump was then switched on and a vacuum was applied by bleeding the vacuum valve located above the condensation trap. After the samples had been freeze dried, the rotor was turned off and the vacuum was gently turned off before the pump was switched off.

7.2.4.5.2 Solvent stability of YADH I CLECs and free YADH I

Five solvents were initially chosen on the basis of their Log P values for the study of solvent stability. The Log P values of the solvents chosen are indicated in brackets: methanol (-0.76), acetonitrile (-0.33), tetrahydrofuran (0.49), chloroform (1.5) and octanol (2.9) (Laane *et al.*, 1987). CLEC and free YADH I preparations were incubated in 50 % (v/v) solutions of the indicated organic solvents. A 100 µL slurry of CLECs (1 $mg.mL^{-1}$) and free YADH I (1 $mg.mL^{-1}$) both in 0.1 M Tris-HCl buffer, pH 7 were combined with equal volumes of the indicated solvents in an Eppendorf tube. The mixtures were vortexed and incubated for two hours while agitating at room temperature. The solvents were subsequently removed by freeze drying. The CLECs and free YADH I, in a powdered state, were then resuspended in 100 µL buffer and assayed according to Section 7.2.1.

7.2.4.6 Stability of CLECs and free YADH I in the presence of proteases

The CLECs and free YADH I preparations were incubated in presence of Pronase^{R} (Sigma, UK), a non-specific protease. The ratio of the Pronase^{R} concentration to CLEC/ free YADH I concentration was 10 : 1 (on a protein basis). A 250 µL slurry of YADH I CLECs (1 $mg.mL^{-1}$) in 0.1 M Tris buffer, pH 7 was mixed with an equal volume of Pronase^{R} solution (10 $mg.mL^{-1}$) to achieve a total volume of 500 µL. Similarly, 250 µL of free YADH I (2 $mg.mL^{-1}$) in 0.1 M Tris buffer, pH 7 was mixed with an equal volume of Pronase^{R} (20 $mg.mL^{-1}$). Both mixtures were incubated at room temperature and aliquots of 100 µL were removed after time interval of several hours and also after 24 hours. The aliquots were pelleted by centrifugation, washed twice with buffer and then resuspended in 100 µL of buffer. The CLECs and free YADH I were then assayed as described in Section 7.2.1.

7.2.4.7 Variation of activity with substrate concentration

The activities of a slurry of YADH I CLECs and free YADH I were measured against a range of increasing ethanol concentrations: 0.01, 0.02, 0.03, 0.04, 0.05, 0.1, 0.2 and 0.8 M. The concentration of the CLECs was kept constant at each ethanol concentration. Hexagonal CLECs had a concentration of 0.25 $mg.mL^{-1}$ while rod

CLECs had a concentration of 0.5 $mg.mL^{-1}$. The concentration of free YADH I was 0.5 $mg.mL^{-1}$. The NAD concentration was kept constant at 1.8 mM.

Reactions with CLECs and free YADH I were performed under the same conditions as described in Section 7.2.1 and 4.2 respectively. The YADH I reaction mix was prepared in 20 mL volume fresh before the experiment. Each 20 mL YADH I mix contained 0.0239 g of NAD and 0.1127 g of Tris buffer. Volumes of ethanol were added to the assay solution to attain the required concentrations. Distilled water was added to make up the volume to 20 mL and the pH of the solution was adjusted to pH 8.8. A plot of specific activity ($Units.mg^{-1}$) against substrate concentration was constructed to determine the kinetic constants such as k_{cat} and K_m of CLECs and free YADH I for ethanol as substrate. k_{cat} is the turnover number of the enzyme. It relates to the number of substrate molecules converted into product by an enzyme in unit time when the enzyme is fully saturated with substrate. K_m is equal to the substrate concentration at which the reaction rate is half of its maximal value (Piszkiewicz, 1977).

7.3 RESULTS AND DISCUSSION

7.3.1 Temperature activity profile of CLECs compared to free YADH I

Reactions with the CLECs and free YADH I were carried out in a stirred vessel by measuring the NADH production over time at different temperatures. The specific activities ($Units.mg^{-1}$) of both rod and hexagonal CLECs increased significantly as the temperature increased, reaching a temperature optimum of 50 °C and remaining steady at 60 °C (Figure 16 a and b). Temperature profiles for the two crystal forms were similar. The temperature optimum of free YADH I was around 40 °C. Free YADH I, however, did not remain active at temperatures greater than 40 °C and only retained 10 % of its activity at 50 °C in comparison to 40 °C and lost all of its activity at 60 °C (Figure 17). In comparison to free YADH I, both CLEC forms are able to retain their activity at higher temperatures.

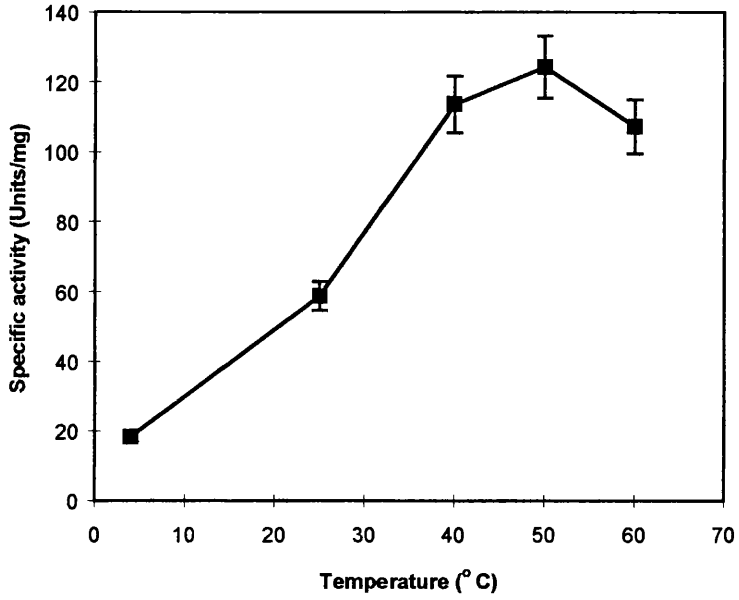

Figure 16 (a): Effect of temperature (°C) on the specific activity of YADH I rod CLECs.

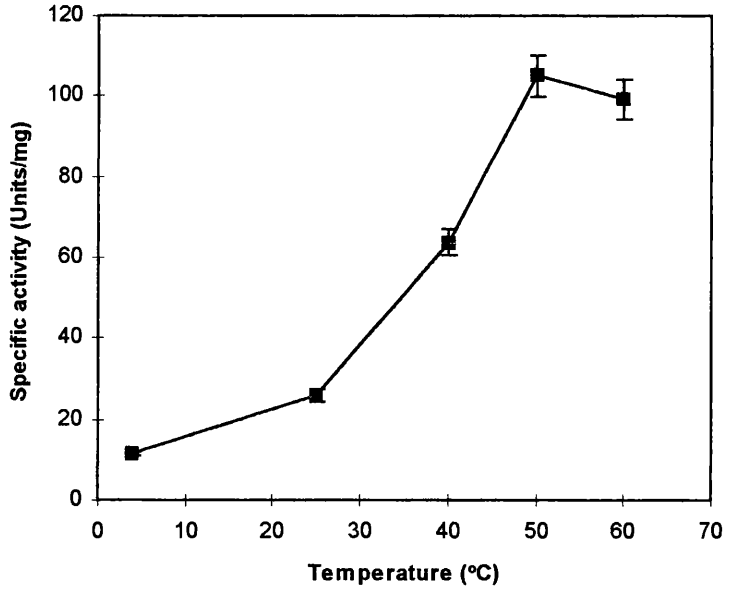

Figure 16 (b): Effect of temperature (°C) on the specific activity of YADH I hexagonal CLECs.

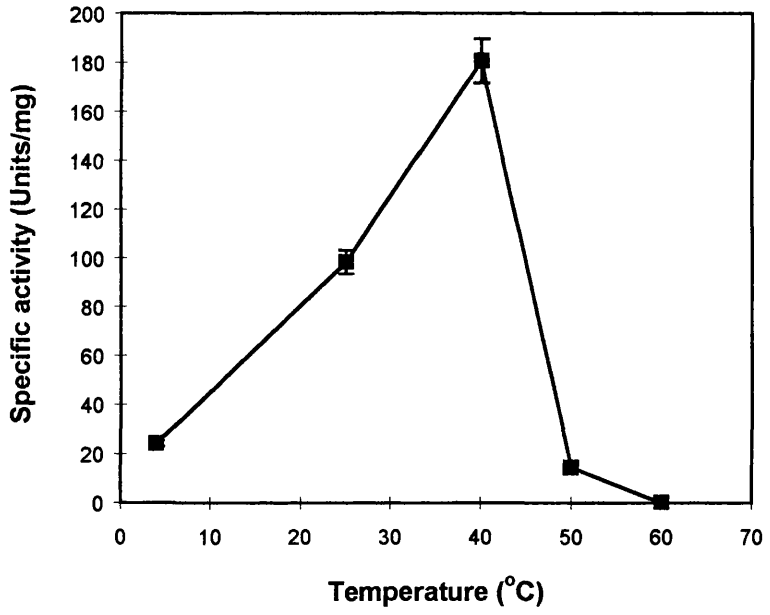

Figure 17: Effect of temperature (°C) on the specific activity of free YADH I.

7.3.2 Temperature stability of CLECs compared to free YADH I

It is also important to identify how stable the CLECs are at temperatures greater than 25 °C in comparison to free YADH I. The specific activities (Units.mg^{-1}) of both CLEC forms and free YADH I were monitored for a period of 4 days at temperatures of 25, 40, 50 and 60 °C.

The rod CLECs were stable at 25 and 40 °C for a period of 4 days in relation to their initial activity (Figure 18a). At 50 °C, the rod CLECs were stable for one day but began to decrease in their activity by the second day, finally retaining only half of their initial specific activity by the fourth day. At 65 °C, the rod CLECs were unstable, only retaining 10 % of their initial activity after the first day and losing all their activity by the third day. The hexagonal CLECs similarly remained stable, maintaining a specific activity of around 80 Units.mg^{-1}, at both 25 and 40 °C for 4 days (Figure 18 b). However, at 50 °C, the hexagonal CLECs still maintained their activity unlike the rod CLECs. The morphological form of the CLECs thus had a significant effect on their temperature stability.

Even though hexagonal CLECs had a lower initial activity of 80 Units.mg^{-1} compared to the rod CLECs' initial activity of 150 Units.mg^{-1}, they still maintained this level of activity after 4 days at 25 to 50 °C. Free YADH I on the other hand remained stable at 25 °C within a period of 3 days. At 40 and 50 °C however, it only retained a third and a tenth of its initial activity respectively after the first day (Figure 19). As observed, both CLEC forms were more stable than free YADH I. Stability might be the result of increased hydrophobic and polar interactions among the protein molecules in the crystalline lattice preventing unfolding (Margolin, 1996).

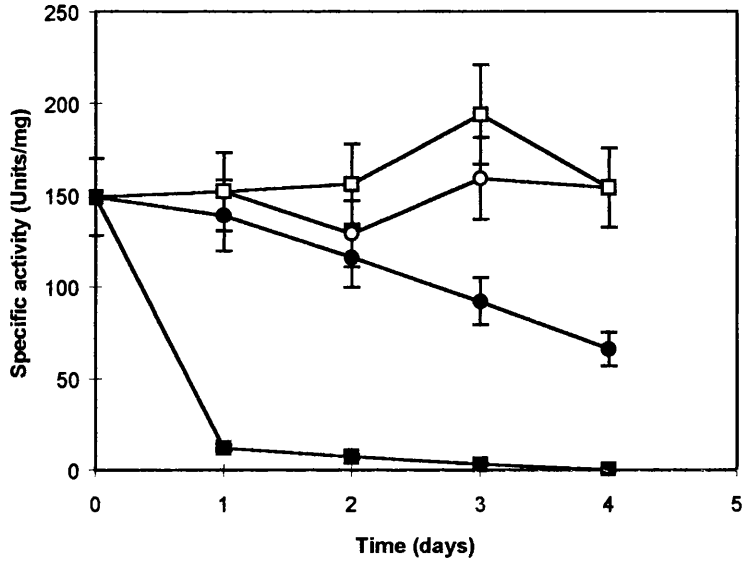

Figure 18(a): Effect of temperature on the specific activity (Units.mg^{-1}) of rod CLECs for a period of 4 days. O, 25 °C, □, 40 °C ,● 50 °C, ■, 65 °C.

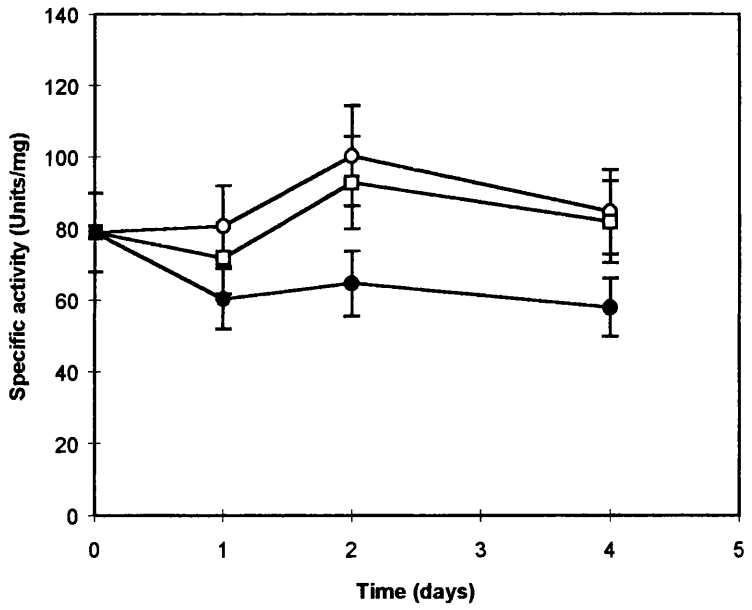

Figure 18(b): Effect of temperature on the specific activity (Units.mg^{-1}) of hexagonal CLECs for a period of 4 days. O, 25 °C, □, 40 °C ,● 50 °C.

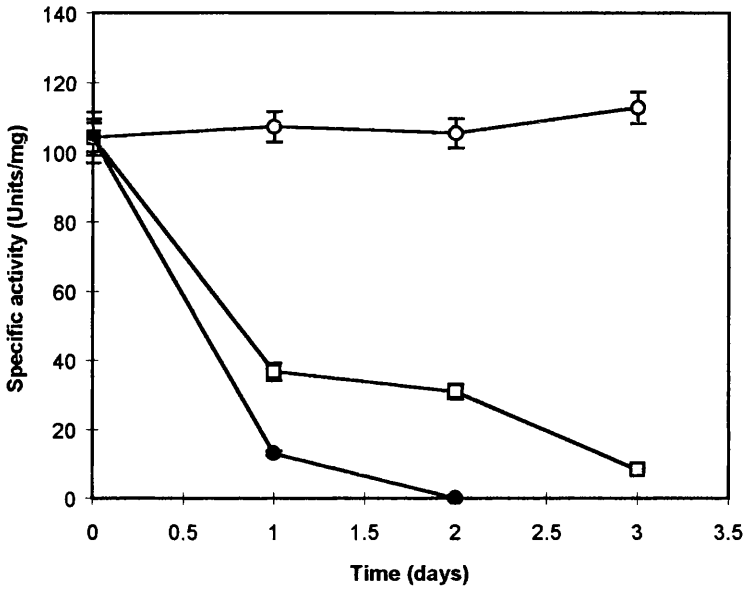

Figure 19: Effect of temperature on the specific activity (Units.mg^{-1}) of free YADH I for a period of 4 days. O, 25 °C, □, 40 °C ,● 50 °C.

7.3.3 pH activity profile of CLECs compared to free YADH I

Reactions with CLECs and free YADH I were carried out in a stirred vessel by measuring NADH production over time at different pHs. The specific activities (Units.mg^{-1}) for both rod and hexagonal CLECs increased significantly as the pH increased from 3 to 11 (Figure 19 a and b). The rod CLECs had a pH optimum around 9, and continued to maintain their activity at pH 11. The specific activity of the hexagonal CLECs gradually increased, remaining active at the higher pH values. The free YADH I, on the other hand, attained a pH optimum of around 9 but showed a decrease in activity as the pH approached 11 (Figure 20). Both forms of CLECs seemed less active than free YADH I at alkaine pHs

7.3.4 pH stability of CLECs and free YADH I

The specific activities (Units.mg^{-1}) of both CLEC forms and free YADH I were monitored for a period of 4 days at pH values of 5 to 11. The rod CLECs were stable at pHs 5, 7 and 9 for a period of 4 days in relation to their initial activity of 150 Units.mg^{-1} (Figure 21 a). However, when the pH exceeded 9, for example at pH 10 and 11, the rod CLECs would dissolve and lose their activity after the first day (data not shown). The difference in pH stability was observed with the hexagonal CLECs (Figure 21 b) when they were exposed to alkaline pHs. Hexagonal CLECs were stable at pH 7 with a specific activity of 80 Units.mg^{-1}. However at pH values of 5, 9, 10 and 11, the CLECs did not redissolve but only maintained a specific activity of around 40 Units.mg^{-1}.

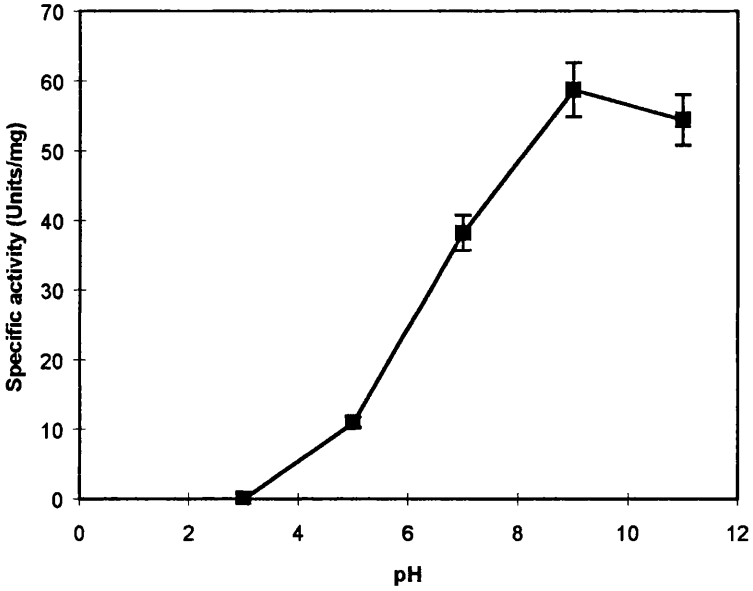

Figure 19(a): Effect of pH on the specific activity (Units.mg^{-1}) of rod CLECs.

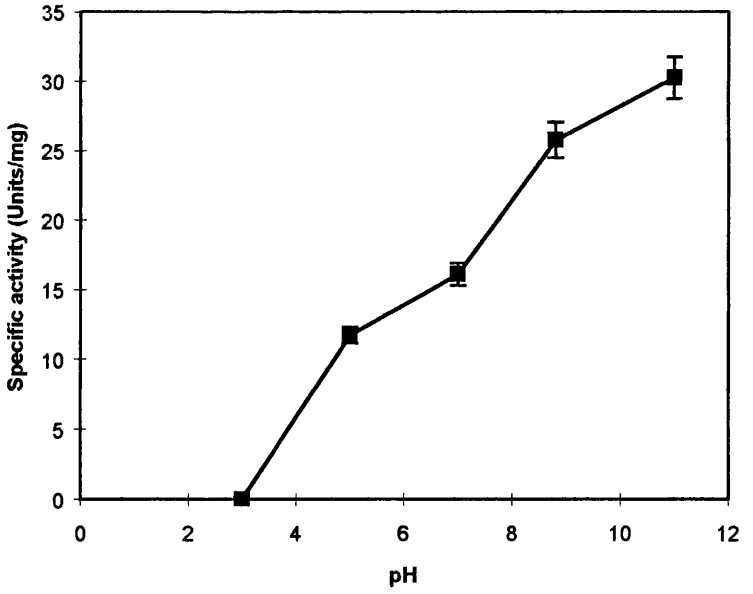

Figure 19(b): Effect of pH on the specific activity (Units.mg^{-1}) of hexagonal CLECs.

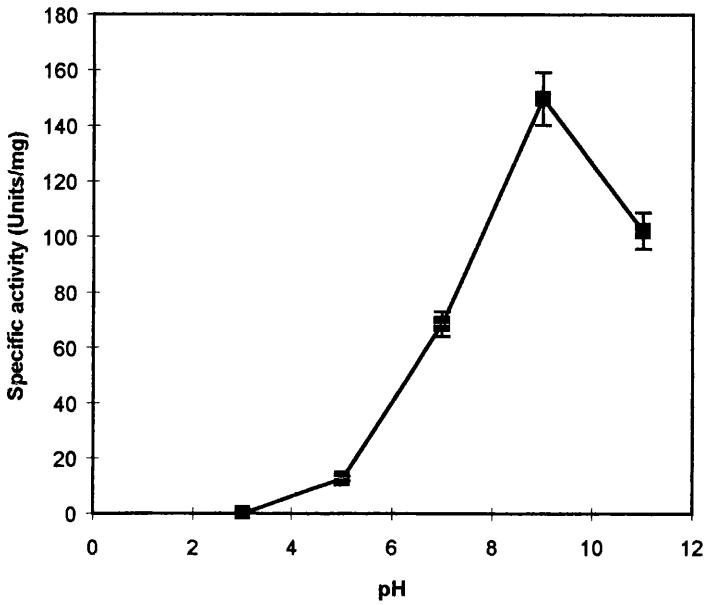

Figure 20: Effect of pH on the specific activity (Units.mg^{-1}) of free YADH I.

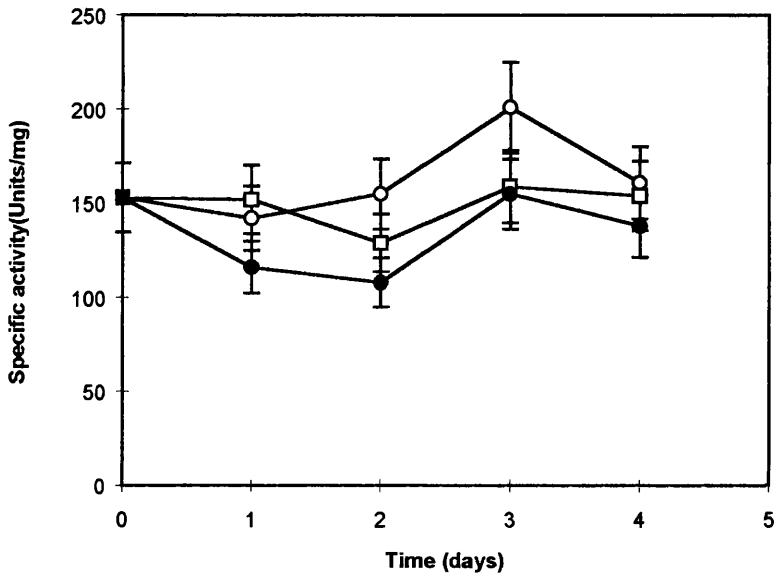

Figure 21(a): Effect of pH on the specific activity (Units.mg^{-1}) of rod CLECs for a period of 4 days. O, pH 5, □, pH 7, ●, pH 9.

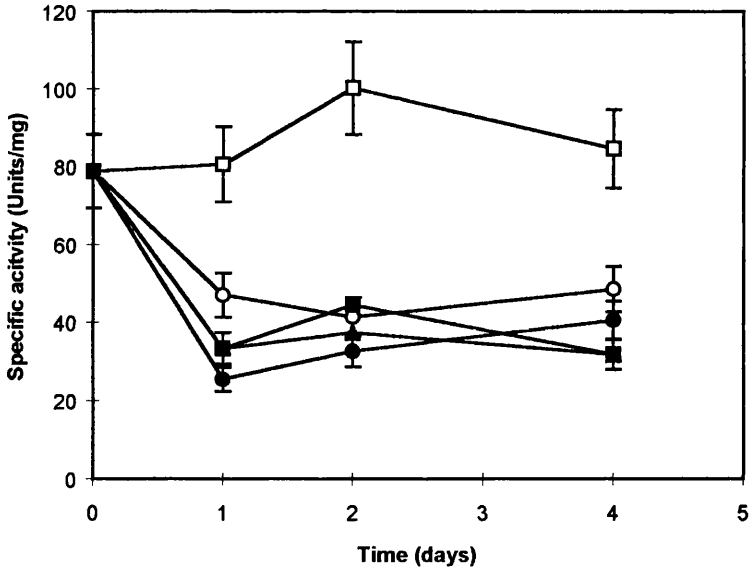

Figure 21(b): Effect of pH on the specific activity (Units.mg^{-1}) of hexagonal CLECs for a period of 4 days. O, pH 5, □, pH 7, ●, pH 9, ■, pH 10, Δ, pH 11.

Similarly, free YADH I remained stable at pH 7 for a period of 3 days. However at pH 5 and 9, it only retained 10 % of its initial activity of 100 Units.mg^{-1} after 1 day and completely lost all activity by the third day (Figure 22). As observed, both CLEC forms are more stable than free YADH I over a wider pH range. The operating pH range from 5 to 9 favours the use of the rod CLECs since they have a higher retained activity of 150 Units.mg^{-1}. However, the operating pH range is wider for hexagonal CLECs in that they can maintain their structural integrity at alkaline pHs of 10 and 11 even though they have a lower retained activity. Therefore the crystal form affects the stability of the CLECs in both acidic and alkaline conditions.

7.3.5 Solvent stability of CLECs and free YADH I

Both forms of CLECs and free enzyme were exposed to five different solvents as described in Section 7.2.4.5.2 for two hours and the percentage retained activity was plotted against the log P of the solvent (Figure 23). High enzymatic activity is generally favoured for higher log P solvents, where the solvent hydrophobicity is greater (Laane *et al.*, 1987). Solvents with higher log P values such as chloroform and octanol are water-immiscible and form a two-phase system with water while polar organic solvents such as acetonitrile and methanol are water-miscible. As shown in Figure 23, both CLEC forms are more stable than free YADH I in polar and hydrophobic solvents.

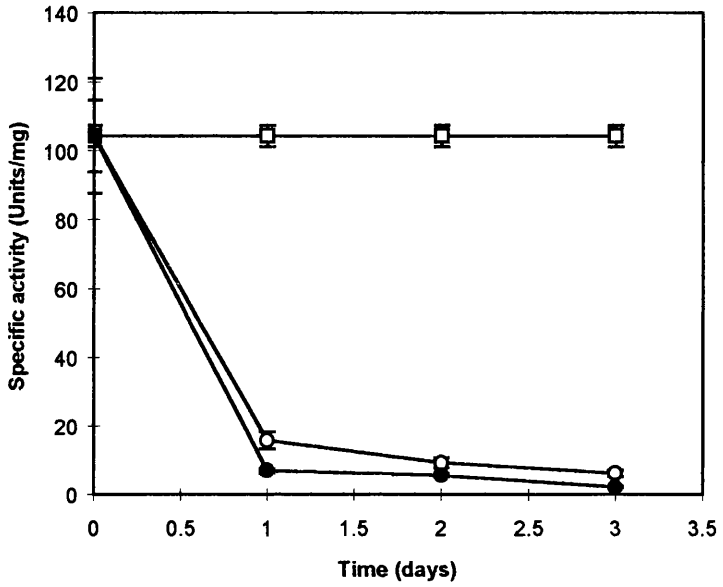

Figure 22: Effect of pH on the specific activity (Units.mg^{-1}) of free YADH I for a period of 3 days. O, pH 5, □, pH 7, ●, pH 9.

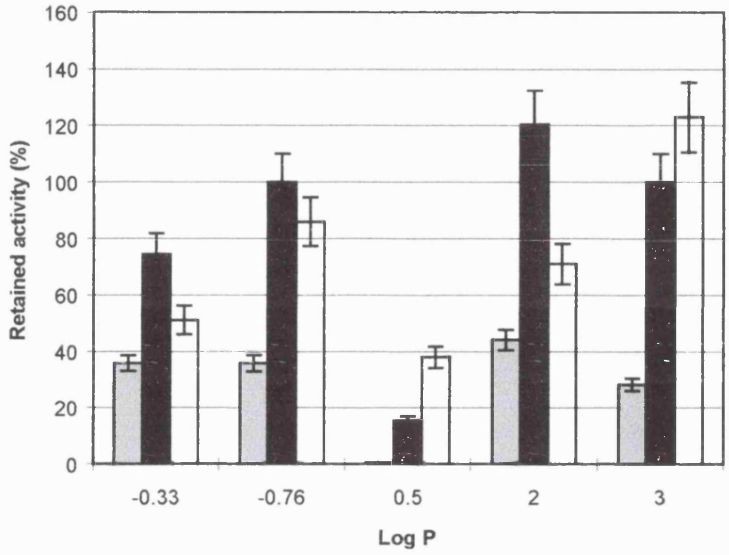

Figure 23: The percent retained activity of rod and hexagonal CLECs and free YADH I with solvent log P. The percent retained activity is the activity after exposure to the solvent relative to the activity in Tris buffer, pH 7. Log P is the logarithm of the partition coefficient in a standard octanol-water two-phase system (Laane *et al.*, 1987). The Log P values of the solvents chosen are indicated as follows: -0.33, acetonitrile, -0.76, methanol, 0.5, tetrahydrofuran, 2, chloroform, 3, octanol. ■, rod CLECs, □, hexagonal CLECs, ■, free YADH I.

The percentage retained activity for both forms of the CLECs was considerably greater in all the solvents tested compared to the free enzyme. No distinction was observed for either the water-miscible solvents (log P –0.33, -0.76 and 0.5) or the water-immiscible ones (log P 2 and 3). Free YADH I, on the contrary, has only managed to retain, in most cases, about 30 to 40 % of its initial activity. The hierarchy of structured tests proposed in Section 5 is useful as it provides a fast, systematic approach in exposing the differences in catalytic activity and stability of the two CLEC forms of YADH I. The hierarchy of tests would also be applicable to test for batch to batch variation.

7.3.6 Proteolytic stability of CLECs and free YADH I

Protease experiments were carried out using Pronase^{R}, a non-specific streptococcal protease capable of digesting proteins to free amino acids (Calbiochem 1990 catalog; LaJolla,CA). Rod CLECs maintained their stability for a period of 6 hours (Figure 24 a) but after 24 hours, they lost their activity completely (data not shown). Hexagonal CLECs maintained their activity for a period of 24 hours (Figure 24 b). Even though, they had a lower specific activity of around 30 Units.mg^{-1}, the hexagonal CLECs proved to be more stable than the rods. Free YADH I in the presence of this protease lost all activity after 40 minutes (Figure 25).

Given the packing of enzyme molecules in a crystalline lattice, one might suggest that the enzyme molecules within a CLEC would be protected from proteolysis and so only those on the surface could be acted upon by the protease. This could be the reason why both CLEC forms are more stable than free YADH I. As shown above, the morphology of the CLEC also seemed to be an important factor in its resistance to proteolysis.

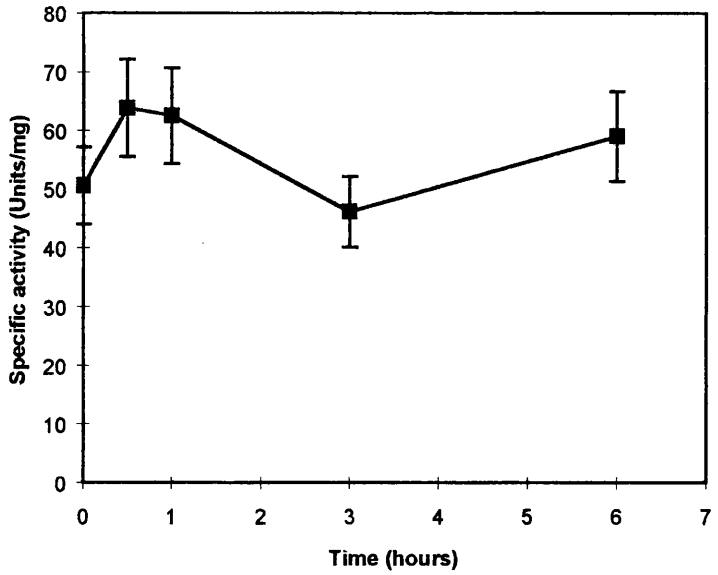

Figure 24(a): Effect of proteases on the specific activity (Units.mg^{-1}) of rod CLECs over 6 hours.

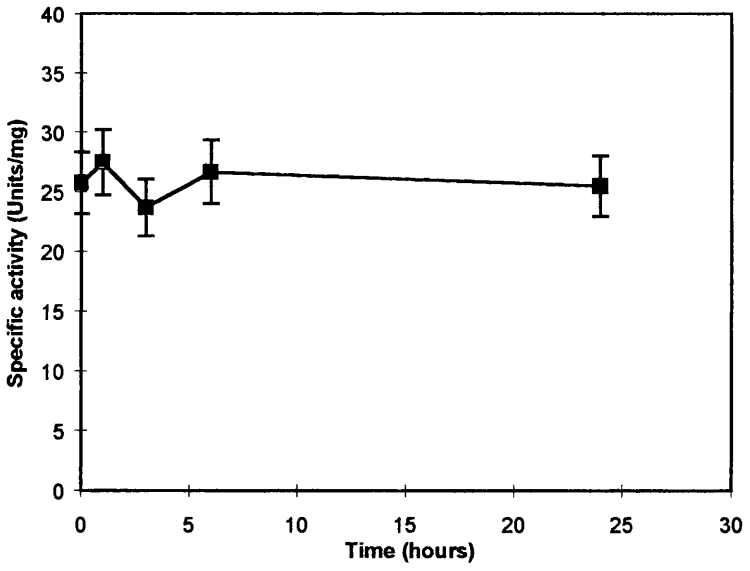

Figure 24(b): Effect of proteases on the specific activity (Units.mg^{-1}) of hexagonal CLECs over 24 hours.

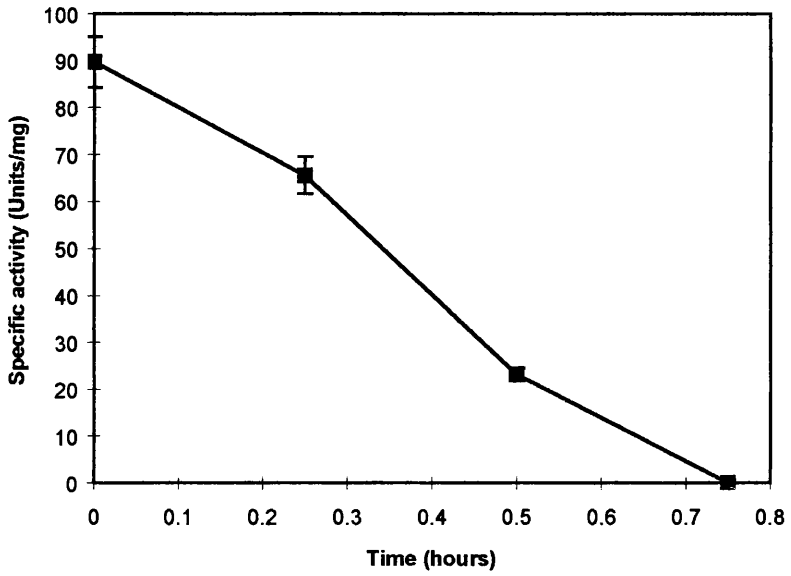

Figure 25: Effect of proteases on the specific activity (Units.mg^{-1}) of free YADH I over 45 minutes.

7.3.7 Variation of activity with substrate concentration

An important parameter to consider when producing an immobilised enzyme such as a CLEC is its catalytic rate. Here, the kinetic parameters of the two forms of CLECs are compared to free YADH I to test whether the enzyme in an immobilised crystalline form is subject to substrate or product diffusional limitations.

Figures 26 (a), (b) and (c) show the variation of specific activity (Units.mg^{-1}) as a function of ethanol concentration for the rod and hexagonal CLECs and free YADH I. Table 5 shows the calculated kinetic constants. These were calculated from Lineweaver-Burk plots of the data shown in Figures 26 (a), (b) and (c). The plots of specific activity versus ethanol concentration for both hexagonal CLEC and free enzyme are very similar. Both hexagonal CLECs and free YADH I have a k_{cat} around 1.5 x 10^3 min^{-1} with K_m values of 20 mM and 15 mM respectively. The K_m value of free YADH I is very close to the one reported in literature (Barman, 1969).

Both hexagonal CLECs and free YADH I have $k_{cat}.K_m^{-1}$ values of 7.5 x 10^2 and 1.0 x 10^3 min^{-1}mM^{-1} respectively. The ratio of $k_{cat}.K_m^{-1}$ is the catalytic velocity

and this value is restricted by the diffusion encounter of enzyme and substrate (Piszkiewicz, 1977). The $k_{cat}.K_m^{-1}$ values of free YADH I and the hexagonal CLECs are similar indicating that the enzyme in an immobilised hexagonal form is not subject to significant substrate diffusional limitation.

The $k_{cat}.K_m^{-1}$ value for rod CLECs was 2.2 x 10^3 $min^{-1}mM^{-1}$ which is double the values of both hexagonal CLECs and free YADH I. Although some of the difference may arise from errors in the colourimetric protein assay applied to the CLECs, the difference in specific activity for the rod CLECs cannot be entirely ascribed to these errors. It is a difference which can be checked with microanalysis of the nitrogen content of the samples.

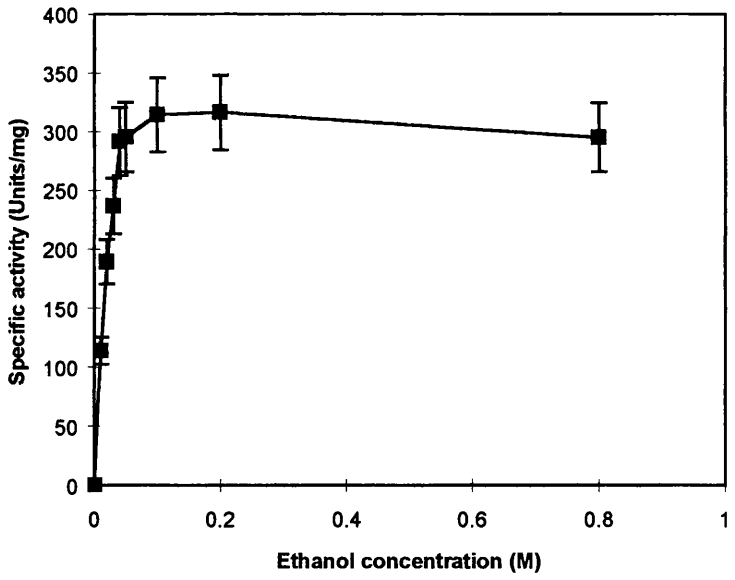

Figure 26(a): A plot of specific activity (Units.mg^{-1}) versus ethanol concentration (M) for rod CLECs.

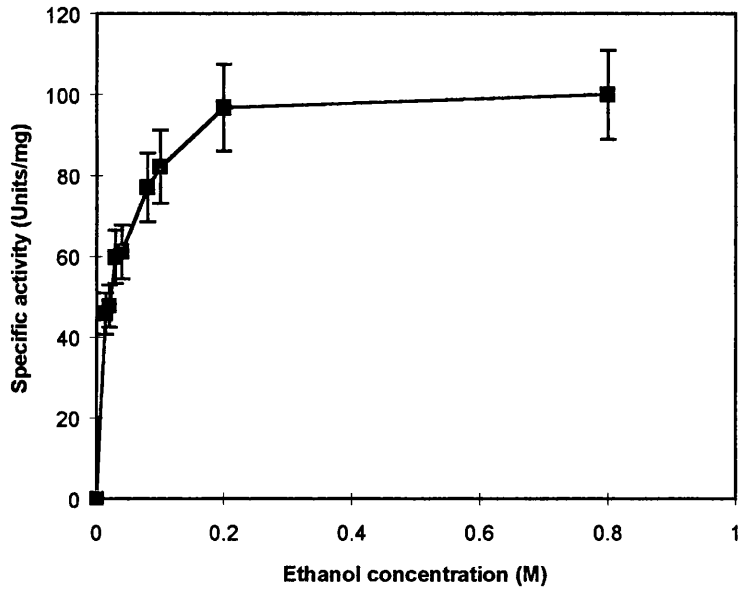

Figure 26 (b): A plot of specific activity (Units.mg^{-1}) versus ethanol concentration (M) for hexagonal CLECs.

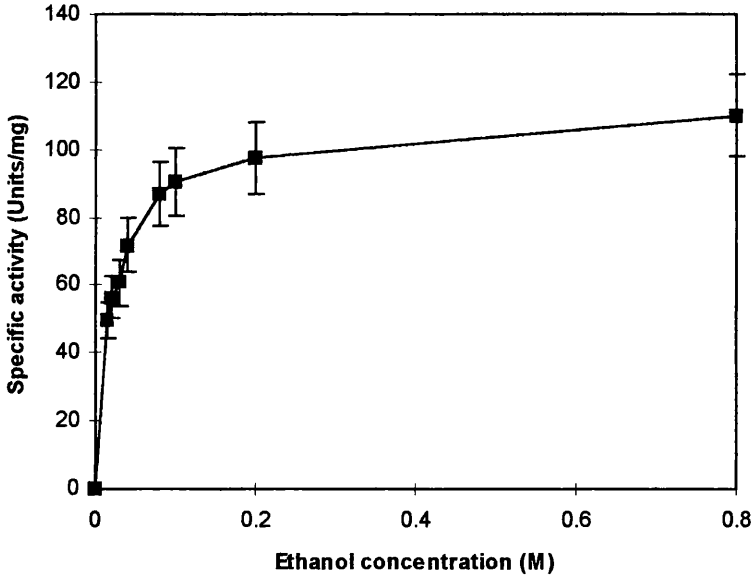

Figure 26(c): A plot of specific activity (Units.mg^{-1}) versus ethanol concentration (M) for free YADH I.

Table 5: Kinetic constants calculated for rod and hexagonal CLECs and free YADH I.

	Rod YADH I CLECs	Hexagonal YADH I CLECs	Free YADH I
V_{max} (Units.mg^{-1})	290	100	100
K_m (M)	0.020	0.020	0.015
k_{cat} (min^{-1})	4.4 X 10^4	1.5 X 10^3	1.5 X 10^3
$k_{cat}.K_m^{-1}$ (min^{-1}mM^{-1})	2.2 X 10^3	7.5 X 10^2	1.0 X 10^3

7.3.8 The effect of solution composition on the stability of the crystal habit

Proteins can be crystallised at constant ionic strength by changes in pH (McPherson, 1990). Where proteins exhibit a number of different solubility minima as a function of pH, each of these minima may afford the opportunity of preparing different crystal forms. For example, in this work hexagonal YADH I crystals are formed at pH 8 (0.1 M sodium phosphate) while rod crystals are formed at pH 7.

It is instructive to note the significance of pH on the growth of the crystal. Salt bridges between protein molecules clearly require protonation of basic residues such as lysine (pK = 10) and arginine (pK = 12) and deprotonation of the acidic groups such as glutamic acid (pK = 4.4) and aspartic acid (pK = 4.4) in order to form. Neutralization of either types of residues, as happened at lower and higher pH values, disrupts those interactions or lessens their rate of formation. It is likely that one method of controlling rapid crystal growth is through careful control of the relative numbers of charged groups and their capacity of engaging in electrostatic interactions (McPherson, 1995).

If crystal growth is the result of reduced electrostatic interactions, then it suggests that the formation of salt bridges is responsible for rapid nucleation leading to showers of microcrystals (McPherson, 1995). This can be seen in the formation of rod YADH I crystals where crystallisation takes place in around 12 hours while the

crystallisation of hexagonal crystals takes 4 days (Section 5.2.1). Hence, the formation of hexagonal plates of YADH I may be the result of other intermolecular interactions such as hydrogen bonding and hydrophobic attraction necessary in maintaining the crystal lattice. If electrostatic interactions are predominant in the core of the rod CLECs, they would be expected to be stable within the the pH range of 5 to 9. This is indeed shown in Figure 21 (a). However, as the pH is increased to more alkaline regions such as 10 and 11, the interactions are weaker due to deprotonation of basic residues resulting in the loss of activity and dissolution. Hexagonal CLECs on the other hand maintain a more stable but lower activity at higher pHs (Figure 21 b) probably due to other interactions (i.e. hydrophobic) which secure the lattice. There are numerous non-polar contacts between side chain residues that could maintain stability of the crystalline YADH I (DeBolle *et al.*, 1995; Xu and Klibanov, 1996).

DeBolle *et al* (1995) have reported that Cys 277 participates in the stabilisation of the tetrameric form of YADH I. In the 3-dimensional model of YADH I, Cys 276 of one subunit could form a disulfide bridge with the Cys 277 of another subunit. The decrease in pH activity of hexagonal CLECs at pHs other than pH 7, as seen in Figure 21 b, may be the result of potential base oxidation of the cysteine residue at higher pHs compared to their sulfhydryl counterparts. The decrease in activity seen at lower pHs, such as 5, may be the result of the protonation of the cysteine residues (pK = 8.5) preventing formation of disulfide bridges to form. However, as mentioned above, the hexagonal CLECs may be secured by other hydrophobic interactions within the lattice which allows them to maintain their activity.

Preliminary crystallographic studies have been performed with YADH I (Ramaswamy *et al.*, 1994) indicating a hexagonal habit with a packing density value, V_m, of 2.9 A^3/ Da. This corresponds to 58 % solvent within the protein channels. The fairly large solvent content allows substrate and buffer component to enter the crystal, possibly making it more susceptible to pH effects. Rod crystals, having stronger electrostatic attraction may have a tighter configuration preventing inactivation at pHs near 7, where basic residues, like lysine and arginine, still retain their positive charge and acidic groups are deprotonated.

7.3.9 The effect of hydrophobicity on the activity of CLECs

It has been demonstrated that water plays the role of a lubricant in enzymes and that it allows enzymes to exhibit the conformational mobility required for optimal catalysis (Almarsson and Klibanov, 1996). Organic solvents lack water's ability to engage in multiple hydrogen bonds and because of their lower dielectric constants, solvents can form stronger electrostatic interaction with proteins (Klibanov, 1997). The highest activity is observed in hydrophobic solvents having higher log P values (log P > 4) (Laane *et al.*, 1987). This is because hydrophobic solvents possess a lesser ability to distort the essential water off the enzyme. Addition of water to the enzyme in anhydrous solvents, or increasing the water activity (a_w), can enhance enzymatic activity by forming hydrogen bonds with the enzyme molecules in organic solvents (Klibanov, 1997; Carrea *et al.*, 1995).

Referring to Section 7.3.5, both of the two crystal forms of YADH I function better than the free YADH I in a variety of mixed organic-water systems. Generally speaking, both hexagonal and rod CLECs retain all their activity in more hydrophobic solvents such as octanol (Log P = 2.9). Tetrahydrofuran, on the other hand, seems to have inhibited both forms of CLECs. It is possible that tetrahydrofuran, being an ether, can form hydrogen bonds with water thereby stripping the essential water off the enzyme and inhibiting its activity. With the exception of tetrahydrofuran, rod CLECs seem more active than hexagonal CLECs in the organic solvents investigated. This could be due to the stabilisation effect via electrostatic interaction of the solvents with the rod CLECs.

The ability of both CLEC forms to be active in lower log P (hydrophilic) solvents allows for the broader application of more solvents for biocatalytic reactions without the need of hydrophilic supports (Laane *et al.*, 1987). One of the remaining challenges would be to understand why CLECs differ in their sensitivity to the nature of the solvent. For example, both forms of CLECs, maintain about 80 % of their activity in higher log P values (i.e. around 3) and low log P values (i.e. around -0.76). However, they are both inhibited in presence of tetrahydrofuran with log P of 0.5.

7.4 Considering diffusion limitations in CLECs

The rate of conversion of a substrate by a suspension of enzyme crystals depends on the rate of diffusion of substrate into and through the crystal, and the rate

of reaction within the crystal (Sluyterman and Graaf, 1969). In large crystals, the substrate would be converted to products near the surface of the enzyme before they have a chance to penetrate into the centre of the crystal. This results in a low activity per mole of enzyme. If the size of the crystals is decreased, then diffusion will no longer be a limiting factor.

This critical size, d_c, (Slyterman and Graaf, 1969) for steady-state conditions equals:

$$d_c = (K_m Di / k_{cat}[E])^{1/2} \quad [3]$$

d_c denotes the smallest diameter of the crystal, K_m and k_{cat} are the Michaelis-Menten parameters of the substrate, Di is the rate of diffusion of substrate inside the crystal and [E] is the free enzyme concentration in moles of enzyme per volume of liquid within the crystal. This correlation between size and $K_m.k_{cat}^{-1}$ is evident in the results presented in Section 7.3.7 with both forms of CLECs using ethanol as the substrate. The rod CLECs, being smaller in size around 5 μm, have a lower $K_m.k_{cat}^{-1}$ ratio of 4.5×10^{-4} while the hexagonal CLEC, being larger around 15 μm, have a higher $K_m.k_{cat}^{-1}$ ratio of 1.3×10^{-3}. Hence, diffusional problems are reduced when the crystal size is also reduced. However, even though the hexagonal YADH I CLECs have a slightly lower $k_{cat}K_m^{-1}$ than free YADH I and rod CLECs, they are a lot more stable and robust over a wider range of experimental conditions.

7.5 CONCLUSIONS

The catalytic activity and stability of CLECs are tested by using a series of hierarchial tests to determine the robustness of the enzyme CLECs in comparison to free enzyme. These include exposure to different temperatures, pHs, Log P solvents, protease and determining their kinetic properties. The experiments have shown that the two forms of the YADH I CLECs exhibit significant differences in their catalytic activity and stability over a range of experimental conditions. Although the free enzyme has been shown to have a higher initial activity, it was shown to be significantly less stable than the two CLEC forms. It seems that the crystal form has a significant effect on the catalytic activity and stability of the CLECs. Several factors affecting the crystal form are solution composition such as pH and the internal molecular interactions (i.e. hydrophobic, electrostatic, disulfide bonding) within the crystal. The hexagonal YADH I CLECs have been shown to be more stable than the rod YADH I CLECs. The hexagonal CLECs, being the larger crystal form, have a lower catalytic velocity ($k_{cat}.K_m^{-1}$) and specific activity than both the rod CLECs and free YADH I

8 MECHANICAL STABILITY OF CROSS-LINKED ENZYME CRYSTALS

8.1 Introduction

8.1.1 The importance of studying the mechanical properties of CLECs

For the industrial application of CLEC biocatalysts an understanding of their mechanical properties is important in relation to process design and operation. The CLECs must be able to withstand the shear forces associated with processing equipment such as stirred-tanks, cross-flow microfilters and pumps which can cause particle attrition and fragmentation. Shear rates can vary from 10^2 - 10^7 s^{-1} depending upon the design and operation of the equipment (Levy *et al.*, 1999). Synowiec *et al* (1993) have shown that two general mechanisms may be responsible for break up of the particles: (i) collision and (ii) fluid turbulence. Within a stirred vessel, the first may occur as a result of crystal-crystal collision, crystal-impeller impact or crystal-vessel impact. Turbulence, on the other hand, relates to the fluid-induced stresses that act on particles. A large amount of work has been performed based on the theory of isotropic turbulence developed by Kolmogorov (1941). Eddies with a size comparable to the size of the dispersed particles induce shear, surface drag and pressure forces as they flow across the particles causing breakage. Eddies larger than the particles, however, tend to entrain the particles causing very little surface stress (Shamlou and Titchener-Hooker, 1993).

Previous work has examined the rate of breakage of inorganic crystals (potassium sulphate and potash alum) in order to predict effects associated with crystal-impeller collisions or turbulent fluid drag-induced attrition (Synowiec *et al.*, 1993). The aim of the current work was to investigate the mechanical stability of YADH I CLECs in dilute agitated suspensions in order to determine the mechanism and rate of crystal breakage in relation to large scale biocatalysis applications involving stirred-tank reactors. A scale-down shear device consisting of a flat rotating-disc in a cylindrical chamber was used to study crystal breakage over a range of energy dissipation rates.

8.2 THEORY

8.2.1 Crystal breakage in turbulently agitated suspensions

Models describing the mechanism and rate of crystal breakage in turbulently agitated suspension have previously been described (Synowiec *et al.*, 1993) and will be only briefly reviewed here. The models assume that breakage of the particles is affected by two opposing factors, namely, the mechanical strength of the crystal and the applied breaking forces. Breakage can occur by two different mechanisms. Attrition is a process by which fines are removed from the surface of the crystal resulting in a gradual decrease in size. Fragmentation, on the other hand, causes a rapid disappearance of the parent particles as they are broken down into smaller entities. The total rate of crystal breakage by attrition is given by:

$$\left.\frac{dn_e}{dt}\right|_{tot} = \left.\frac{dn_e}{dt}\right|_{imp} + \left.\frac{dn_e}{dt}\right|_{turb} \qquad [4]$$

where the total rate of fines generated in an agitated vessel is equal to the fines resulting from impact ($\left.\frac{dn_e}{dt}\right|_{imp}$) and those resulting from turbulent fluid forces ($\left.\frac{dn_e}{dt}\right|_{turb}$). These two components are considered further in the following sections.

8.2.1.1 Impact attrition

The attrition rate due to *crystal-impeller impact* was assumed to be affected by five factors (Synowiec *et al.*, 1993): (i) the stirring intensity, f_{st} (ii) impact energy applied per unit energy needed to produce an attrition fragment from the parent crystal (E_{ci}/e_{ci}) (iii) the target efficiency, η_T, which is the probability of impact of a crystal with an impeller (Metzner and Otto, 1957) (iv) the mechanical properties of

the crystal and stirrer and (v) the total number of parent particles within the vessel, n_c. The rate of attrition of crystals due to impact with the impeller can be expressed as:

$$\left.\frac{dn_e}{dt}\right|_{ci} = f_{st}(E_{ci} / e_{ci})\eta_T m n_c \qquad [5]$$

Synowiec *et al* (1993) derived relationships for all the terms in Equation [5] and obtained the following final equation:

$$\left.\frac{dn_e}{dt}\right|_{ci} = \frac{\pi^2}{2} k_v L^3{}_o \rho_c \frac{Q_o}{P_o} \varepsilon \eta_T \left(\frac{1+\sigma_c}{1+\sigma_{st}} \frac{Y_{st}}{Y_c}\right) \frac{n_c}{e_{ci}} \qquad [6]$$

Equation [6] suggests a linear dependence of impact attrition rate on the power input, ε.

The attrition rate due to *crystal-crystal collision* was considered to be affected by three factors (Synowiec *et al.*, 1993): (i) the crystal-crystal collision frequency, f_{cc} (Ottens and deJong, 1973) (ii) the crystal-crystal impact energy per unit energy needed to produce an attrition fragment, (E_{cc}/e_{cc}) and (iii) the total number of parent particles within the vessel, n_c. The rate of attrition of crystals due to crystal-crystal impact was expressed as:

$$\left.\frac{dn_e}{dt}\right|_{cc} = f_{cc}\left(E_{cc} / e_{cc}\right) n_c \qquad [7]$$

From Equation [7], the following expression was derived for the rate of attrition (Synowiec *et al.*, 1993):

$$\left.\frac{dn_e}{dt}\right|_{cc} = K_2 L_o{}^8 \varepsilon^{3/2} n^2{}_c \qquad [8]$$

Equation [8] indicates a 1.5 order dependence of the attrition rate on power input.

8.2.1.2 Turbulent attrition

The break-up of crystals as a result of the action of *fluid-induced forces* in turbulent eddies is dependent on three factors: (i) the frequency of eddies, f_e (Levich, 1962) (ii) the drag and shear components of turbulent energy measured in proportion to the energy required to generate an attrition particle either through drag (E_d/e_d) or through shear (E_s/e_s) forces, and (iii) the total number of parent crystals, n_c. The turbulent attrition rate is defined by Equation [9] (Synowiec *et al.*, 1993) from which Equation [10] can be derived:

$$\left.\frac{dn_e}{dt}\right|_{turb} = f_e\left(\frac{E_d}{e_d}+\frac{E_s}{e_s}\right)n_c \qquad [9]$$

$$\left.\frac{dn_e}{dt}\right|_{turb} = 0.258k_v L_o^{\,8}\left[\frac{\varepsilon}{\nu}\right]\left[2.55x10^{-2}L_o^{\,2}\Delta\rho\left[\frac{\varepsilon}{\nu}\right]^{1/2}\frac{1}{e_d}+\frac{\mu}{e_s}\right]n_c$$

[10]

Equation [10] indicates a 1-1.5 order dependence of the turbulent attrition rate on the energy input, ε, whereby a first order dependence would signify attrition due to shear, while a 1.5 order dependence would demonstrate attrition as a result of drag forces within the vessel.

8.2.2 Energy dissipation rate in the rotating-disc chamber

The rotating-disc shear device used in this work consists of a rotating-disc within a closed, air-tight cylindrical chamber (Levy *et al.*, 1998). The tip velocity, v_∞, of flow over the disc of diameter, R, can be analysed using the Navier-Stokes equations (Levich, 1962; Schlichting, 1979; Wang, 1992; Cherry and Papoutsakis, 1986). Wang (1992) has previously applied these to the steady-state condition of a rotating-disc of angular velocity, ω, to derive equations for shear stress, τ, torque, T, power, P and energy dissipation rate per unit mass, ε, as a function of rotational speed of the device, N. The disc Reynolds number is given by:

$$\mathrm{Re}_{disk} = \frac{\omega R^2}{\nu} \qquad [11]$$

where ν is the kinematic viscosity of the continuous phase fluid. The transition point from laminar to turbulent flow, according to Schlichting (1979), occurs at a disc Reynolds number of $3x10^5$.

For rotational speeds at which the Reynolds number is below $3x10^5$, representing the conditions of interest to the current work, the shear stress, τ, shear rate, γ, torque, T, power input, P, and energy dissipation rate per unit mass, ε, are given by Equations [12] to [16] respectively.

$$\tau_{max} = 0.332 \mu v_\infty \left[\frac{v_\infty}{\nu x}\right]^{1/2} \qquad [12]$$

$$\gamma = \frac{\tau}{\mu} \qquad [13]$$

$$T = 0.664 \mu \pi v_\infty \left[\frac{v_\infty}{\nu}\right]^{1/2} \left[\frac{16R^{5/2}}{15}\right] \qquad [14]$$

$$P = 2\pi NT \qquad [15]$$

$$\varepsilon = \frac{P}{\rho v} \qquad [16]$$

This energy is either dissipated through the whole body of the liquid or in the boundary layer. The boundary layer is a region close to the disc in which the energy dissipation is the greatest. Although a very high level of turbulent energy is created in the small volumes of liquid close to the rotating-disc, the average energy dissipated per unit volume of liquid is about two orders lower than this. The volume of the boundary layer is the liquid volume within which the energy dissipation given by Equation. [17] occurs. This volume can be obtained using (Schlichting, 1979):

$$V = 2\pi\left[5R^2\left(\frac{vR}{v_\infty}\right)^{1/2} - \frac{10Rv_\infty}{3v}\left(\frac{vR}{v_\infty}\right)^{3/2} + \left(\frac{vR}{v_\infty}\right)^{5/2}\left(\frac{v_\infty}{v}\right)^2\right] \qquad [17]$$

Finally, the length scale of turbulence is also a critical factor in the breakage of the crystals. The size of the Kolmogorov microscale of turbulence (λ) is given by (Shamlou and Titchener-Hooker, 1993):

$$\lambda = \left(\frac{v^3}{\varepsilon}\right)^{1/4} \qquad [18]$$

In the current investigation the rotational speed of the disc was varied between 4, 000 and 27, 000 rpm. Average values of the physical and hydrodynamic parameters of the system, based on the entire liquid volume of the chamber, calculated according to Equations [11] to [18] are shown in Table 6. The maximum values of the parameters, based on the volume of the liquid boundary layer surrounding the rotating-disc are shown in Table 7.

Speed (rpm)	ω (rad.s^{-1}) (x10^3)	Re_{disk} (x10^5)	τ_{ave} (N.m^{-2}) (x10^3)	γ_{ave} (s^{-1}) (x10^6)	T_{ave} (N) (x10^{-2})	P_{ave} (W) (x10^1)	ε_{ave} (W.kg^{-1}) (x10^3)	λ_{ave} (μm)
4, 000	0.42	0.92	0.085	0.085	0.060	0.025	0.022	15
10, 000	1.0	2.3	0.33	0.33	0.23	0.25	0.22	8.2
15, 000	1.6	3.5	0.61	0.61	0.43	0.68	0.60	6.4
20, 000	2.1	4.6	0.95	0.95	0.67	1.4	1.2	5.3
24, 000	2.5	5.5	1.2	1.2	0.87	2.2	2.0	4.8
27, 000	2.8	6.2	1.5	1.5	1.0	3.0	2.6	4.4

Table 6. Average values of the physical and hydrodynamic parameters within the chamber of the rotating-disc shear device. Values calculated taking the density, ρ, and viscosity, μ of the liquid as 980 kg.m^{-3} and 0.001 Pa.s respectively.

Speed (rpm)	τ_{max} (N.m^{-2}) (x10^3)	γ_{max} (s^{-1}) (x10^6)	T_{max} (N) (x10^{-2})	P_{max} (W) (x10^1)	$V_{boundary}$ (m^3) (x10^{-7})	ε_{max} (W.kg^{-1}) (x10^5)	λ_{max} (μm)
4, 000	0.095	0.095	0.096	0.040	1.9	0.022	4.6
10, 000	0.37	0.37	0.38	0.40	1.2	0.34	2.3
15, 000	0.69	0.69	0.69	1.1	0.96	1.2	1.7
20, 000	1.1	1.1	1.1	2.2	0.83	2.8	1.4
24, 000	1.4	1.4	1.4	3.5	0.76	4.7	1.2
27, 000	1.7	1.7	1.7	4.8	0.72	6.8	1.1

Table 7. Maximum values of the physical and hydrodynamic parameters within the boundary layer of the rotating disc shear device. Values calculated taking the density, ρ, and viscosity, μ of the liquid as 980 kg.m^{-3} and 0.001 Pa.s respectively.

8.3 MATERIALS AND METHODS

8.3.1 Crystallisation and cross-linking

Different crystal forms of YADH I were prepared as previously described (Lee *et al.*, 1999a). The rod-shaped CLECs were crystallised at a protein concentration of 14 $mg.mL^{-1}$, 12 % (v/v) PEG 4000 and pH 7 while the hexagonal-shaped crystals were prepared at a protein concentration of 12 $mg.mL^{-1}$, 10 % (v/v) PEG 4000 and pH 8. Both types of crystal were crystallised in the presence of 2 mM β-nicotinamide adenine dinucleotide (β-NAD) in 50 mM Tris-HCl buffer, instead of phosphate buffer, at the appropriate pH in a total liquid volume of 300 mL. A 200 μL seed crystal suspension was used to seed each of the 300 mL batches; these had previously been prepared at a 5 mL scale under similar crystallisation conditions for each of the required crystal forms. The 300 mL batches were then gently stirred on a Vibrax vibrating platform (Janke & Kunkel GmbH, Germany) at 100 rpm and room temperature for 3 days. Previous experiments have shown that the crystallisation process was complete after this time (Lee *et al.*, 1999).

Before being cross-linked, the crystals in the 300 mL batches were first allowed to settle overnight. 3 mL of a 5 % (v/v) aqueous solution of glutaraldehyde was then added and the crystals were cross-linked at room temperature with gentle shaking for 2 hours. After cross-linking was complete, both forms of CLECs were then centrifuged for 1 hour at 1, 000 rpm in a Beckmann J2-M1 centrifuge and the supernatant was removed. The crystals were washed once in 300 mL of 50 mM Tris buffer, pH 8, and then resuspended in the same buffer volume and stored at 4°C until required.

8.3.2 Rotating shear device experiments

The rotating-disc shear device consisted of a rotating-disc in a sealed perspex chamber as shown in Figure 27, and was designed and built in-house (Levy *et al.*, 1998). This had previously been used to study the shear sensitivity of a range of

biological materials including protein precipitates (Boychyn *et al.*, 1999) and plasmid DNA (Levy *et al.*, 1998; Levy *et al*, 1999). The disk was driven by a high speed motor (Groupher Speed 500 BB Race, UK) connected to a battery which was charged continuously by a power supply (RDP transducer E 308). The shear device consisted of an 11 mL total volume chamber with 1.5 mm diameter inlet and outlet ports on the top and bottom covers (not shown in Figure 27) for adding and removing samples. The diameter and height of the chamber were 4 and 1 cm respectively, while the diameter and thickness of the disc were 3 and 0.1 cm respectively. The disc was mounted 0.4 cm from the base of the chamber. The energy dissipation generated as shown in Tables 6 and 7 increased as a function of the rotational speed of the motor.

Before each experiment the chamber was washed with 20 to 30 mL of fresh distilled water. About 10 mL of a CLEC suspension, at the desired concentration, was used to fill the chamber and the inlet and outlet lines were pinched off with clips in order to prevent air from entering. The sample was sheared for a pre-determined length of time at a fixed speed. After shearing the contents of the chamber were carefully removed and analysed for particle size distribution or activity as required. All experiments were performed in triplicate.

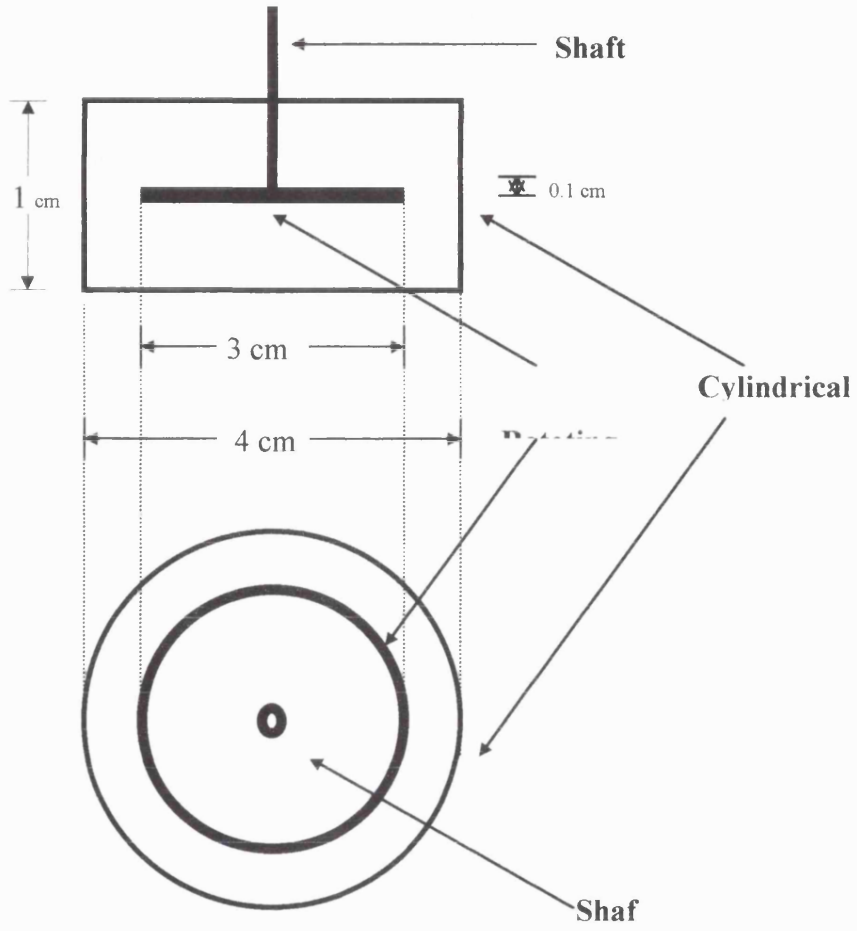

Figure 27: Schematic diagram of the rotating shear device.

8.3.3 Determination of crystal density

The densities of both forms of CLECs were determined using Percol density gradients (Pharmacia Biotech, UK) with appropriate marker beads of specified density (Pharmacia Biotech, UK). 10 mL of a diluted Percol solution was prepared in each of two centrifuge tubes by mixing 5.0 mL Percol (1.1 $g.mL^{-1}$), 1 mL of 1.5 M NaCl and 4.0 mL of distilled water. 20 μL of the coloured marker beads were added to one tube while 50 μL of a CLEC suspension was added to the other. Both tubes were then spun in a Beckmann J2-M1 centrifuge at 10, 000 rpm for 40 minutes. The density of the CLECs was then determined by comparing their settled distance from the meniscus with the distance travelled by the coloured marker beads of known density. All density determinations were performed in triplicate. The coefficient of variance was 2.0%.

8.3.4 Determination of crystal size distribution

The size distribution of CLECs before and after shearing was determined using an Elzone 282 PC particle size analyser. The technique determines the number and size distribution of particles suspended in an electrolyte solution as they pass through an orifice. The changes in electrical impedance as particles pass through the orifice produces pulses whose amplitudes are proportional to the volume of the particles. The amplified pulses are sized and counted and from this data the particle size distribution can be determined. Cumulative crystal size distribution curves are produced by plotting the percentage of particles by volume having particle diameters equal to or less than a given particle size as a function of the particle size itself. These curves clearly show any shift to smaller particles as a result of breakage due to shear.

Crystal breakage is also evident from the rate of change of the median particle diameter. This diameter characterises a particle whose diameter is equal to or less than 50 % of the total population of particles. The data is plotted as a dimensionless ratio (d_{50}) which compares the median diameter after a fixed period of shearing (3, 4,

5, 10 seconds) to the median diameter for the unsheared particles. The initial slope of the curve represents the initial breakage rate.

The crystals to be analysed were suspended in a stirred electrolyte solution consisting of 1.3 % (w/v) lithium chloride buffered to pH 4 using acetic acid. The electrolyte solution also contained 0.01 % (w/v) sodium azide and was filtered through a 0.2 μm cellulose nitrate membrane (Whatman, Inc.) to remove any other particles before use. In all experiments a 95 μm orifice was used to record the raw data (the operating range of each sensor was around 2 to 60 % of the orifice diameter). All measurements were performed in triplicate. The coefficient of variance for the measurement of sheared and unsheared CLECs was 7.5%.

8.4 RESULTS AND DISCUSSION

8.4.1 Physical properties of YADH I crystals

The physical properties of the YADH I CLECs are summarised in Table 8. Photographs of the hexagonal and rod-shaped CLECs immediately after manufacture, *i.e.* before being exposed to shear, are shown in Figure 28 (a) and Figure 28 (b) respectively. As previously found it is clear that the size and morphology of the CLECs are strongly dependent on the crystallisation conditions (Lee *et al.*, 1999). Both crystal forms, have a density of about $1.1x10^3$ kg.m^{-3}.

Crystallisation conditions	12 mg.mL^{-1} YADH I, 10% (w/v) PEG 4000 pH 8	14 mg.mL^{-1} YADH I 12 % (w/v) PEG 4000 pH 7
CLEC morphology	Hexagonal	Rod
Median size (μm)	12 ± 1.0	4.6 ± 0.7
Density (kg.m^{-3})	$1.10x10^3 \pm 0.002$	$1.09x10^3 \pm 0.003$

Table 8. Physical properties of YADH I CLECs as a function of crystallisation conditions.

8.4.2 Breakage of cross-linked crystals as a function of disc rotational speed

The mechanical stability of the CLECs plays an important role in determining whether or not breakage will occur under a given set of operating conditions in a stirred vessel. Quantifying the extent of breakage and understanding the mechanism responsible for this will be of importance in relation to the industrial application of CLEC technology. Figures 29 and 30 show the cumulative size distributions (undersize) of hexagonal-shaped and rod-shaped CLECs respectively before and after subjecting the sample to shear (data only shown at four rotational speeds for clarity). The shearing experiments for hexagonal CLECs (Figure 29) indicate a significant

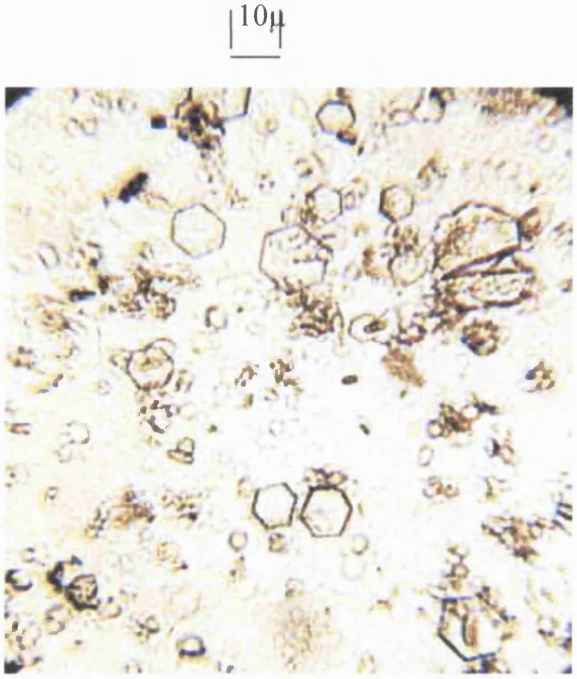

Figure 28(a): Hexagonal YADH I CLECs before shearing.

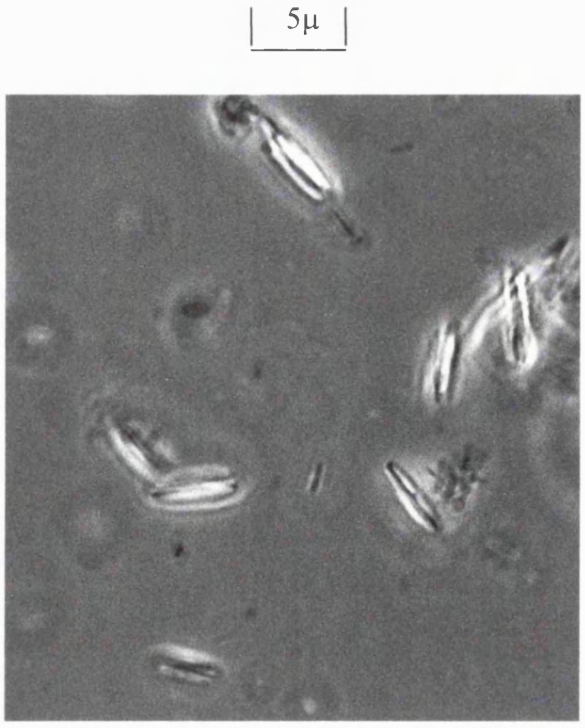

Figure 28(b): Rod YADH I CLECs before shearing.

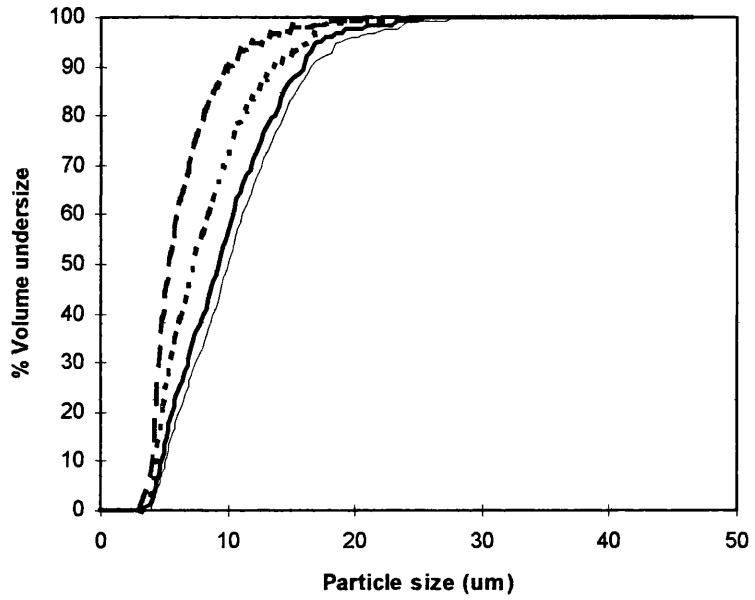

Figure 29: Cumulative size distributions of hexagonal-shaped CLECs as a function of disc rotational speed. —, control, _ _ _ 10,000 rpm, ...,15, 000 rpm, – – –, 27, 000 rpm.

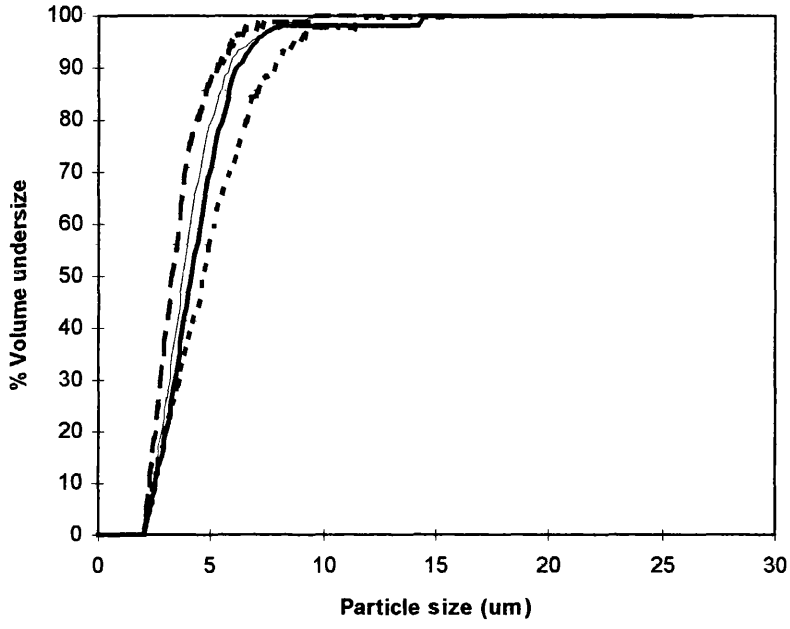

Figure 30: Cumulative size distributions of rod-shaped CLECs as a function of disc rotational speed. —, control,— ,10,000 rpm, ...,15, 000 rpm, – – –, 27, 000 rpm.

shift to smaller size distributions for disc rotational speeds greater than 15, 000 rpm (Re_{disc} $3.5x10^5$, ε_{max} $1.2x10^5$ $W.kg^{-1}$). There is clearly a threshold speed around 10, 000 rpm (Re_{disc} $2.3x10^5$, ε_{max} $3.4x10^4$ $W.kg^{-1}$) below which no damage to the crystals could be detected. The median crystal size decreases from an initial value of 10 μm to around 5 μm after shearing at 27, 000 rpm.

In contrast to the data for the hexagonal-shaped CLECs, the results indicate that there was no significant difference between the sheared samples and the original CLECs suspension. Taken together, Figures 29 and 30 indicate that the crystal size and form will be significant parameters with regard to the mechanical stability of CLECs and consequently their industrial application. The length scales of turbulence based on the physical properties of the continuous liquid phase were calculated in Tables 6 and 7 to be in the range 1.1-15 μm. Breakage of hexagonal CLECs occurred at a tip velocity of 24 $m.s^{-1}$ and a length scale of turbulence of 1.7 μm. Under most operating conditions, these are smaller than the size of the hexagonal-shaped CLECs, though not necessarily of the rod-shaped CLECs. This might explain the different extent to which each crystal form is broken.

Photographs of hexagonal and rod-shaped CLEC suspensions after being sheared at 27, 000 rpm are shown in Figures 31(a) and 31(b) respectively. The rod-shaped CLECs are visually unaltered compared to their appearance before being sheared (*c.f.* Figure 28(b)). In contrast, the hexagonal-shaped CLECs show significant rounding of the edges of the crystals and a gradual reduction in the size of the parent crystals (*c.f.* Figure 28(a)). This suggests that the mechanism of breakage is primarily due to attrition rather than fragmentation. Glutaraldehyde cross-linking significantly increases the mechanical stability of the crystals. There is significant attrition even under the relatively mild conditions at 10, 000 rpm which would have no effect on them after they are cross-linked. The comparison between the control sample of uncross-linked crystals and the sample of the CLECs which was unaffected by the shear show in this instance that the cross-linking does not affect the crystal size (Figure 32).

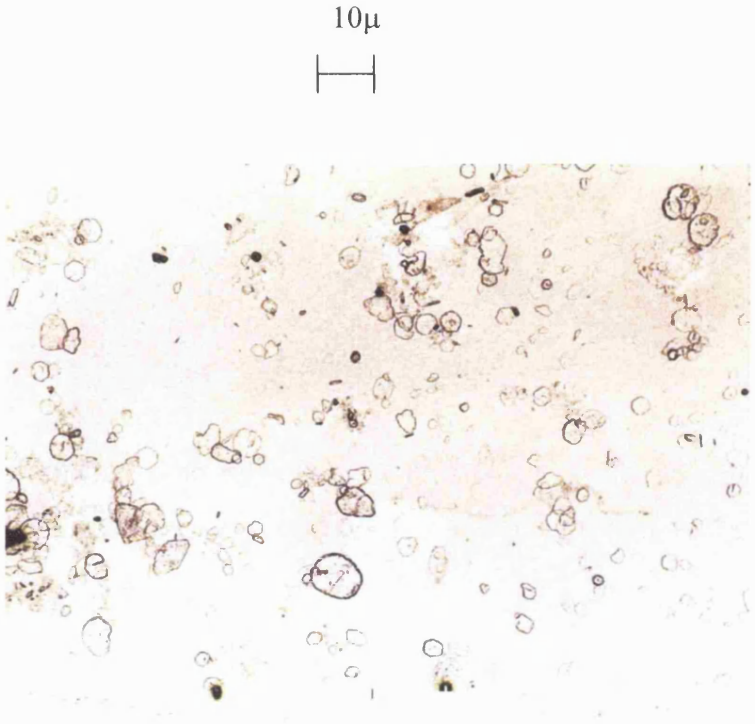

Figure 31(a): Hexagonal CLECs sheared at 27, 000 rpm.

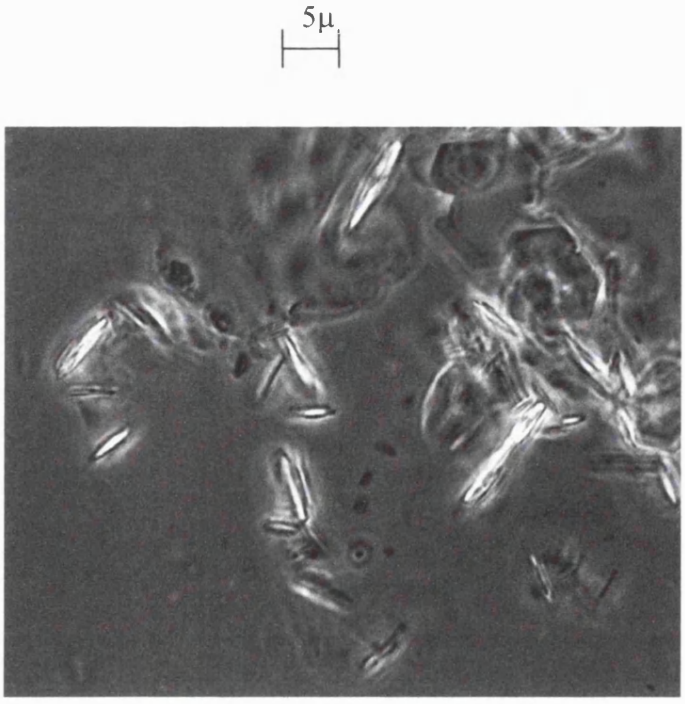

Figure 31(b): Rod CLECs sheared at 27, 000 rpm.

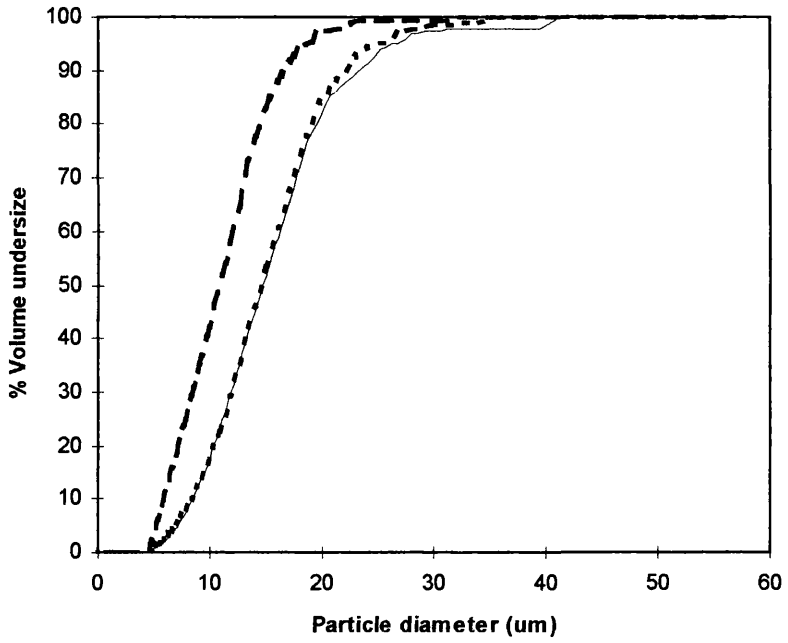

Figure 32: Cumulative size distributions of hexagonal YADH I crystals and CLECs after shearing. —, Control: uncross-linked YADH I crystals; _____, Crystals:uncross-linked YADH I crystals after shearing for 10 seconds at 10, 000 rpm; ...., CLECs: Cross-linked YADH I crystals after shearing for 10 seconds at 10, 000 rpm.

8.4.3 Breakage rate as a function of crystal concentration

In order to identify the cause of attrition of the hexagonal-shaped CLECs the rate of breakage as a function of crystal concentration was examined. Figure 33 shows the change of crystal size during the initial period of shearing at a CLEC concentration of 0.26 $mg.mL^{-1}$ for rotational speeds at which breakage was observed. No data was collected between one to two seconds as the disc was still accelerating to the pre-set speed during this period and the data is presented as a dimensionless d_{50} normalised against the initial crystal size. In all cases the CLEC suspension had achieved a steady-state size within 5-10 seconds. Figure 34 shows similar data obtained at a higher CLEC concentration of 1.04 $mg.mL^{-1}$. In both cases the results indicate that for the hexagonal-shaped CLECs the initial breakage rate is strongly dependent on the rotational speed of the disc but is largely independent of the CLEC concentration. If the rate of breakage increased with increasing CLEC concentration this would imply that the observed attrition of the CLECs was primarily due to crystal-crystal collision as a consequence of the increased probability of crystal-crystal impact. This does not appear to be the case here, however, over the range of CLEC concentrations investigated.

Experiments to determine the initial rate of breakage of the rod-shaped CLECs at concentrations of 0.26 and 1.04 $mg.mL^{-1}$ and an impeller speed of 27, 000 rpm were also performed. The results again indicated that no significant breakage of the rod-shaped CLECs occurred.

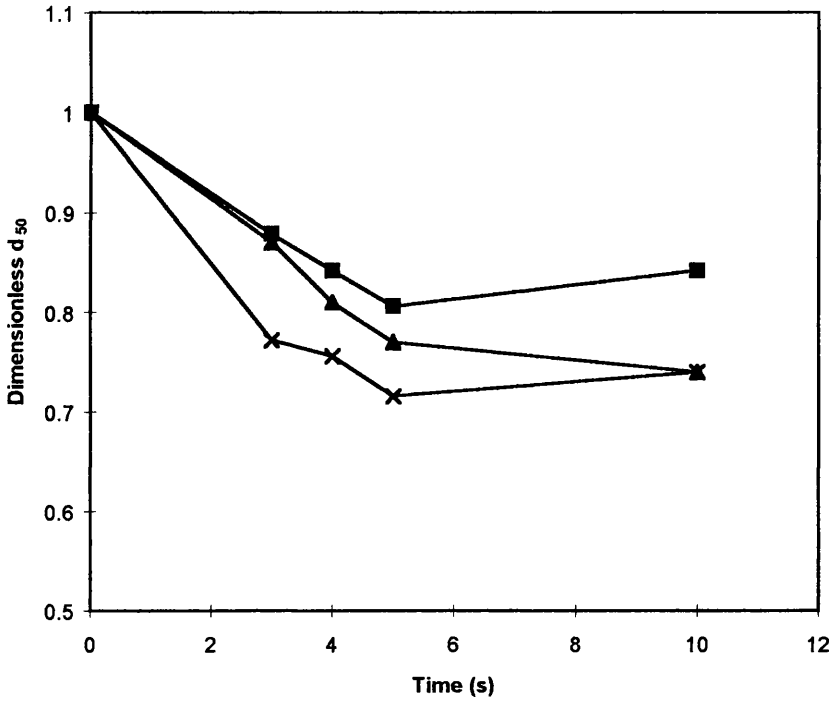

Figure 33: Variation of crystal size as a function of time and disc rotational speed (hexagonal-shaped CLECs, 0.26 mg.mL^{-1}). ■, 15, 000 rpm, ▲, 24, 000 rpm, x, 27, 000 rpm.

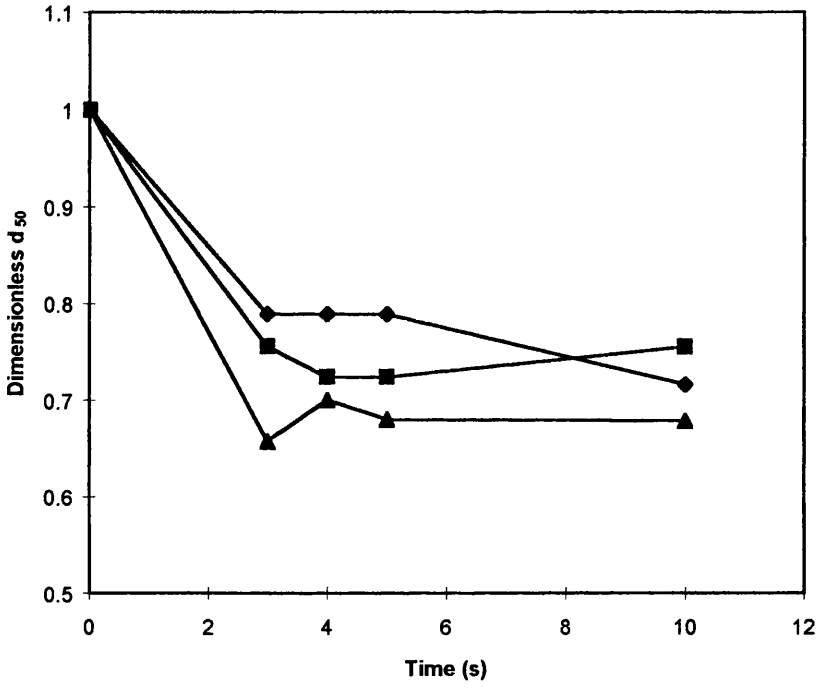

Figure 34: Variation of crystal size as a function of time and disc rotational speed (hexagonal-shaped CLECs, 1.04 mg.mL^{-1}). ◆, 15, 000 rpm, ■, 24, 000 rpm, ▲, 27, 000 rpm.

8.4.4 Breakage rate as a function of energy dissipation

In order to further elucidate the cause of attrition of the hexagonal-shaped CLECs the initial breakage rate (d_{50}/d_t) was plotted as a function of energy dissipation as shown in Figure 35. Experiments were performed over a range of different CLEC concentrations from 0.26 - 2.5 $mg.mL^{-1}$. The results from each CLEC concentration fall approximately on a straight line and the slopes of individual lines, fitted by linear regression, were in the range 0.7-0.9. These are close to a theoretical slope of 1 which indicates a first-order dependency of initial breakage rate on energy dissipation. This suggests then that the mechanism of breakage can be attributed to turbulent shear forces (Equation [10]) and/or crystal-impeller collisions (Equation [6]). Breakage due to crystal-crystal collision (Equation [8]) or turbulent drag forces (Equation [10]) can be neglected as both would be expected to display a 1.5 order dependency of breakage rate on energy dissipation.

To distinguish between breakage of the hexagonal-shaped CLECs due to either turbulent shear forces or crystal-impeller collisions it is necessary to consider both the density of the CLECs and the observed mechanism of breakage. Breakage due to crystal-impeller collisions would be expected to result in fragmentation of the CLECs rather than the pattern of attrition shown in Figure 31(a). Furthermore, given the similar density of the dispersed CLECs (Table 8) and the continuous phase it is unlikely that the individual particles will have sufficient momentum to travel across the streamlines surrounding the rotating-disc. Thus the conclusion is that over the range of conditions investigated breakage of the hexagonal-shaped CLECs occurs primarily by shear-induced attrition.

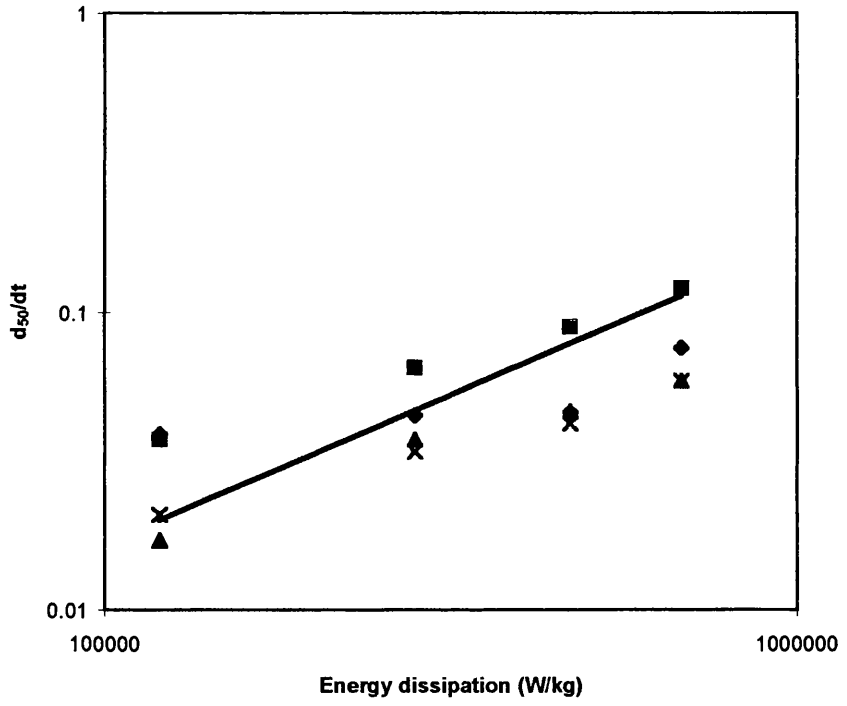

Figure 35: Initial rate of breakage of hexagonal-shaped CLECs as a function of energy dissipation and crystal concentration. ◆, 0.26 mg.mL^{-1}, ■, 0.52 mg.mL^{-1}, ▲, 2.08 mg.mL^{-1}, x, 2.5 mg.mL^{-1}, —, slope =1.

8.4.5 Catalytic activity of sheared CLEC suspensions

In addition to exhibiting mechanical stability it is important that the CLECs also maintain their catalytic activity and that this is not decreased as a result of exposure to the physical environment within the reactor. The catalytic activities of both hexagonal and rod-shaped CLECs are shown in Table 9 before and after shearing at different speeds. In general it can be seen that the specific activity of both CLEC forms do not change significantly after exposure to shear.

Disc rotational speed (rpm)	Activity (Units.mg^{-1})	
	Hexagonal (x10^3)	Rod (x10^3)
0	0.87 ± 0.02	0.87 ± 0.04
4, 000	1.2 ± 0.27	0.84 ± 0.05
10, 000	1.2 ± 0.71	0.89 ± 0.08
15, 000	0.97 ± 0.15	0.93 ± 0.05
20, 000	0.95 ± 0.03	0.96 ± 0.05
27, 000	1.1 ± 0.52	1.0 ± 0.16

Table 9. Catalytic activity of hexagonal and rod-shaped CLECs before and after being subject to shear (period of rotation 10s).

8.4.6 Implications for large-scale biocatalysis

Industrial biocatalytic processes using immobilised enzyme preparations are generally operated batchwise in either packed-bed or stirred-tank reactors. Given the

size and morphology of CLEC preparations, operation in stirred-tank reactors is probably the favoured configuration due to the low voidage and hence high pressure drops likely to be found in packed-beds of these catalysts. Indeed, the only large scale (100L) use of CLECs currently reported in the literature describes the use of a stirred-tank reactor followed by dead-end filtration through a 5 μm filter cloth for recovery of the CLECs (Collins *et al.*, 1998). For the successful design of such a process it is important to avoid breakage of the CLECs during reactor operation otherwise valuable catalyst will be lost from the reactor as 'fines' during filtration, causing a decrease in reactor productivity with each batch and further downstream processing problems.

In order to relate the breakage of the hexagonal-shaped CLECs in the rotating shear device to that which might occur in an industrial scale stirred-tank reactor it is necessary to compare physical and hydrodynamic parameters such as energy dissipation rate and the length scale of turbulence. For the rotating-disc shear device these were shown previously in Tables 6 and 7, while calculated values for a $5m^3$ stirred vessel over a range of impeller speeds are given in Table 10. These were calculated assuming a stirred-tank of standard geometry (H_T:D_T = 3:1, D_i/D_T = 0.33 *etc*) fitted with two equally spaced 6-bladed Rushton turbine impellers (P_o = 5.7) and four equally spaced baffles. Values of the average energy dissipation rate, ε_{avg}, and length scale of turbulence, λ_{avg}, are based on the entire liquid volume in the reactor. The maximum values, ε_{max} and λ_{max}, are based on the local rate of energy dissipation in the region of the impeller assuming that all the energy is dissipated in a liquid volume equal to $0.075D_i^3$ (Aloi and Cherry, 1996).

As previously shown in Figure 29, breakage of the hexagonal-shaped CLECs in the scale-down shear device starts at rotational speeds greater than 15, 000 rpm where ε_{max} is greater than $1.2x10^5$ $W.kg^{-1}$ and λ_{max} is less than 1.7 μm. In relation to the 5 m^3 vessel these conditions correspond to a rotational speed above 1, 000 rpm. This suggests two things. Firstly that at rotational speeds of 200 - 600 rpm, we can expect to see little damage to the CLEC catalyst. Secondly, that the rotating-disc shear device is a useful scale-down tool to test the mechanical stability of CLEC preparations in relation to damage potentially caused by shear-induced attrition.

Speed (rpm)	Re_i ($x10^5$)	P (W) ($x10^5$)	ε_{ave} ($W.kg^{-1}$) ($x10^2$)	λ_{ave} (μm) ($x10^1$)	ε_{max} ($W.kg^{-1}$) ($x10^4$)	λ_{max} (μm) ($x10^1$)
100	2.9	0.0061	0.0016	5.0	0.0054	1.2
200	5.9	0.048	0.013	3.0	0.044	0.69
400	12	0.39	0.10	1.8	0.35	0.41
800	24	3.1	0.83	1.0	2.8	0.24
1, 000	29	6.1	1.6	0.89	5.5	0.21
1, 500	44	20	5.4	0.66	18	0.15

Table 10. Physical and hydrodynamic conditions in a 5 m^3 stirred-tank reactor. Values calculated taking the density, ρ, and viscosity, μ of the continuous phase liquid as 980 $kg.m^{-3}$ and 0.001 Pa.s respectively.

8.5 CONCLUSIONS

In this work the crystallisation conditions used for the preparation of YADH I CLECs, such as protein concentration, pH, and precipitant concentration have been shown to influence not only the size and morphology of the enzyme crystals formed but also their mechanical stability. Using a scale-down, rotating-disc shear device it was shown that the small rod-shaped YADH I CLECs were not damaged over the range of energy dissipation rates investigated. In contrast, the larger hexagonal-shaped YADH I CLECs showed significant breakage. In this case breakage was shown to occur due to shear-induced attrition rather than fragmentation. The energy dissipation rates at which breakage of the hexagonal-shaped CLECs occurred in the shear device were generally higher than those found in typical industrial scale reactors. This obviously has important consequences for the design and operation of large scale biocatalytic reactors, micro-filters and centrifuges using CLEC-based catalysts.

9 FILTRATION STUDIES INVOLVING THE TWO CLEC FORMS

9.1 INTRODUCTION

9.1.1 The importance of studying filtration

The basis of CLEC technology lies in the crystallisation of the protein catalyst followed by cross-linking of the crystals with a bi-functional reagent such as glutaraldehyde. CLECs have been reported so far to be active in environments that can be detrimental to enzyme function, including prolonged exposure to high temperatures, pH values, proteases and aqueous-organic solvent mixtures. Furthermore, CLEC particles have also shown to be more mechanically stable than uncross-linked crystals in agitated conditions using the small-scale shear device. This section explores the recovery and reuse of the YADH I CLECs using dead-end filtration. The study of filtration is important if a stirred-tank reactor incorporating an internal membrane is to be designed for the recovery of CLECs downstream of a reactor (Collins *et al.*, 1998).

The ability to recover the catalyst by filtration simplifies downstream processing while the stability of the catalyst would allow for multiple reuse of the catalyst. Here the effect of the two CLEC forms (rod and hexagonal) on the filtration characteristics of the catalyst is being studied.

9.1.2 Factors affecting the filtration of CLECs

Two types of filtration play an important role in product purification. Crossflow filtration is often the primary process used in purifying biopharmaceutical products (Brose *et al.*, 1996). The fluid to be filtered flows perpendicular to the filtrate or permeate stream. The crossflow generates shear that limits the thickness of the filter cake and prevents the clogging of the membrane deposits (Bowen, 1993). The more conventional dead-end filtration is the process by which the fluid flow is parallel to the filtrate stream and the filter cake builds up with time resulting in a cessation of flow (Brose *et al.*, 1996). Conventional filtration will be used for this study on the recovery of CLECs.

A typical filtration operation contains the filter medium, in this case a membrane, its support and the layer of solids, or filter cake, which has formed

(Wolthius and Dichiaria, 1997). The cake gradually builds up on the medium and the resistance to flow progressively increases. The factors affecting the rate of filtration will be: (1) the drop in pressure from the feed to the far side of the filter medium, (2) the area of the filtering cake, (3) the resistance of the filter cake, (4) the viscosity of the filtrate, (5) the resistance of the filter medium and initial layers of cake.

9.2 DEAD-END FILTRATION THEORY

In a batch filter, if the pressure is kept constant, then the rate of flow will progressively dimish. The flow of filtrate through the cake can be represented as follows (Coulson and Richardson, 1991):

$$\mu_c = \frac{1}{A}\frac{dV}{dt} = \frac{1}{5}\frac{e^3}{(1-e)^2 S^2}\frac{-\Delta P}{\mu l} \qquad [19]$$

In this equation, V is the volume of filtrate which passes in time t. A is the total cross-sectional area of the filter cake, μ_c is the superficial velocity of the filtrate, l is the cake thickness, S is the specific particle surface, e is the voidage, μ is the viscosity of the filtrate and ΔP is the applied pressure difference (Coulson and Richardson, 1991).

Under the assumption that the filter cake formed during filtration is incompressible, e in Equation [19] can be taken as a constant. This is because the cake resistance is not affected significantly by the pressure difference or by the rate of material deposition but only by the physical properties, such as its geometry and surface structure, attributed to the particle. The quantity $e^3/[5(1-e)^2S^2]$ should be constant for the particles forming the cake (Coulson and Richardson, 1991).

Therefore Equation [19] can be rearranged as:

$$\frac{1}{A}\frac{dV}{dt} = \frac{-\Delta P}{\alpha \mu l} \qquad [20]$$

where α is the cake resistance ($m.kg^{-1}$).

The volume of cake deposited by unit volume of filtrate, v, can be written as:

$$\upsilon = \frac{lA}{V} \qquad [21]$$

where l is the cake thickness (Coulson and Richardson, 1991). By substituting Equation [21] into Equation [20], the resulting expression is as follows:

$$\frac{dV}{dt} = \frac{A^2(-\Delta P)}{\alpha \mu \upsilon V} \qquad [22]$$

Two important filtration operations are considered: (i) where pressure difference is constant and (ii) rate of filtration is maintained constant (Hermia, 1982).

For filtration at a constant rate,

$$\frac{dV}{dt} = \frac{V}{t} = \text{constant}$$

so that

$$\frac{V}{t} = \frac{A^2(-\Delta P)}{\alpha \mu \upsilon V}$$

or

$$\frac{t}{V} = \frac{\alpha\mu\upsilon V}{A^2(-\Delta P)} \qquad [23]$$

For filtration at a constant pressure difference,

$$\frac{t}{V} = \frac{\alpha\mu\upsilon V}{2A^2(-\Delta P)} \qquad [24]$$

Thus for a constant pressure filtration, there is a linear relation between V^2 and t or t/V and V (Svarovsky, 1981). A similar equation developed by Russotti *et al* (1995) can be used for the calculation of cake resistance of both CLEC forms in a batch dead-end filter. By integrating Equation [24] over time, the expression in Equation [25] can be obtained.

$$\frac{t - t_{ss}}{V - V_{ss}} = \frac{\alpha\mu c}{2A^2P}(V + V_{ss}) + \frac{\mu R_m}{AP} \qquad [25]$$

In this equation, c is the concentration of CLEC particles in the feed, R_m is the membrane resistance, t_{ss} and V_{ss} is the time and volume respectively at the beginning of a steady state region of flux. Here $t-t_{ss}$ represents the time of the constant pressure filtration and $V-V_{ss}$, the corresponding volume of filtrate obtained in the steady state region of flux. By plotting $(t-t_{ss})/(V-V_{ss})$ against V for this steady state region and measuring the slope of the linear correlation, the cake resistance, α, (Russotti *et al.*, 1995) can be determined.

9.3 MATERIAL AND METHODS

9.3.1 Filtration test for CLECs

A dead-end pressure filtration test was developed to evaluate the recoverability and mechanical stability of the CLECs. A pressure filter (Laboratory Filter "60", Schenk Laboratory Systems Limited, Oxton, Wirral, UK) fitted with a 0.2 μm cellulose nitrate membrane (Whatman, UK) with a filter area of 2×10^{-3} m^2 was used to process 60 mL of CLEC suspension. The CLEC suspension was poured into the filtration vessel and the pressure inside the vessel was adjusted to the prescibed value by the setting of a valve on the N_2 gas cylinder. Filtration of rod and hexagonal YADH I CLEC suspensions at 1.5 $mg.mL^{-1}$ concentration were tested at 3 feed pressures (50, 100 and 200 kPa). After a CLEC suspension was filtered, fresh buffer (50 mM Tris, pH 8) was added to the pressure filter device and the contents were mixed by repeated slow aspiration using a 5 mL Gilson pipette. Filtration then resumed for another cycle until 5 cycles were completed. The mass of the filtrate was recorded for each filtration cycle every few seconds using a balance. The change in the permeate volume (V) in grams with time (t) in seconds was measured under constant pressure. The cake resistance, α ($m.kg^{-1}$), was calculated from the plot of t/V versus V using Equation [25].

For each filtration cycle, the cake resistance due to the CLECs was calculated. Other measurements performed included size distributions (Section 8.3.4), activity (Section 7.2.1) and protein concentration of CLECs (Section 7.2.3) in both the retentate and permeate. The filtration experiments were performed in triplicate. A protein concentration of 1.5 $mg.mL^{-1}$ was picked because it had reasonable filtration rates using a 0.2 μm membrane. When the CLEC concentration was increased to 5 $mg.mL^{-1}$, the flux was slightly slower. The decrease in flux due to an increase in particle concentration can be seen in other systems such as yeast cells (Hashim *et al.*, 1997). At larger membrane pore sizes, such as 1.0 μm, the liquid would begin to flow through before any pressure was applied.

9.4 RESULTS AND DISCUSSION

9.4.1 Effect of pressure on the cake resistances of the two YADH I CLEC forms

The flux of the liquid using both hexagonal and rod YADH I CLECs can be calculated by plotting t/V versus V, according to Equation [25], and measuring the slope of the steady-state region of the flux. As can be seen in Figures 36 and 37, the hexagonal CLECs had a slope of 0.12 while the rod CLECs had a slope of 0.01 at a pressure of 50 kPa during the first cycle of filtration respectively. The slope for the experiments of the rod CLECs is about an order of magnitude lower than the hexagonal CLECs. These slopes correlate well with the cake resistances of both hexagonal and rod CLECs where the cake resistances are in the order of 10^{14} and 10^{12} $m.kg^{-1}$ respectively (Table 11).

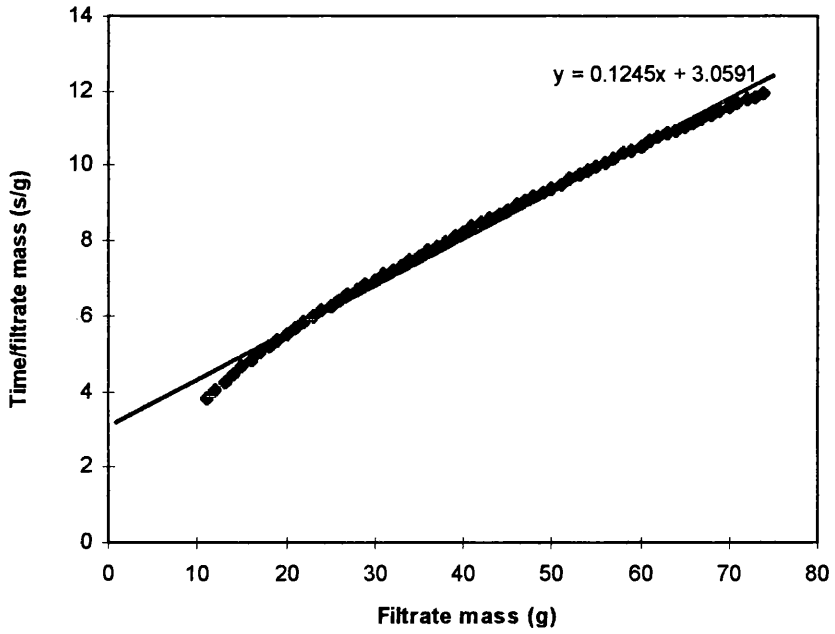

Figure 36: A plot of time/filtrate mass (s/g) versus filtrate mass (g) for hexagonal CLECs filtered at a pressure of 50 kPa. Solid line fitted by linear regression.

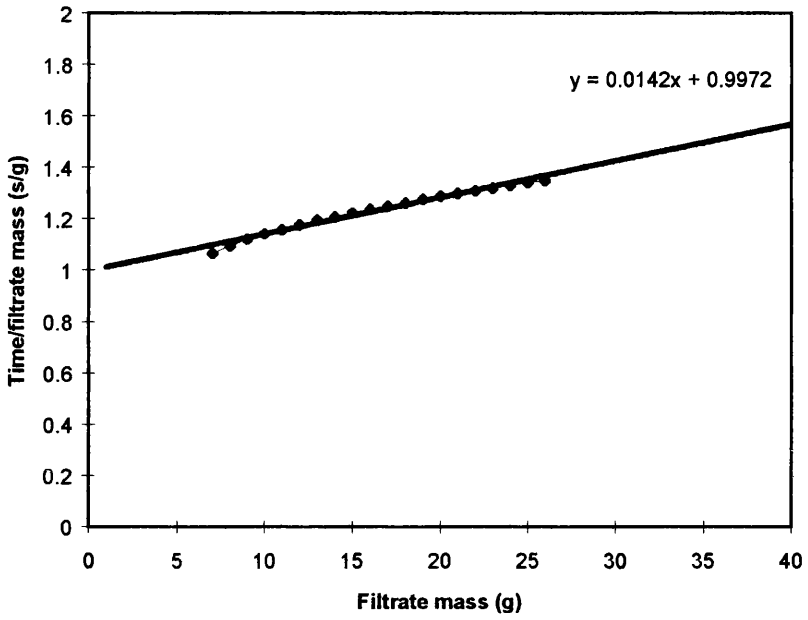

Figure 37: A plot of time/filtrate mass (s/g) versus filtrate mass (g) for rod CLECs filtered at a pressure of 50 kPa. Solid line fitted by linear regression.

CLEC morphology	Pressure (kPa)	Cake resistance α (x 10^{13} m.kg^{-1})
Hexagonal	50	10 ± 3.0
Hexagonal	100	20 ± 13
Rod	50	0.32 ± 0.16
Rod	100	0.94 ± 0.47

Table 11: The effect of pressure on the cake resistances (α) of the CLEC forms using a 0.2 μm membrane filter. Cake resistance is the average over 5 filtration cycles.

The mechanical integrity of both forms of YADH I CLECs (hexagonal and rod) were tested under 3 different pressures by calculating the cake resistance. Cake resistance is a measure of the compressibility of the cake which also indicates the mechanical integrity of the CLEC particles. The cake resistance (m.kg^{-1}) at each of the 5 cycles at the particular pressure was constant, therefore an average value for the

5 filtration cycles for the particular pressure was obtained (Table 11). From Table 11, it can be observed that rod-shaped YADH I CLECs have on average a lower cake resistance than the hexagonal CLECs. Rod CLECs, being more cylindrical in shape than the hexagonal CLECs, may allow for more voidage within the cake, thus reducing the cake resistance. Hexagonal CLECs, on the other hand, are mainly flat plates which can stack on top of each other thus increasing the compression of the cake and thereby increasing the cake resistance.

The cakes formed by hexagonal and rod YADH I CLECs were both compressible at a pressure of 200 kPa. The cake resistances for hexagonal and rod crystal forms dramatically increased to a maximum reading of $3.0 \pm 1.5 \times 10^{14}$ m.kg^{-1} after 5 cycles of filtration. For the rod CLECs, this corresponded to a cake resistance that was 100 fold greater than at 50 kPa. Nakanishi *et al* (1987) evaluated the mean specific resistance of the cakes of various micro-organisms. As seen from Table 12, the cake resistances of both forms of YADH I CLECs fell within the ranges obtained for most micro-organisms.

Particles	**Cake resistance α (x 10^{12} m.kg^{-1})**
E.coli	1000
Hexagonal YADH I CLECs	200
R. spheroides	40
B. cirulans	40
Rod YADH I CLECs	9.4
M. glutamicus	4.0
Bakers'yeast	0.4
Filter-Cel latex beads	0.1

Table 12: The cake resistance (α) of various micro-organism, latex beads and CLECs at 20°C at a pressure of 100 kPa (Nakanishi *et al.*, 1987).

As observed in Table 11, due to the large standard deviation, the specific cake resistance of hexagonal and rod CLECs seemed unchanged as a function of the pressure, ranging from 50 to 100 kPa. This indicated a relatively incompressible cake within these pressure readings for both rod and hexagonal YADH I CLECs. Specific cake resistance seemed to increase at pressures of 200 kPa for both rod and hexagonal CLECs. This may be attributed to cake compressibility or by smaller contaminants retained by the 0.2 μm membrane at higher pressures. As a result, voids within the membrane were filled with these particles thereby increasing cake resistance.

9.4.2 Effect of pressure on the mean size and activity of the YADH I CLEC forms

The specific activities (Units.mg^{-1}) of both rod and hexagonal YADH I CLECs at each of the 5 cycles at the particular pressure were not significantly different from each other and therefore an average value for the 5 filtration cycles was obtained (Table 13). The specific activities were the activities of the CLECs retained in the retentate. The permeate was also assayed for activity but there was no activity present indicating none of the enzyme, either in CLEC or free soluble forms, had passed through the membrane. In addition to exhibiting mechanical stability, it is important that the CLECs also maintained their catalytic activity and that this is not decreased due to the exposure to the physical environment during the filtration step. The sizes of both hexagonal and rod CLECs did not change as a function of pressure (Table 13). The hexagonal and rod CLECs maintain their mean size of 12 and 5 μm respectively after each of the 5 filtration cycles at pressures 50 to 200 kPa.

CLEC morphology	Pressure (kPa)	Specific Activity (Units.mg^{-1})	Mean size (d_{50}) (μm)
Hexagonal	50	63 ± 6.3	12 ± 0.9
Hexagonal	100	50 ± 7.0	12 ± 0.9
Hexagonal	200	53 ± 5.0	12 ± 0.9
Rod	50	91 ± 9.1	5.0 ± 0.38
Rod	100	96 ± 9.6	5.0 ± 0.38
Rod	200	100 ± 10	5.0 ± 0.38

Table 13: The effect of pressure on the average size and activity of the CLEC forms using a 0.2 μm membrane filter after 5 cycles of filtration.

9.4.3 Variation of protein concentration of CLECs in the retentate with filtration cycle

A CLEC suspension with a protein concentration of 1.5 mg.mL^{-1}, assayed using the Lowry method (Section 7.2.3), was used for filtration. The protein concentration (mg.mL^{-1}) of hexagonal CLECs measured at each of the 5 cycles at the particular pressure was not significantly different from each other and therefore an averaged value was obtained for the 5 filtration cycles (Table 14). The permeate was also assayed for protein but there was no significant amount present. As observed in Table 14, the protein concentration of hexagonal CLECs in the retentate was independent of the pressure (kPa). This indicated that most of the hexagonal CLECs could be retained after filtration and that the cake resistance, not pore plugging, was the main resistance to the flux as the pressure was increased to 200 kPa.

Pressure (kPa)	Protein concentration ($mg.mL^{-1}$)
50	1.5 ± 0.08
100	1.3 ± 0.03
200	1.3 ± 0.06

Table 14: The concentration of hexagonal CLECs in the retentate after 5 cycles of filtration.

In contrast, the rod YADH I CLECs showed a decrease in protein concentration in the retentate as a function of filtration cycle for all the pressures investigated. A starting protein concentration of 1.2 $mg.mL^{-1}$, assayed using the Lowry method (Section 7.2.3), for the rod CLECs was used for filtration. As shown in Figure 38, the concentration of rod CLECs in the retentate decreased as a function of filtration cycles at 100 kPa reaching a steady-state value of 0.6 $mg.mL^{-1}$ after the second cycle. At 200 kPa, the concentration of rod CLECs in the retentate also showed a similar trend where the protein concentration continued to decrease as a function of filtration cycle (data not shown). After filtering the rod CLECs at 100 kPa, the 0.2 μm membrane was assayed for protein concentration using the Lowry method. A protein concentration of 0.61 $mg.mL^{-1}$ was recorded indicating that a majority of the rod CLECs were retained in the pores. The rod particles, due to their small sizes, could be the reason for pore plugging of the membrane resulting in the main resistance to flux at higher pressures of 200 kPa.

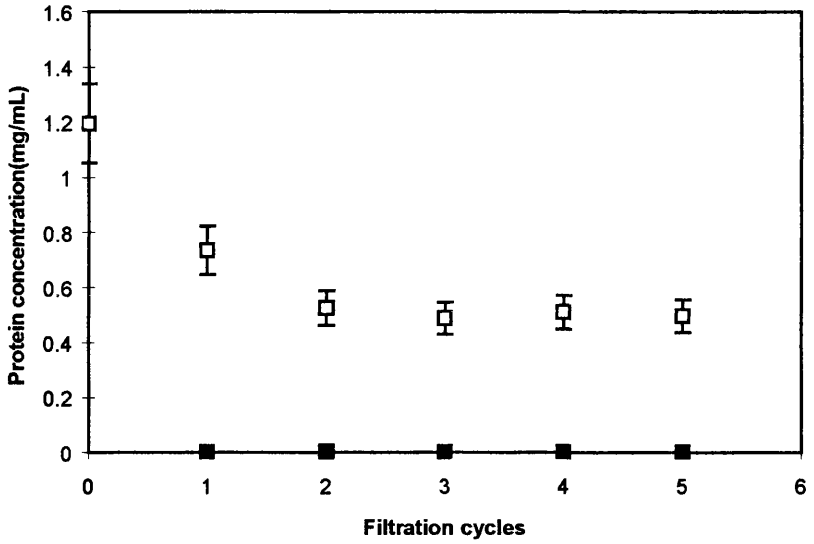

Figure 38: Protein concentration of rod CLECs in the retentate and permeate over 5 filtration cycles at 100 kPa. □, retentate, ■, permeate.

9.4.4 The effect of morphology on the filtration characteristic of rod CLECs

The process performance of rod CLECs can be examined in detail by understanding the microscopic nature of the rod CLECs particles. One way is to examine the crystallisation conditions that determine the formation of rod crystals.

The rate of growth of protein crystals are affected by the transport of molecules to the face of the growing crystal and the frequency the molecules orient and attach themselves to the growing surface. The rate at which protein crystals nucleate and grow depends on the rate of attachment (McPherson, 1990). Molecules to be incorporated into the growing crystal have to be correctly oriented and form proper chemical interactions with neighbouring molecules. The frequency of attachment can be enhanced by optimising the charge state of the proteins by adjusting the pH of the system (McPherson, 1990).

It has been discussed in Section 7.3.8 that the formation of salt bridges is responsible for rapid nucleation leading to showers of microcrystals (McPherson, 1995). Rod YADH I crystals are formed overnight at pH 7, 25 °C (Section 5.3.1), with a crystal recovery greater than 70 % (Section 5.3.2). They may be formed due to the formation of salt bridges caused by the protonation of the basic residues and deprotonation of the acidic groups of the YADH I enzyme.

Rapid crystallisation leading to showers of microcrystals form very strong electrostatic interactions among the protein molecules (McPherson, 1995). It is possible that in the rapid process of crystallisation of rod YADH I crystals that contaminating proteins may also be incorporated within the lattice inhibiting the attachment rate and terminating crystal growth. The particle size distribution of rod crystals (Figure 30) indicates that rod crystals have a smaller median size of 4.6 μm in comparison to the hexagonal plates of 10 μm in size. The purity of the rod YADH I crystals can be seen in gel 2 where lower molecular weight contaminants are present in the redissolved crystals. These contaminants could also be the reason for pore plugging of the membrane resulting in the main resistance to flux at higher pressures.

9.5 CONCLUSIONS

Using a scale-down filtration device, small rod-shaped YADH I CLECs were shown to have a greater permeate flux and hence a lower cake resistance than the larger hexagonal YADH I CLECs. The specific cake resistance of rod and hexagonal YADH I CLECs maintained constant during several filtration cycles at 50 and 100 kPa using a 0.2 μm membrane. The specific cake resistance of rod CLECs was in the range of 3-9 x 10^{12} $m.kg^{-1}$ while that of the hexagonal CLECs was in the range of 1-2 x 10^{14} $m.kg^{-1}$ up to pressures of 100 kPa.

The rod CLECs, due to their small size may have led to pore plugging of the membrane when operated at higher pressures. The hexagonal YADH I CLECs, on the other hand, showed cake compressibility at higher pressures of 200 kPa. Hence, the effectiveness of using CLECs in a " dead-end" filtration unit would depend on the operational pressure and size of the CLECs. Size and activity measurements showed that no breakage of crystal forms occur as a result of pressure. The calculation of filtration time of the CLEC catalyst is difficult since the intercept on the t/V axis for the calculation of R_m, membrane resistance, is not reproducible (Coulson and Richardson, 1991). However, by maintaining a constant specific cake resistance at a particular pressure, the filtration time of the CLEC catalyst may be roughly estimated at a process scale under various operating conditions.

10 REACTOR STUDIES EVALUATING THE PERFORMANCE OF CLECs

10.1 INTRODUCTION

10.1.1 Evaluation of the industrial performance of *C.rugosa* lipase CLECs

The purpose of this final section is to use the small-scale shear (Section 8.3.2) and filtration studies (Section 9.3.1) developed here to test the mechanical performance and recovery of a batch of *Candida rugosa* lipase CLECs in a standard stirred-tank reactor. The lipase CLECs were chosen instead of the hexagonal YADH I CLECs for the reactor study because the reaction they catalyse does not require cofactor recycling. Previous work by Collins *et al* (1998) have mentioned that a stirred-tank design incorporating a 0.2 μm flat filter at the outlet would be an ideal reactor in which CLECs might be used industrially. In this section, a standard stirred-tank reactor (100 mL) with a tank diameter the same as the diameter of the pressure filter (Laboratory Filter "60", Schenk Laboratory Systems Limited, Oxton, Wirral, UK) was used to simulate this reactor design. The experiments will investigate the performance of the lipase CLECs in the stirred-tank reactor with regard to their mechanical stability and recovery over four cycles of reaction and separation. The key issues to consider with regard to the evaluation of the industrial application of CLECs are as follows:

1) Use of the small-scale shear device to predict the breakage associated with the process scale equipment.
2) Use of the small-scale filtration unit to predict the specific cake resistance of the CLECs over a number of reaction cycles.
3) To relate the mechanical stability of the CLECs to the catalyst recovery.
4) To determine the retained specific activity of the CLECs as the catalyst is being recycled through a number of cycles.

10.2 MATERIALS AND METHODS

10.2.1 Purification of *C.rugosa* lipase by propanol precipitation

Crude lipase from *C.rugosa* was a gift from Biocatalysts Ltd. (Pontypridd, Wales). 20 g of crude lipase was dissolved in 200 mL of RO water for 1 hour on ice.

Cold isopropanol (40 mL) was added dropwise to the enzyme solution which was left stirring on ice for 2 hours. The precipitate was removed by centrifugation at 10, 000 rpm, 4 °C for 10 minutes. The supernatant was dialysed twice against RO water in prepared dialysis tubes and then concentrated by placing the dialysed enzyme in PEG 8000 for 5 hours until the volume of the enzyme solution was about 50 mL.

10.2.2 Crystallisation and cross-linking of *C.rugosa* lipase

The purified lipase was crystallised using the hanging-drop conditions as described by Rubin *et al* (1991). Crystallisation of lipase involved combining 50 mL (approximately 2 $mg.mL^{-1}$ final protein concentration) of concentrated lipase solution, 105 mL 2-methyl-2,4-pentanediol (42 % (v/v) MPD), 1.5 mL of a 0.1 M calcium chloride solution (0.6 mM $CaCl_2$) and 93.5 mL of a 50 mM MES buffer, pH 5.9 in a final volume of 250 mL in a 500 mL Duran bottle. The components were seeded with a 1 mL seed lipase crystal solution crystallised under the same crystallisation conditions in a 0.5 mL Eppendorf (Lee *et al.*, 1999). The contents were agitated gently on a IKA-VIBRAX-VXR vibrating platform (Janke & Kunkel GmbH & CO., Germany) at 200 rpm. Crystallisation of lipase was completed within 2 days at room temperature. Cross-linking of lipase crystals was performed by adding directly
2.5 mL of a 50 % (v/v) glutaraldehyde aqueous solution to the 250 mL crystal suspension. The final concentration of glutaraldehyde in the crystal mixture was 0.5 % (v/v). The crystals were cross-linked for 1 hour after which time they were washed twice with 50 mM MES buffer at pH 5.9.

10.2.3 Titrimetric assay for CLEC *C.rugosa* lipase activity

The activity of the lipase CLECs was measured at 25 °C using 20 % (S)-ethyl lactate in 10 mM NaCl as the substrate. The substrate solution formed a single phase and had physical properties similar to that of water. The assays were carried out in a pH stat (Radiometer ETS822 end-point titration system). After the lipase CLECs had been washed, they were resuspended in 10 mM NaCl and placed in the Rushton stirred-tank reactor such that the volume of the CLEC mixture was 60 mL. To the

CLEC mixture, 15 mL of ethyl lactate was added to the reactor and the reaction was autotitrated at pH 7. The final protein concentration of lipase CLECs in the final volume (75 mL) was 0.5 $mg.mL^{-1}$. This was the concentration suggested by Collins *et al* (1998) for their scale-up work with CLECs.

The rate of addition of 2 M NaOH was recorded and used to calculate the initial linear rates. The linear rates ($mL.min^{-1}$) were converted to $Units.mL^{-1}$ by taking into account the dilution of enzyme in the substrate solution. One unit is defined as the release of 1 μmole of acid per minute. The assay lasted for 15-20 minutes. The specific activity of the lipase CLECs was calculated by dividing the Units per mL by the final concentration of the CLECs in the reactor as determined by the Lowry assay (Section 7.2.3). The coefficient of variance of this assay was 11 %.

10.2.4 Shear device experiments

Lipase CLECs cross-linked with 0.5 % (v/v) glutaraldehyde were sheared for 10 seconds at speeds 4, 000 to 27, 000 rpm. The size distribution of the sheared CLEC suspension was analysed using the Elzone 282 PC particle size analyser.

10.2.5 Filtration experiment

The specific cake resistance of the lipase CLECs was determined by filtering the CLECs (protein concentration of 0.5 $mg.mL^{-1}$) using a dead-end pressure filter fitted with a 0.2 μm cellulose nitrate membrane with applied pressure of 100 kPa as described in Section 9.3.1. The CLECs were filtered for 4 cycles.

10.2.6 A biotransformation in a Rushton turbine stirred-tank reactor with lipase CLECs

In order to relate the breakage of the lipase CLECs in the rotating shear device to that which might occur in a stirred-tank reactor, it is necessary to compare the hydrodynamic parameters such as energy dissipation and shear rate. A 100 mL stirred-tank of standard geometry ($H_T:D_T = 3:1$, $D_i/D_T = 0.5$) was fitted with a 6-bladed Rushton turbine impeller ($P_0 = 5$, $D_i = 2.4$ cm), situated at a position 1.6 cm from the base of the vessel with four equally spaced baffles (Atkinson and Mavituna,

1987). The volume of the liquid was filled up to 75 % of the vessel. The impeller was driven by a motor (IKA Labortechnik, Germany) and the speed adjusted in the range of 200 and 1, 000 rpm. The maximum calculated value of ε_{max} is based on the local rate of energy dissipation in the region of the impeller assuming all the energy is dissipated in the liquid volume equal to $0.075D_i^3$ (Aloi and Cherry, 1996). The maximum calculated value of G_{max} refers to the local shear rate in the region of the impeller assuming the maximum shear is located in the liquid volume equal to $0.075D_i^3$ (Shamlou and Titchener-Hooker,1993). The reaction was carried out in the Rushton stirred-tank reactor controlled by the pH stat and lasted for 15 to 20 minutes. The supernatant was filtered off and the CLECs were resuspended in 10 mM NaCl (60 mL) to which 15 mL of ethyl lactate was again added. Another reaction cycle was resumed until 4 cycles have been completed.

10.3 RESULTS AND DISCUSSION

10.3.1 Rotating-disc shear device and filtration experiments

To investigate breakage of the lipase CLECs, the influence of the rotational speed of the disc in the shear device on the size distribution of the diamond flat-shaped lipase CLECs was studied. Experiments were carried out by varying the disc rotational speed from 4000 to 27000 rpm with a constant shearing time of 10 seconds and at a crystal concentration of 0.5 $mg.mL^{-1}$. Figure 39 shows the cumulative size distribution (undersize) of lipase CLECs before and after shearing. The results indicated a shift to smaller size distribution for disc rotational speed greater than 15, 000 rpm (Re_{disc} 3.5×10^5, ε_{max} 1.2×10^5 $W.kg^{-1}$, G_{max} 3.4×10^5 s^{-1}). The energy dissipation for the breakage of lipase CLECs were very similar to the ones for the hexagonal YADH I CLECs (Re_{disc} 3.5×10^5, ε_{max} 1.2×10^5 $W.kg^{-1}$, G_{max} 3.4×10^5 s^{-1}).

The specific cake resistance of lipase CLECs was determined over a period of 4 cycles at a crystal concentration of 0.5 $mg.mL^{-1}$. To investigate the compressibility of the lipase CLECs during filtration, filtration experiments were performed at 100 kPa for 4 cycles. Figure 40 indicated that the cake resistance for the CLECs were maintained at a constant value of 2.6×10^{13} $m.kg^{-1}$ over a period of 4 cycles. The cake resistance ($m.kg^{-1}$) for lipase CLECs was lower than the hexagonal YADH I

CLECs ($\alpha = 2.0 \times 10^{14}$ m.kg^{-1}). Hence, according to the filtration equation at constant pressure devised by Russotti *et al* (1995), the time taken to filter the total contents of the reaction (75 mL) would be approximately 2.1 minutes.

10.3.2 Relationship between CLEC breakage in the shear device with that in the Stirred-tank reactor

The hydrodynamic conditions such as Reynolds number (Re_i), power, P and maximum energy dissipation rate, ε_{max}, were calculated as previously described in Section 8.2.2. As shown previously in Figure 39, breakage of lipase CLECs in the scale-down shear device occurred at rotational speeds greater than 15, 000 rpm where G_{max} is 3.4×10^5 s^{-1}. In relation to the 100 mL standard Rushton stirred-tank reactor, these conditions corresponded to rotational speed greater than 1, 000 rpm and above (Table 15).

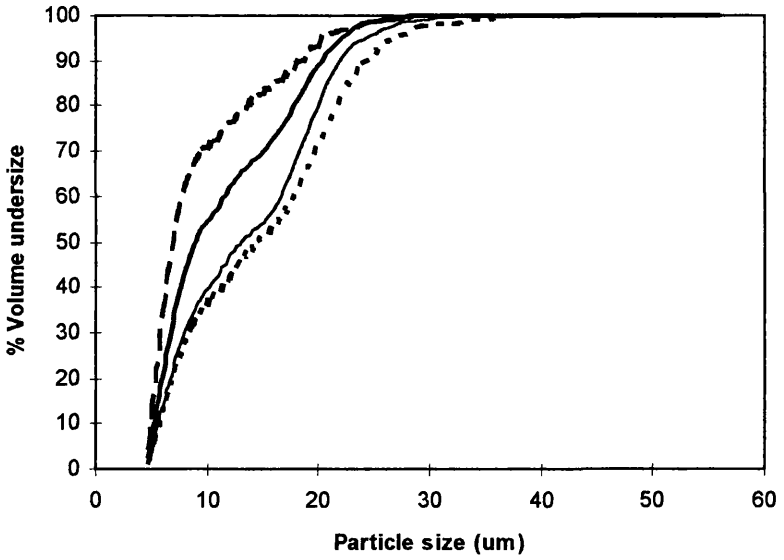

Figure 39: Cumulative size distribution (undersize) of lipase CLECs cross-linked with 0.5% glutaraldehyde as a function of disc rotational speed. —, control, ..., 4, 000 rpm, —, 15, 000 rpm, – –, 27, 000 rpm.
Crystal concentration, 0.5 mg.mL^{-1}, time of shearing, 10 seconds.

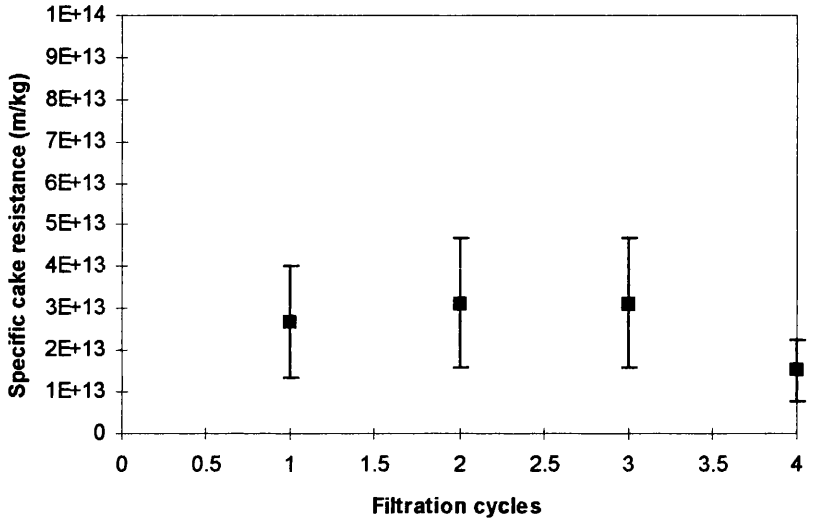

Figure 40: Specific cake resistance of lipase CLECs (0.5 mg.mL^{-1}) over 4 filtration cycles at 100 kPa.

Speed (rpm)	Re_i (x10^3)	Power (W)	ε_{max} (W.kg^{-1})	G_{max} (s^{-1})
100	1.0	$2.7x10^{-4}$	0.2	$4.8x10^2$
200	2.1	$2.2x10^{-3}$	1.8	$1.4x10^3$
400	4.2	$1.7x10^{-2}$	14	$3.8x10^3$
1, 000	10	0.28	$2.4x10^2$	$1.5x10^4$

Table 15: Physical and hydrodynamic conditions in a 100 mL stirred-tank reactor. Values calculated taking the density, ρ and viscosity, μ of the continuous phase liquid as 1000 kg.m^{-3} and 0.001 Pa.s respectively.

By comparing the median particle diameters of the lipase CLECs stirred at 200 and 1, 000 rpm in the Rushton turbine stirred-tank reactor, breakage occurred at 1, 000 rpm after the third reaction cycle (Figure 41). However, no breakage occurred for lipase CLECs stirred at 200 rpm. This suggests three things. Firstly, we can expect little damage to the CLEC catalysts at rotational speeds of 200 rpm. Secondly, the rotating shear device is a useful scale-down tool to test the mechanical stability of a CLEC preparation and predict the likelihood of damage caused by shear-induced attrition. Thirdly, the maximum shear rates at which breakage of lipase CLECs occurred in the shear device are generally higher than those found typically in industrial scale reactors.

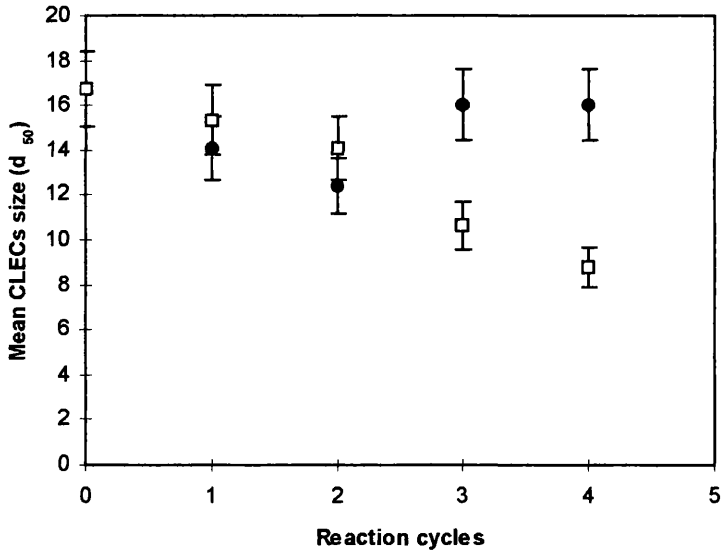

Figure 41: Trend in mean sizes of lipase CLECs, stirred at 200 and 1, 000 rpm, after each reaction cycle in the Rushton turbine stirred-tank reactor. ●, 200 rpm, □, 1, 000 rpm.

10.3.3 The effects of breakage on the filtration and recovery of Lipase CLECs

As shown in Figure 40, the cake resistance of the lipase CLECs was constant at a value of 2.6×10^{13} $m.kg^{-1}$ which corresponded to a filtration time of 2.1 minutes to remove the contents of the reaction vessel. According to Coulson and Richardson (1991), the true determination of cake resistance is difficult because the resistance depends on the way the pressure is developed within the fitering device. Small variations in the support geometry can influence the measurement of the cake resistance. Therefore, due to the level of error in the experiments, the filtration time may not be accurately determined.

Damage to the CLEC catalysts, due to shear-induced attrition, can also affect the recovery of the catalyst. Figure 42 shows that a majority of CLECs, stirred at 1, 000 rpm in the reactor were lost after the third cycle where breakage had occurred. This could be due to the small fines, generated by attrition, clogging the membrane and not being able to be recovered. CLECs stirred at 200 rpm, did not show any damage due to attrition and were recovered after each reaction cycle (Figure 43).

10.3.4 Catalytic activity of the CLECs over 4 reaction cycles

The catalytic activities of the lipase CLECs are shown in Figures 44 and 45 for 4 reaction cycles. At a stirrer speed of 200 rpm, the lipase CLECs showed relatively constant specific activity up to the third cycle. Very little activity was observed for the CLECs at the fourth cycle. At an impeller speed of 1, 000 rpm (Figure 45), the activity of lipase CLECs decreased significantly after each reaction cycle.

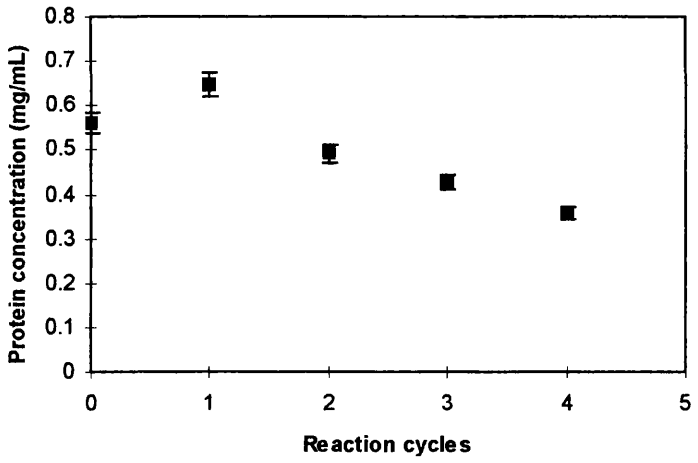

Figure 42: Protein concentration ($mg.mL^{-1}$) of lipase CLECs, stirred at 1, 000 rpm, recovered in the retentate after each reaction cycle.

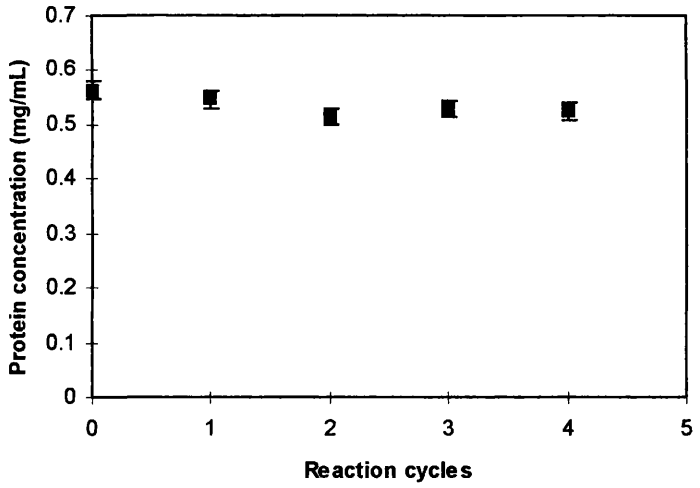

Figure 43: Protein concentraion ($mg.mL^{-1}$) of lipase CLECs, stirred at 200 rpm, recovered in the retentate after each reaction cycle.

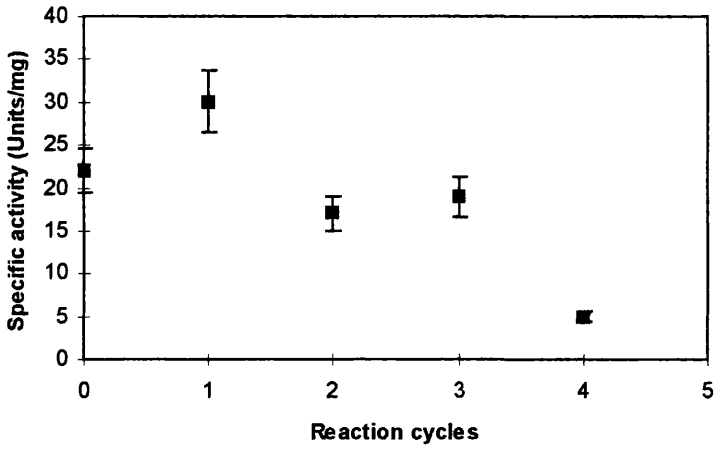

Figure 44: Specific activity (Units.mg $^{-1}$) of lipase CLECs , stirred at 200 rpm, after each reaction cycle.

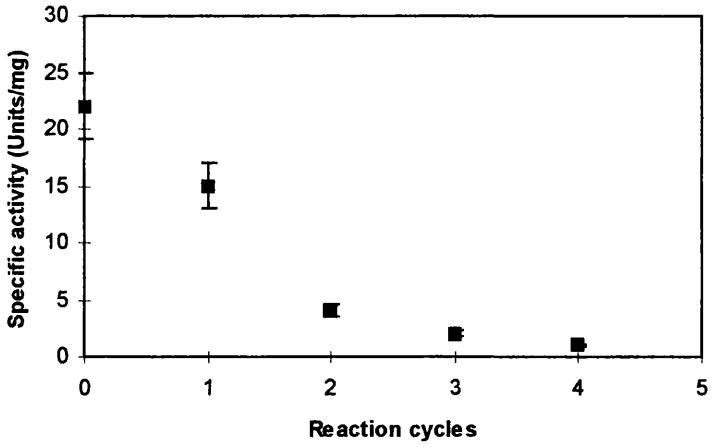

Figure 45: Specific activity of lipase CLECs, stirred at 1, 000 rpm, after each reaction cycle.

Tischer and Kasche (1999) have reported that the activity of immobilised enzymes can be affected significantly by formation of proton gradients within the

carrier in low buffer and ionic strength solutions. Such static pH gradients can be formed in enzyme crystals at low ionic strengths. The charge groups within the crystal can act as a cation exchanger and partitioning of protons can give rise to a static pH gradient. It has been reported with carrier-fixed α-chymotrypsin that pH shifts within the carrier, in low buffer and high substrate solutions, can significantly reduce the enzyme activity (Tischer and Kasche, 1999).

In Figure 44, the reaction rate of lipase CLECs, stirred at 200 rpm, for the first 3 cycles indicated substrate-related diffusional control. However, at the fourth cycle, the enzyme activity is significantly lowered, possibly indicating control by pH shifts within the enzyme crystals. This may be due to the lack of buffer and low ionic strength (10 mM NaCl) in the enzyme assay. Also, the lack of washing of the CLEC catalyst after each cycle could cause an increase of protons within the crystal causing its inactivation.

10.4 Conclusions

In this work, the small-scale shear device has been shown to be a useful scale-down tool to predict the breakage of CLECs associated with process scale equipment such as a Rushton turbine stirred-tank reactor. It is also useful in estimating the rotational speed that damage to the CLECs might occur due to shear-induced attrition. The small-scale microfiltration device can be used to predict the cake resistance of the CLECs. The reactor work has shown that breakage of the CLECs can reduce the recovery of the catalyst possibly due to membrane clogging by fines generated by shear-induced attrition. The specific activity of CLECs is more difficult to predict than its mechanical stability. It has been observed that CLECs stirred at lower rotational speeds (200 rpm) retained their initial activity for a longer period. Loss of activity could be due to the pH shifts established within the crystals.

11 GENERAL CONCLUSIONS

11.1 Summary

Temperature, protein concentration, pH, ionic strength and the presence of coenzymes are all important variables influencing the crystallisation behaviour of a protein. The definition of an operational window for crystallisation is a convenient technique to optimise the large-scale production of crystals, whether as an aid for protein purification or for the manufacture of CLECs as biocatalysts.

Starting with published conditions in the hanging drop at a 1 μL scale, the crystallisation diagram explores systematically an appropriate range of conditions at a 1 mL scale in Eppendorf tubes. The diagram clearly shows how the combination of variables affect the crystallisation, and it allows a process window to be quickly identified with its regions of optimum recovery and of different crystal forms, while regions of precipitation or high solubility are avoided. From this window, the successful conditions can be increased to a 0.5 L scale with little or no change in crystallisation behaviour either of recovery or crystal habit. The approach allows for the formation of two crystal habits (rod and hexagonal) of YADH I that are controlled by pH and temperature.

Chemical cross-linking of the enzyme crystals (CLECs) stabilises the crystals to harsh conditions such as high temperature, extremes of pH and high concentrations of organic solvents. A hierarchy of tests has been developed to determine the robustness of these CLECs under process conditions. The control of crystallisation conditions may allow for the selection of the crystal habit most chemically stable for the process. Catalytic studies show that hexagonal CLECs are more stable than rod CLECs at higher temperatures, in acidic and alkaline conditions and in the presence of proteases. Rod CLECs however are more active than hexagonal CLECs in aqueous-organic solvents ranging from log P values of -0.76 to 3.0. Kinetic studies show that the catalytic velocity, $k_{cat}.K_m^{-1}$, of rod CLECs is double that of hexagonal CLECs and free YADH I.

Crystallisation conditions, such as protein concentration, pH and precipitant concentration, used for the preparation of YADH I CLECs influence not only the physical properties, such as the size and morphology, of the enzyme crystals formed but also their mechanical stability under shear conditions. Using a scale-down, rotating shear device, small rod YADH I CLECs are not damaged over a range of

energy dissipation rates investigated. In contrast, hexagonal YADH I CLECs show significant breakage due to shear-induced attrition. This is important for the design and operation of large-scale biocatalytic reactors using CLEC-based catalysts. The recovery of the CLEC catalysts via filtration can simplify downstream processing. Both rod and hexagonal YADH I CLECs are not damaged as a result of pressure during filtration. Rod CLECs have a greater filtration flux and lower cake resistance than the hexagonal CLECs up to 100 kPa of pressure. Both CLEC forms maintain a constant specific cake resistance during filtration up to 100 kPa of pressure.

The rotating shear device is a useful scale-down tool to predict the breakage of a batch of CLECs. Breakage can reduce the recovery of the catalyst due to possible membrane fouling generated by shear-induced attrition. The shear device is a useful tool to estimate the impeller speeds where breakage of the CLEC catalysts might occur in a stirred-tank reactor. It has been shown that no breakage of CLECs, at speeds sufficient to disperse the crystals, would occur in a standard Rushton turbine reactor.

11.2 Future Work

In this research project, the crystallisation conditions of enzymes, their subsequent cross-linking followed by the catalytic and mechanical studies of their robustness have been investigated. Even though these CLEC biocatalysts have been shown to be catalytically and mechanically more stable than free enzyme and their crystalline counterpart, the sceening procedure to determine the crystalline window of optimum recovery and crystal form can be very labour-intensive and time-consuming. A possible solution may be to employ an automated system to carry out the screening as well as the defined catalytic and mechanical tests of a batch of CLECs that may have industrial interest and importance.

A robotic automated system, such as the Multiprobe®II (Packard BioScience Company) operated under Windows NT®, may simplify the work by reducing the workload, reagent costs and sample supply. It has been used in other areas such as clinical diagnostics, molecular biology and immunoassays (Multiprobe®II handbook, Packard BioScience Company). The automated system utilises a range of microplates that can be combined with ancillary equipment (Multiprobe®II handbook,

Packard BioScience Company) such as microplate readers and mixers for the assaying of enzyme activity, pH probing for studying activity in different pHs and thermal cyclers for temperature stability studies. The system is resistant to organic solvents, making it ideal for solvent stability studies. The mechanical studies with CLECs can be simplified by incorporating a rotating-disc in wells for studying shear. The capacity to withdraw fluids from below the well (Multiprobe®II handbook, Packard BioScience Company) will simplify the study of filtration of the CLEC biocatalysts. Areas of interest that could be simplified by this automated system would be the screening of the crystallisation conditions of *E.Coli* transketolase for its optimum recovery. This would allow a more detailed study on the different variables such as pH and precipitant type and concentration on the crystallisation of transketolase.

Reactor studies with *C.rugosa* lipase CLECs in a Rushton turbine, stirred at 200 rpm, have shown that the reaction rate decreases significantly after the third reaction cycle. This could possibly be due to pH gradients formed within the enzyme crystals at low ionic strengths (Tischer and Kasche, 1999). Further work could involve washing the CLECs between reaction cycles and also measuring their activity in the presence of buffer. The activity of CLECs may require a different assay for the determination of the protein content in the CLECs. The Lowry assay used in the determination of protein concentration may not be accurate since the reactive amino groups are protected from inactivation by glutaraldehyde cross-linking (Visuri *et al.*, 1999). The nitrogen content of cross-linked samples can be measured by a Kjeldahl method to obtain the protein content (Visuri *et al.*, 1999). Visuri *et al* (1999) have used this method for the determination of specific activity of glucose isomerase CLECs.

One fundamental obstacle to the use of NAD(H)-dependent oxidoreductases on a large-scale has been the expense of their cofactors. Nicotinamide cofactors cost too much to be used as stoichiometric reagents on a large-scale. If nicotinamide cofactor-dependent enzymes like YADH I are to be employed as catalysts for preparative chemistry, *in situ* cofactor regeneration must be employed. In the case of

YADH I, a second system, the regenerative system, must be used. The regenerative system may involve a combination of oxidising or reducing reagents and enzymes. A possible method may be to use malate, through the action of malate dehydrogenase, to regenerate the NAD cofactor.

A fundamental problem in cofactor regeneration is the instability of the cofactor in acidic and alkaline conditions (Chenault and Whitesides, 1987). It is therefore important to determine the pH of the system in which cofactor regeneration is to be carried out. Destruction of oxidised cofactor is minimised by acidic conditions and destruction of reduced cofactor is minimised by alkaline conditions. Selective hydrolysis of either form would decrease the total concentration of NAD cofactor. An estimate of the rate of destruction of total cofactor requires a knowledge of the rate constant for the hydrolysis of each cofactor form and the steady-state concentration of each of the two forms. The steady-state concentrations of the two cofactor forms depend on three parameters: (a) the total concentration of NAD (oxidised and reduced), (b) the relative Michaelis constants (k_m) for NAD and NADH of the enzymes catalysing oxidation and reduction respectively, and (c) the relative activities present of the two enzymes. Once the relative steady-state concentrations of NAD and NADH are known, the rate of decomposition of the mixture may be calculated (Chenault and Whitesides, 1987).

The reaction used for regeneration should proceed in high yield, and the total turnover numbers for the cofactor should be high (TTN = total turnover number = total number of moles of product formed per mole of cofactor present). The TTN number is an important factor as it indicates the loss of cofactor caused by degradation. In order to determine the amount of product (acetaldehyde) converted as a function of time, an assay has to be devised. A possible method of determining the amount of acetaldehyde produced is through a highly sensitive colorimetric method developed by Paz *et al* (1965). In this first step, the reagent N-methyl benzothiazolone hydrazone hydrochloride (MBTH) couples with the carbonyl group to form an azine. The azines formed from aldehydes have an active hydrogen which can react with the $FeCl_3$ oxidized form of MBTH to give rise to tetraazopentamethine cyanine dyes used in the colorimetric procedure. The method is very sensitive in that microgram amounts of the carbonyl compound can be identified and accurately measured (Paz *et al.*, 1965).

12 CRYSTALLISATION OF TRANSKETOLASE

12.1 Introduction

To date, the major applications of CLECs have been in organic synthesis, such as in the production of high fructose corn syrup, the resolution of chiral compounds, peptide synthesis and the formation of C-C bonds (Margolin, 1996). It is this last area of CLEC application which is the focus for the crystallisation of *E.coli* transketolase (TK) for its potential use in C-C formation. Unlike YADH I, the difficulty in the crystallisation of transketolase is the number of steps it takes to bring the enzyme to a state of purity for crystallisation.

Recombinant *E.coli* PQR 700 cells expressing transketolase intracellularly were disrupted in a Lab 40 homogeniser to release the intracellular components for analysis. The enzyme was removed from the crude homogenate by centrifugation and used for crystallisation. Many purification methods such as salting-out using ammonium sulphate followed by dialysis, FPLC ion-exchange column chromatography, batch separation using DE-52 beads and FPLC gel filtration chromatography were used to bring the clarified transketolase extract to a state of partial purity for its subsequent crystallisation. The crystallisation diagrams established in Section 5 have been used to see how effective the diagrams were in developing a window of crystallisation for transketolase.

12.2 Materials and Methods

12.2.1 Preparation of crude extract using a Lab 40 homogeniser

E.Coli pQR 700 cells containing transketolase was resuspended in buffer A [50 mM Tris-HCl pH 7.5, 1 mM ethylenediamine tetraacetic acid (EDTA), 0.006 M β-mercaptoethanol and protease inhibitors phenylmethylsulfonyl fluoride (PMSF) and benzamidine (BAM) at concentrations of 1 x 10^{-4} M and 2 x 10^{-5} M respectively. 12.5g of cells were resuspended in 50 mL of buffer A, by stirring for 1 hr at 4°C, to give a 25% (w/v) suspension. Crude extracts (50mL) were prepared by high pressure homogenisation (4 passes at 1100 bar) and aliquoted into 1.5 mL Eppendorf tubes for small-scale studies.

12.2.2 Clarification using a Microcentaur centrifuge

The transketolase enzyme in Eppendorf tubes was clarified by centrifugation using a laboratory bench-scale centrifuge at 13, 000 rpm for 15 minutes. This process removed the cellular debris from the clear supernatant containing the tranketolase enzyme.

12.2.3 Batch separation technique as a purification method

1 mL of DE 52 (Whatman, Inc.), a cellulose ion exchanger, was resuspended in 20 mM Tris-HCl, pH 7.6. An equal volume of clarified TK extract at 130 Units.mL^{-1} was added to the beads and gently stirred for 30 minutes at room temperature.

The beads were sedimented by centrifuging at 1, 000 rpm and the supernatant was assayed for TK activity to determine the amount of TK that bound to the beads. The beads were then washed again in 20 mM Tris-HCl, pH 7.6 and assayed for TK activity. This was followed by a batch procedure in which the beads were stirred with increasing salt (NaCl) concentrations of 100 mM to 500 mM in 20 mM Tris-HCl, pH 7.6, while assaying for TK activity at each stage. This was to determine at which salt concentration TK was eluted. The purity of TK was determined by SDS-PAGE electrophoresis as described in Section 4.4.

12.2.4 Laboratory scale enzyme purification and crystallisation

12.2.4.1 Protamine sulphate precipitation

A final aqueous protamine sulphate (Grade X from Salmon, Sigma chemical co.) concentration of 0.05 % (w/v) was added to a clarified crude extract (10 mL). The resulting suspension was stirred at 4 °C for 30 minutes and the precipitate was removed by centrifugation (30 minutes, 15, 000 rpm) to leave the TK enzyme in the supernatant.

12.2.4.2 Ammonium sulphate precipitation

Solid ammonium sulphate was added slowly, while stirring, to the supernatant at 4°C (29.5 g in 100 mL) to give 50% (w/v) saturation (Boistelle and Astier, 1988). After 30 minutes, the precipitate was removed by centrifugation (30 minutes, 15, 000 rpm) using a JA-20 Beckmann centrifuge at 4 °C. The clarified supernatant was made up to 75% (w/v) ammonium sulphate (48.3 g in 100 mL to afford 75% (w/v) saturation), while stirring at 4 °C. After 30 minutes, the precipitate was centrifuged at 15, 000 rpm for 30 minutes and the resulting pellet was resuspended in 2 mL of buffer A (Section 12.2.1).

12.2.4.3 Preparation of dialysis tubing

Dialysis tubing (Medicell International Ltd.) with a molecular weight cut-off of 12-14 kD was boiled for 30 minutes in a solution of a 5% (w/v) sodium bicarbonate ($NaHCO_3$) and 50 mM EDTA. The tubes were mixed with a glass rod and rinsed several times with distilled water. The membranes were then rinsed several times in buffer A (Section 12.2.1) prior to dialysis.

12.2.4.4 Dialysis

The precipitate containing TK was redissolved in buffer A (2 mL) (Section 12.2.1) and poured into a preprepared dialysis tubing. The tubing was then submerged into a 2 L solution of buffer A (Section 12.2.1) and gently stirred at 4 °C. After equilibrium was reached (approximately 3 hours), the dialysing buffer solution was changed and dialysis was repeated for another 3 hours.

12.2.4.5 Ion-exchange using Fast Protein Liquid Chromatography (FPLC)

The FPLC system (Pharmacia) consists of a P-500 pump monitored by a liquid chromatography controller LCC-500 plus. The pumps are connected to a mixer (Pharmacia) which is connected to the column. The mixer allows a gradient to be applied to the system. The protein eluted is detected by the LKB-UV-MII (Pharmacia) monitor and chart recorder. The protein is collected by the automated Frac-100 fraction collector (Ion Exchange Chromatography Principles and Methods, Pharmacia Biotech).

The dialysed protein sample was loaded via a 2 mL superloop onto a Fast-Flow Q (FFQ) Sepharose ion-exchange XK-26 column (Pharmacia). The column was prepacked up to a final bed volume of 25 mL and equilibrated with 4 column volumes of both high salt buffer A (Section 12.2.1) containing 1 M NaCl and low salt buffer A (Section 12.2.1). The transketolase enzyme was eluted using a salt gradient: Buffer A (Section 12.2.1) to Buffer A (Section 12.2.1) containing 1 M NaCl at 4 $mL.min^{-1}$.

12.2.5 Size exclusion chromatography

For this particular study, the fractions, after ion-exchange chromatography, containing the most TK activity were concentrated and loaded onto two size exclusion columns.

One fraction was loaded onto a column (30 x 1 cm) of Superose 12 (Pharmacia Biotech). Another fraction was loaded onto a column (30 x 1 cm) of Superdex 75 (Pharmacia Biotech). The samples were washed with 30 mL of Buffer A (Section 12.2.1) and collected using the automated fraction collector. The sample loop volume for this study was fixed at 0.5 mL (Gel Filtration Principles and Methods, Pharmacia Biotech).

12.2.6 Concentration of protein solution

The fractions containing the most TK were concentrated in a Centricon 10 (Amicon, Inc.) protein filter membrane by centrifugation using a JA-20 Beckmann centrifuge at 4 °C. The speed for centrifugation was set at 7, 000 rpm. The protein was concentrated to a final protein concentration of 20 $mg.mL^{-1}$. Protein concentration was measured using a protein assay method mentioned in section 4.3. The sample was washed twice with piperizine-N,N'-bis 2-ethanesulphonic acid (PIPES) buffer (50 mM, pH 6.4) containing thamine pyrophosphate (TPP) (2mM) and calcium chloride ($CaCl_2$) (9 mM).

12.2.7 Crystallisation of transketolase

For the crystallisation of transketolase, lanes on 24-well Linbro plates (Hampton research, Inc.) were set up using the hanging drop method. A range of ammonium sulphate conditions (40-65% (w/v) in PIPES buffer, pH 6.4) were investigated. A lane would consist of aqueous saturated ammonium sulphate (1 μL) and PIPES washed TK (9 μL) on the cover slip equilibrated against aqueous ammonium sulphate solution (40-65% (w/v) in PIPES buffer, 1 mL) in the wells (Littlechild *et al.*, 1995). Vacuum grease was applied around the rim of the well as a seal and the cover slip was placed directly above the well. The hanging-drop vapour diffusion method allowed for the withdrawal of water from the drop thereby concentrating the protein in the drop causing it to crystallise.

12.2.8 Large-scale crystallisation using a split-petri dish

A split petri dish (BDH, Merck) was used in the large-scale crystallisation of transketolase similar to that of the hanging-drop vapour diffusion method (Section 2.4.4). One side of the dish consisted of the reservoir buffer containing 5 mL of an aqueous ammonium sulphate solution (40-65%(w/v)) in 50 mM PIPES buffer, pH 6.4. The other side of the dish contained 100 μL of a TK protein solution (17 $mg.mL^{-1}$) and 11 μL of the reservoir buffer. This corresponded to a 9:1 ratio of protein solution to reservoir buffer. The volumes of protein solution and reservoir

buffer were scaled up according to this ratio. The concentrated salt solution in the reservoir buffer equilibrated with the protein solution through a small opening, above the split, after the cover of the petri dish had been sealed with vacuum grease.

12.2.8.1 Linked enzyme assay for transketolase

The assay system used by Heinrich *et al* (1972) was used to quantitate the amount of TK activity. This assay involved adding the substrate ribose-5-phosphate (ribose-5-P) in the presence of linking enzymes and cofactors in the cascade pathway which eventually led to the oxidation of NADH in the final step. The assay could be monitored spectrophotometrically at 340 nm, indicated by a decrease in absorbance (Figure 46).

The assay involved adding ribose-5-phosphate, the linking enzymes, cofactors and magnesium ions in excess so that each component was not limiting. Under the assumption that the TK catalyzed step was the limiting step, the rate of NADH oxidation (indicated by a decrease in absorbance at 340 nm) was directly proportional to the concentration of TK in the assay.

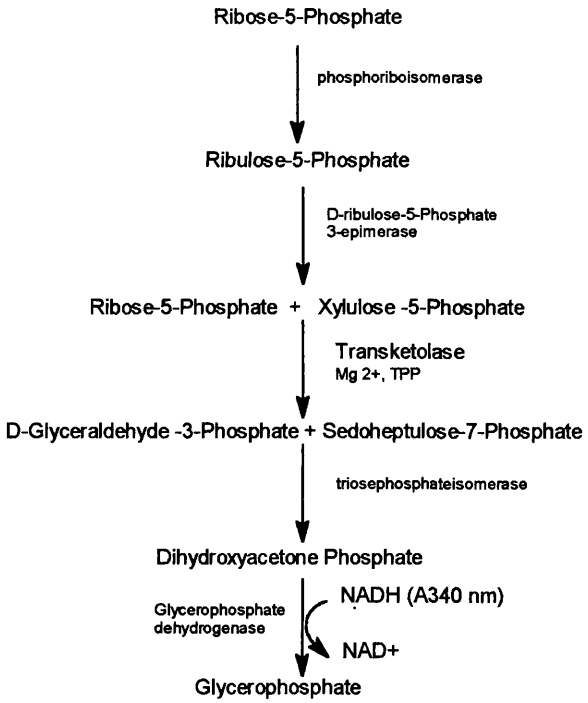

Figure 46: The enzyme linked assay system of transketolase.

The assay consisted of adding the following reagents expressed in their final concentrations, in a 1.5 mL cuvette: TPP, 0.211 mM; $MgCl_2.6H_2O$, 9 mM; NADH (di-sodium salt), 0.228 mM; α-glycerophosphate dehydrogenase-triosephosphate isomerase (α-GDH-TPI), 0.2 Units.mL^{-1}; phosphoriboisomerase, 0.2 Units.mL^{-1}; D-ribulose-5-phosphate-3-epimerase, 0.2 Units.mL^{-1}; glycylglycine buffer, 30 mM, pH 7.6 and TK source, 0.001-0.03 Units.mL^{-1}. After an initial lag phase of 10 minutes, D-ribose-5-phosphate (0.84 mg.mL^{-1}) was then added to the above mixture and the decrease in absorbance of 340 nm, due to NADH oxidation, was recorded with time. All the above assay mixtures with the exception of TK and ribose-5-P were preprepared and stored at -20°C. Glycylglycine buffer, pH 7.6 was preprepared at a concentration of 0.1 M with 0.5 mg.mL^{-1} Bovine Serum Albumin (BSA).

A lag period exists in the multi-enzyme linked assay (Egan and Sable, 1981) due to the dependence of the product accumulation from previous steps. Also, equilibrium must be achieved for the first two enzymatic steps, as there is competition between phosphoriboisomerase and transketolase for ribose-5-P. These features contributed to the initial lag stage. Once steady state is reached, the rate of NADH oxidation becomes constant and the value can be recorded in the calculation.

The rate of NADH oxidation (ΔA/t) and TK concentration can be derived as follows using Beer-Lambert's law: $C = A/ \epsilon l$

where C = concentration, A = absorbance, ϵ = extinction coefficient and l = light path length.

$$C/t = (\Delta A/ \Delta t) / \epsilon l$$

where C/t = (μmole.mL^{-1}) / min = Units.mL^{-1} = TK concentration in the assay and $\Delta A/ \Delta t = min^{-1}$.

ϵ_{NADH} based on 1 cm light path = 6.3 mL.μmole^{-1} (Harris, 1995).

$$\Rightarrow \text{[TK] in assay} = \frac{\text{rate of NADH oxidation (min}^{-1})}{\epsilon_{NADH}\ (\text{mL.}\mu\text{mole}^{-1})}$$

$$= (\mu\text{mole.mL}^{-1})\ \text{min}^{-1}$$

$$= \text{Units.mL}^{-1}$$

The total assay volume is 1.5 mL:

$$\text{Units of TK in assay} = 1.5 \text{ mL (rate of NADH oxidation) } \text{min}^{-1} / 6.3 \text{ } \mu\text{mole}^{-1}$$
$$= 0.238 \text{ (rate of oxidation) } \mu\text{mole.min}^{-1}.$$

$$\text{Activity of TK in sample} = \frac{\text{TK in assay (Units) X Dilution factor}}{\text{Volume of sample added (mL)}}$$

$$= \text{Units.mL}^{-1}$$

Therefore the TK concentration in the sample takes into account the final dilution in the assay.

12.3 Results and Discussion.

12.3.1 Crystallisation from a crude TK extract

Transketolase (TK) was crystallised previously from a clarified crude extract by techniques mentioned earlier. One of these methods used was batch crystallisation (Ducruix and Giege, 1992) using increasing concentrations of salt such as sodium chloride, ammonium sulphate, ammonium citrate, sodium acetate, calcium acetate and increasing percentage (v/v) of dimethyl sulphoxide in water. The protein concentration in the clarified extract was 20 $mg.mL^{-1}$. This method was used to bring the solution to a state of supersaturation by adding the precipitant increasingly and setting the mixture aside until crystallisation had occurred. This technique resulted only in precipitation.

Another method included a 50 % (w/v) and 75 % (w/v) ammonium sulphate precipitation (Section 12.2.4.2) followed by dialysis against water (Ducruix and Giege, 1992) and low salt buffer (50 mM Tris-HCl, pH 7.0) (Section 12.2.4.4). Other methods included the temperature shift method (King, 1964), increasing the protein concentration and adjusting the pH to the pI of transketolase. These methods only resulted in the formation of precipitate. A purification method devised by Littlechild (1995) was used to produce TK crystals.

12.3.2 Purification of TK and crystallisation using hanging-drop method

The purification strategy involved resuspending *E.coli* pQR 700 cells containing transketolase in 50 mM Tris-HCl, pH 7.5, 1 mM EDTA, β-mercaptoethanol, PMSF and benzamidine (Boistelle and Astier, 1988) (Section 12.2.1). The resuspended cells were homogenised at 1100 bar with 4 passes through the Lab 40 homogeniser (Section 12.2.1). The homogenised TK extract was clarified in Eppendorf tubes using a Microcentaur centrifuge (Section 12.2.2). Protamine sulphate was added to the clarified TK extract at a concentration of 0.01 % (w/v) to remove any DNA present in the preparation (Section 12.2.4.2). The removal of DNA

was essential since it might interfere with the binding of TK onto an ion-exchange column later on in the purification procedure.

A 50% (w/v) ammonium sulphate precipitation (Section 12.2.4.2) was used to remove any contaminating proteins in the TK extract. Dialysis of TK against a larger volume (2 litres) of Buffer A (Section 12.2.1) through a semipermeable membrane was to remove the sulphate ions that were inhibitory to the transketolase (Littlechild *et al.*, 1995). Sulphate and phosphate ions were found to inhibit transketolase approximately 50% between concentrations of 0.01 and 0.02 M (Littlechild *et al.*, 1995). Dialysing the TK twice minimised inhibition by reducing the sulphate concentration down to 3.3 pM.

The dialysed transketolase was then loaded onto an FPLC ion-exchange column using a Fast-Flow Q (FFQ) sepharose as a support (Section 12.2.4.2). The FFQ Sepharose ion exchangers are highly cross-linked agarose beads of high chemical and physical stability (Ion Exchange Chromatography Principles and Methods, Pharmacia Biotech). These 90 μm beads have a triethyl aminoethyl functional which remain charged over a wide pH range. A pH of 7.5, greater than the pI of transketolase, was chosen so that TK would exist in its negatively-charged state for binding onto the ion-exchanger.

TK was eluted off the column by applying a gradient of salt (NaCl) from 0-1 M. The counter ion Cl^- competes with TK for binding to the ion exchanger and at a specific concentration displaces TK from the column. The total activity of TK was assayed at each stage using the enzyme linked assay system (Section 12.2.9.1).

Table 16 of *Escherichia coli* transketolase:

Stage	Volume (mL)	Amt. protein (mg)	Total Units (U*)	Activity ($U^*.mg^{-1}$)	% Yield	Purification Factor
Crude extract	10	180	2600	14.4	100	1.00
protamine sulphate precipitation	9.5	142.5	3990	28.0	153	1.94
50-75% (w/v) ammonium sulphate precipitation	9.5	38	950	25	36.5	1.74
Dialysis	20	20	800	40	30.8	2.78
ion-exchange	10	6.28	680	108	26.2	7.50

*μmole of NADH utilised per minute at 308K, pH 7.6 in the linked assay system.

Percentage yield represents the total units of enzyme after each stage divided by the total units in the crude extract

Purification Factor represents the specific activity after each stage divided by the specific activity in the crude extract

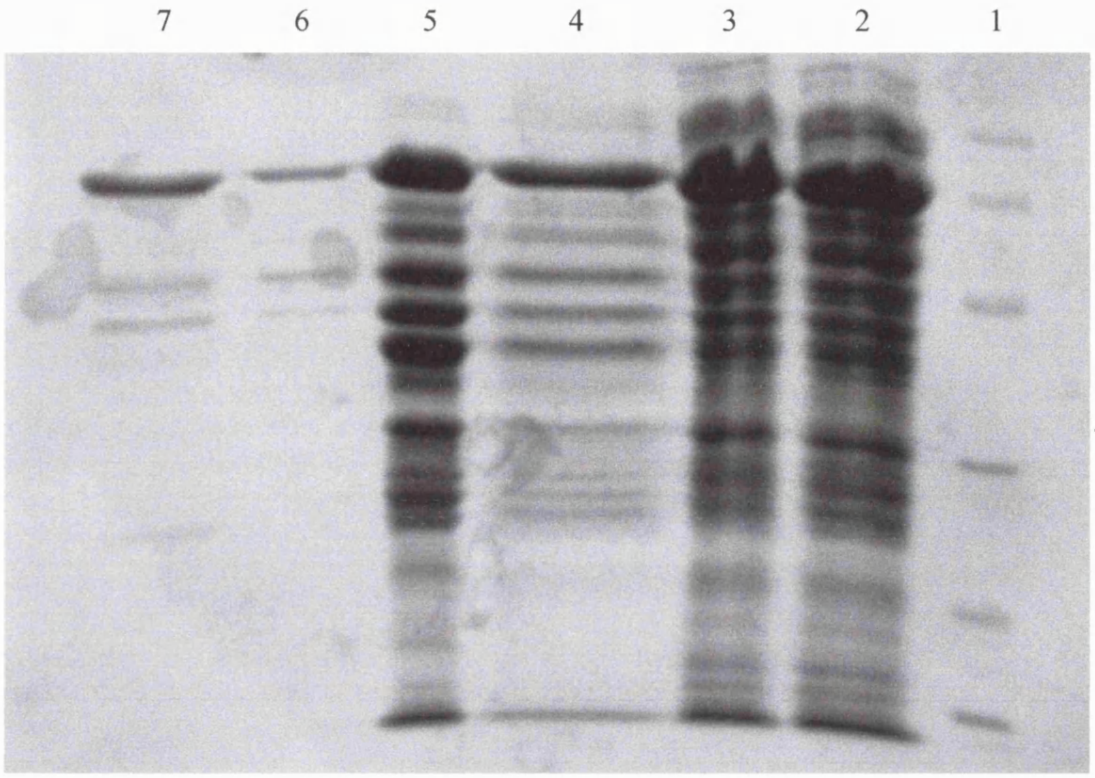

Gel 3: A 12.5% SDS-PAGE gel of the purification of TK. Lane 1 is the low molecular weight markers. Lane 2 is clarified crude TK extract. Lane 3 is TK treated with protamine sulphate. Lane 4 is TK treated with 50 %-75 % (w/v) ammonium sulphate. Lane 5 is TK after dialysis. Lanes 6 and 7 are TK after FFQ Sepharose column chromatography.

Using this strategy, transketolase was purified to a factor of 7.5 with a final yield of 26.2 % as recorded in Table 16. The TK after ion-exchange chromatography appeared quite pure (Gel 3) and was used for crystallisation according to the Hanging-drop vapour diffusion technique (Section 2.4.4). Crystals were grown in 50 % (w/v) ammonium sulphate containing 2 mM Thiamine Diphosphate (TPP) , 9 mM $CaCl_2$ in 50mM PIPES buffer at pH 6.4. These crystals had a needle-like morphology characteristic of transketolase as shown by Littlechild (1995).

12.3.3 Batch purification of TK

A batch separation method (Section 12.2.3) using DE 52 beads (Whatman, Inc.) was used to purify TK in bulk. Batch separation is a very rapid technique with

no technical difficulties caused by swelling or shrinking of of ion exchanger beads. Most of the TK were bound to DE 52 at low salt concentration (20 mM Tris-HCl, pH 7.6) and were eluted at 200 mM salt concentration (Figure 47). The percentage yield of TK recovery according to Table 17 was very high (98.8%), however TK was only purified to a factor of 2.7. Gel 4 (lane 3) showed that this purification method removed the contaminating proteins of higher molecular weights in the preparation. The purification factors obtained using the batch method and FFQ Sepharose column were the same (PF = 2.7). Comparing Tables 16 and 17, the percentage yield using the batch method was better than the FFQ column. The batch method was also much simpler and cheaper to operate at a larger scale.

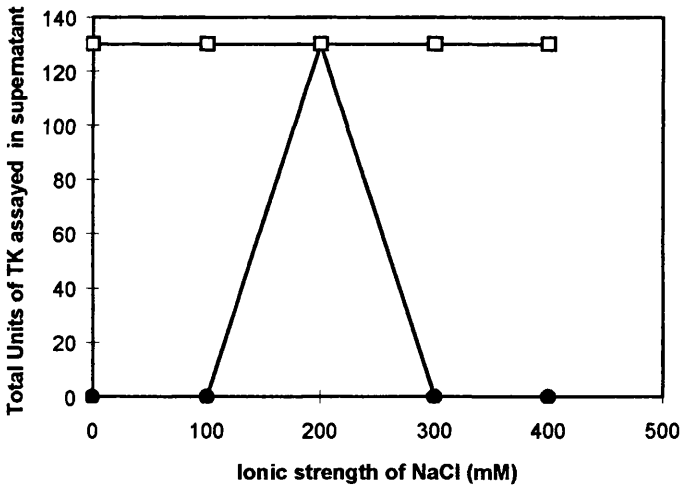

Figure 47: Elution profile of TK using DE52 beads. □, total units of TK bound onto the DE52 beads by assaying the supernatant after the beads were washed in low salt buffer. ●, total units of the eluted TK after each salt concentration.

Table 17: Purification using batch separation method

Stage	Volume (mL)	Amt. protein (mg)	Total Units(U*)	Activity ($U^*.mg^{-1}$)	% Yield	Purification Factor
Crude extract	1	20	130	6.5	100	----
Batch separation	1.8	7.2	126	17.5	98.8	2.7

* µmole of NADH utilised per minute at 308 K, pH 7.6 in the linked assay system.

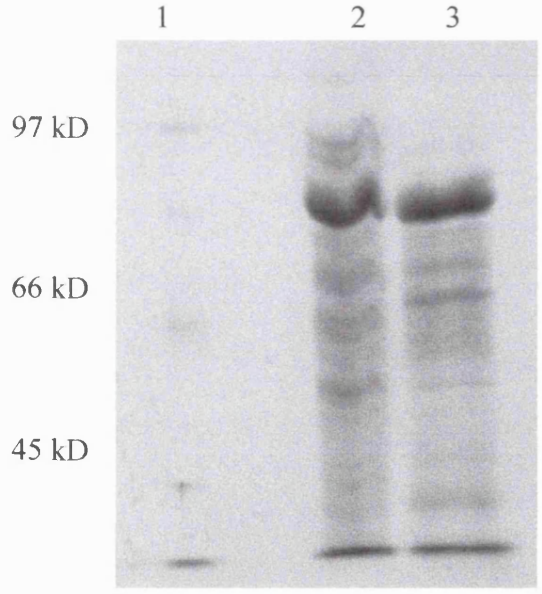

Gel 4: A 12.5 % SDS-PAGE showing the batch separation purification. Lane 1 shows the low molecular markers. Lane 2 shows clarified crude TK. Lane 3 is the TK purified using the batch separation method.

12.3.4 Purification of TK using an ion-exchange followed by gel-filtration

Another crystallisation strategy was devised to purify transketolase using fewer steps. This involved loading the transketolase onto the FFQ-Sepharose ion-exchanger after protamine sulphate precipitation.

Chromatography, as shown on Gel 3 (lanes 6 and 7), had been very effective in removing most of the contaminating proteins. This procedure omitted the need for ammonium sulphate precipitation and dialysis which reduced the yield of transketolase greatly. Almost 70% of transketolase was lost in those two steps according to Table 16.

Purification of *E.coli* transketolase using Fast Flow Q ion-exchange and Superdex 75/ Superose 12 gel filtration chromatography

Table 18(a): Using FFQ ion-exchange and Superdex 75 gel filtration

Step	Volume (mL)	Amt. protein (mg)	Total Units (U*)	Activity ($U*mg^{-1}$)	% Yield	Purification Factor
Crude extract	4	64	1360	21.25	100	-
Protamine sulphate precipitation	3	39	1020	26.15	75	1.23
FFQ ion-exchange	2.5	5.25	550	62.86	40.4	2.96
Superdex 75 gel filtration	5	3.5	300	85.7	22	4.03

*μmole of NADH utilised per minute at 308K, pH 7.6 in the linked assay system (Heinrich *et al.*, 1972).

Table 18(b): Using FFQ ion-exchange and Superose 12

Step	Volume (mL)	Amt. protein (mg)	Total Units (U*)	Activity ($U^*.mg^{-1}$)	% Yield	Purification Factor
Crude extract	4	64	1360	21.25	100	-
Protamine sulphate precipitation	3	39	1020	26.15	75	1.23
FFQ ion-exchange	5	6	470	31.3	34.6	1.47
Superose 12 gel filtration	8	1	384	96	28.2	4.52

*μmole of NADH utilised per minute at 308K, pH7.6 in the linked assay system (Heinrich *et al.*, 1972).

One fraction (gel 5, lane 4) of the purified TK was loaded onto a Superdex 75 gel filtration column (Section 12.2.6) while another fraction (gel 5, lane 6) was loaded onto a Superose 12 gel filtration column (Section 12.2.6). The purpose was to determine how efficient these two size exclusion columns were in removing the lower molecular weight contaminants that were 45 kDa and lower (Gel 5 , lanes 4 and 6).

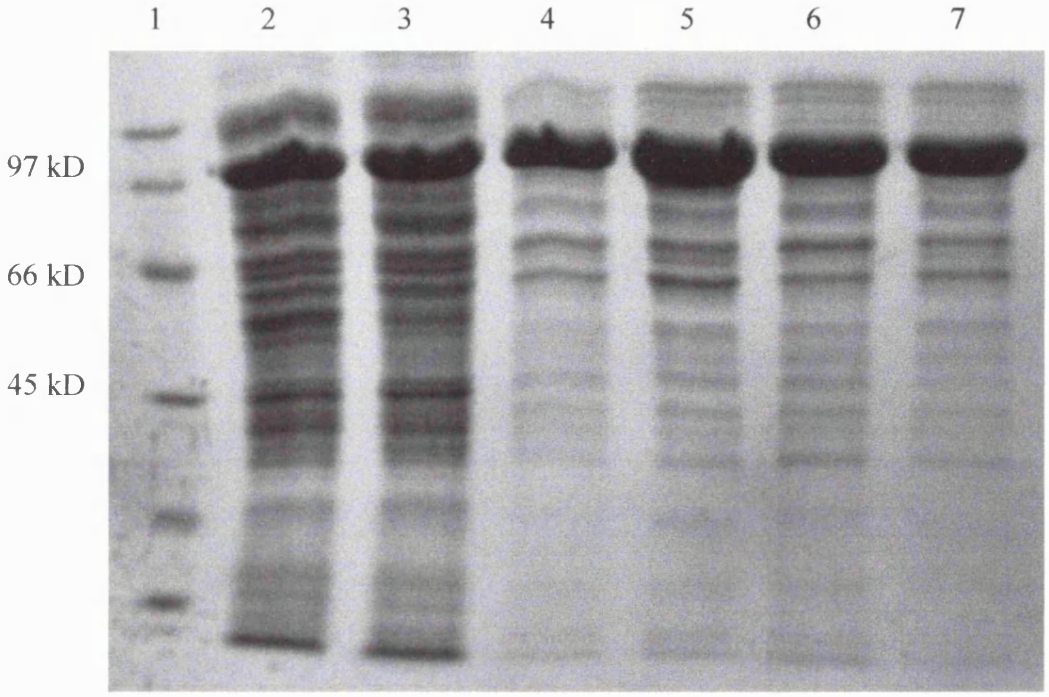

Gel 5: A 12.5 % SDS-PAGE gel showing purification of TK using FFQ-Sepharose and the 2 gel filtration columns, Superdex 75 and Superose 12. Lane 1 is the low molecular weight markers. Lane 2 is the clarified TK. Lane 3 is the TK treated with protamine sulphate. Lanes 4 and 6 are TK purified with FFQ-Sepharose. Lane 5 is TK purified with Superdex 75 after FFQ-Sepharose. Lane 7 is TK purified with Superose 12 after FFQ-Sepharose.

Superdex 75 consists of highly cross-linked porous agarose beads that fractionate protein between 3 to 70 kD in molecular weight (Boistelle and Astier, 1988). TK, being 73 kD, was eluted near the beginning since it is larger than the largest pores in the gel. Hence, transketolase is confined to the void volume. Superose 12, on the other hand, can fractionate proteins between 1 to 300 kD in molecular weight (Gel filtration Principles and Methods, Pharmacia Biotech). TK, using this gel support, was eluted in the middle of the elution profile.

TK was purified to the factors of 4.03 and 4.52 by using a Superdex 75 and a Superose 12 gel filtration columns respectively according to Table 18. However, purification to homogeneity was not evident by using these two size exclusion columns (Gel 5, lanes 5 and 7). There were proteins in the region of 45 kD that could not be removed.

12.3.5 Crystallisation of TK after Superose 12 gel filtration

Crystallisation was attempted using the TK preparation after Superose 12 gel filtration. This was done to determine if transketolase could be crystallised from a partially purified preparation. By using the hanging-drop vapour diffusion method (Section 12.2.8) as before, crystals were evident in 60 %, 58 % and 54 % ammonium sulphate with 2 mM TPP and 9 mM $CaCl_2$ in 50 mM PIPES buffer, pH 6.4. The protein concentration was set at 17 $mg.mL^{-1}$. The crystals had the same needle-like morphology as mentioned before and were surrounded by precipitate in the droplet.

12.3.6 Crystallisation using split petri dish

Crystallisation was attempted on a larger scale using the split petri dish method (Section 12.2.9). Crystals and precipitate appeared at 60% ammonium sulphate using the TK purified after the superose 12 gel filtration (Gel 5, lane 7). The total units of TK used for the crystallisation was 22.5 $\mu mole.min^{-1}$ at a protein concentration of 17 $mg.mL^{-1}$. The crystals were washed in a 70% ammonium sulphate mother liquor (McPherson, 1990). The crystal suspension was pelleted at 7, 000 rpm for 10 minutes and redissolved in 200 µL of a 50 mM PIPES buffer, pH 6.4.

By using the TK linked assay system (Section 12.2.9.1), the total units of TK was 3.04 $\mu mole.min^{-1}$ which was 13.5 % of the total input of TK used for the crystallisation trial. Further experiments will require screening for conditions in which crystallisation of transketolase will be favoured.

12.3.7 Batch crystallisation of TK using a crystallisation diagram

Yeast transketolase has been crystallised previously by Nilsson (1993) using the hanging-drop method. Crystals were obtained from wells containing 13 to 16 % (v/v) PEG 6000 in 50 mM glycyl-glycine buffer, pH 7.9 with 5 mM $CaCl_2$ and

5 mM TPP cofactor. Yeast TK has also been crystallised using 46 % (w/v) ammonium sulfate in the presence of PEG 6000 in 50 mM glycylglycine buffer (Littlechild, 1991; Kuimov *et al.*, 1992).

A crystallisation diagram was set up for *E.coli* TK using the crystallisation conditions from yeast. The diagram took into account the three variables, protein concentration ($mg.mL^{-1}$), PEG 6000 and ammonium sulphate concentrations (Figure 48). *E.coli* PQR 700 cells were suspended in 50 mM glycylglycine buffer, pH 7.6, homogenised, and the clarified extract was used for crystallisation without further purification. The TK solution also included 2 mM TPP cofactor.

The window of crystallisation of TK is shown in Figure 48 to be around 8.4 to 10 $mg.mL^{-1}$ protein concentration, 27 to 35 % (v/v) PEG 6000 and 10 to 70 mM ammonium sulphate concentration. The morphology of the crystals were prism-shaped similar to yeast TK (Kuimov *et al.*, 1992). However, a relatively low crystal activity recovery, 4 %, was obtained during the screening. Other possible experiments could use this method to crystallise TK after one column of purification with Sepharose Q. By using the Hampton screening kit (Hampton research, Inc.), crystals were obtained from conditions from the following conditions: (a) 0.1 M Tris-HCl, pH 8.5, 0.2 M sodium citrate, 30 % (v/v) PEG 400, and (b) 0.2 M Calcium chloride, 0.1 M sodium HEPES, pH 7.5 and 25 % (v/v) PEG 400.

It would be useful to screen in batches using the above conditions for the optimisation of TK crystals.

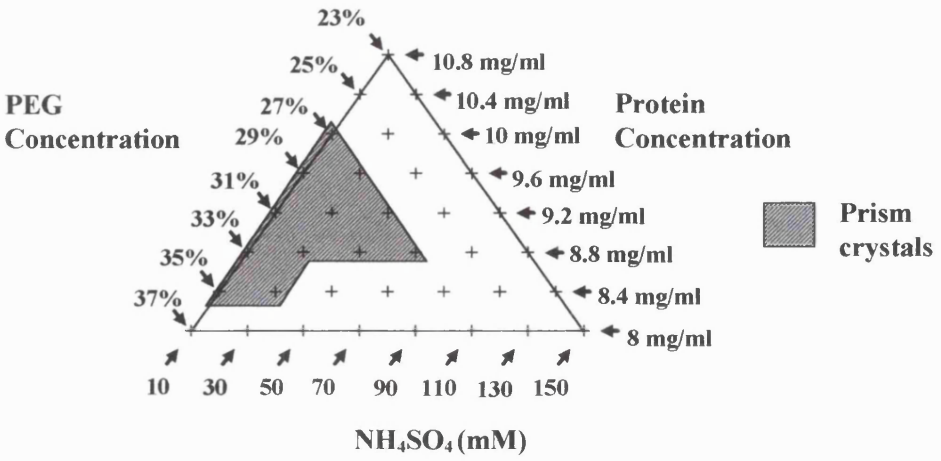

Figure 48: A crystallisation window for the crystallisation of *E.coli* transketolase.

12.4 Conclusions

This section shows that crystallisation and the optimisation of crystallisation conditions can be difficult. Even though YADH I and *C. rugosa* lipase have been successfully crystallised on a large-scale using the crystallisation window technique, this technique may be more difficult for some enzymes. In the experiments, a relatively low crystal activity recovery was obtained during screening. This was possibly due to the fact that the region of optimum recovery of transketolase crystals was not yet achieved. More screening of crystallisation conditions for the optimum recovery of transketolase crystals may be required. The crystallisation 'windows' technique may possibly be used in conjunction with a purification step, such as ion-exchange chromatography, to aid the crystallisation process.

13 REFERENCES

Abergel, C., Moulard, M., Moreau, H., Loret, E., Cambillau, C., and Fontecilla-Camps, J.C. (1991). Systematic use of the incomplete factorial approach in the design of protein crystallization experiments. *J. Biol. Chem.* **266**, 20131-20138.

Allen, T. (1997). ' Stream scanning methods of particle size measurements' in particle size measurement 1 (Chapman and Hall, eds). London, U.K.

Almarsson, Orn and Klibanov, A. (1996). Remarkable activation of enzymes in nonaqueous media by denaturing organic cosolvents. *Biotech. Bioeng.* **49**, 87-92.

Aloi, L.E. and Cherry, R.S. (1996). Cellular response to agitation intensity characterised by energy dissipation at the impeller tip. *Chem. Eng. Sci.* **51**, 1523.

Ataka, M., and Tanaka, S. (1978). Effect of pH on the Dimorphic Crystal Growth of Lysozyme. *J. Phys. Soc. Japan* **45**, 1779-1780.

Atkinson, B. and Mavituna, F. (1991). 'Gas-Liquid contacting in mixing vessels' in Biochemical Engineering & Biotechnology Handbook. Macmillan Publishers Ltd, England.

Bar, R., Gainer, J.L., and Kirwan, D.J. (1986). Immobilisation of Acetobacteraceti on cellulose ion exchangers: Absorption isotherms. *Biotechnol. Bioeng.* **28**, 1166.

Barman, T. E. (1969). 'Alcohol dehydrogenase' in Enzyme Handbook (Springer-Verlag, eds). Berlin Heidelberg, N.Y.

Bedell, B.A., Mozhaev, V.V, Clark, D.S. and Dordick, J.S. (1998). Testing for diffusion limitations in salt-activated enzyme catalysts operating in organic solvents. *Biotech. Bioeng.* **58**, 654-657.

Bergmeyer, H.V., Grabl, M., and Walter, H.E. (1983). *Methods of Enzymic Analysis*, Vol. **2**. *Verlag chemie, Weinham*, 126.

Betts, L., Frick, L., Wolfenden, R., and Carter Jr., C.W. (1979). Incomplete factorial search for conditions leading to crystals of *Escherichia Coli* cytidine deaminase complexed to a transition-state analog inhibitor. *J. Biol. Chem.* **264**, 6737-6740.

Boistelle, R. and Astier, J.P. (1988). Crystallisation mechanisms in solution. *J. Crystal Growth* **90**, 14-30.

Borman, S. (1992). Cross-Lined Enzyme Crystals show promise for industrial, clinical uses. *Science/Technology*, 40-43.

Bowen, R. (1993). Understanding flux patterns in membrane processing of protein solutions and suspension. *TIBTECH* **11**, 451-460.

Boychyn, M., Yim, S.S.S., Shamlou, P.A., More, J., Bulmer, M. and Hoare, M. (1999). Characterisation of the response of shear sensitive species in the feed zone of continuous centrifuge. *Biotech. Bioeng.*, submitted.

Bradford, M. (1976). A rapid and sensitive method for the quantitation of microgram quantities of protein utilizing the principle of protein-dye binding. *Anal. Biochem.* **72**, 248-254.

Branden, C.I., Jornvall, H., Eklund, H. and Furugren B. (1975). The Enzymes, Vol. **11**. Academic Press, New York,103-190.

Brose, D., Dosmar, M., Cates, S. and Hutchison, F. (1996). Studies on the scale-up of crossflow filtration devices. *PDA Journal of Pharmaceutical Science and Technology* **50**, 252-260.

Brose, D.J., Cates, S. and Hutchison, F.A. (1994). Studies on the scale-up of microfiltration membrane devices. *PDA Journal of Pharmaceutical Science and technology* **48**, 184-188.

Byrne, A.P., Stites, W.E. (1995). *Protein Science* **4**, 2545-2558.

Carrea, G., Ottolina, G. and Riva, S. (1995). Role of solvents in the control of enzyme selectivity in organic media. *TIBTECH* **13**, 63-70.

Carter Jr., C.W. (1990). Efficient factorial designs and the analysis of macromolecular crystal growth conditions. *Methods, Companion Methods Enzymol.* **1**, 12-24.

Carter Jr., C.W., and Carter, C.W. (1979). Protein crystallization using incomplete factorial experiments. *J. Biol. Chem.* **254**, 12219-12223.

Carter Jr., C.W., Baldwin, E.T., and Frick, L. (1988). Statistical design of experiments for protein crystal-growth and the use of a precrystallization assay. *J. Cryst. Growth* **90**, 60-73.

Chantal, A., Moulard, M., Moreau, H., Loret, E., Cambillau, C. and Fontecilla-Camps, J.C. (1991). Systematic use of the incomplete factorial approach in the design of protein crystallisation experiments. *J. Biol. Chem.* **266**, 20131-20138.

Chenault, H.K. and Whiteside, G.M. (1987). Regeneration of nicotinamide cofactors for use in organic synthesis. *Appl. Biochem. Biotech.* **14**, 1470173.

Cherry, R.S. and Papoutsakis, E.T. (1986). Hydrodynamic effects on cells in agitated tissue culture reactors. *Bioprocess Engng.* **1**, 29.

Collins, A.M., Maslin, C. and Davies, R.J. (1998). Scale-up of a chiral resolution using cross-linked enzyme crystals. *Org. Process Res. Dev.* **2**, 400.

Coulson, J.M. and Richardson, J.F. (1991). 'Filtration' in Chemical Engineering, Particle Technology and Separation Processes, Volume **2**, 4th Edition (Backhurst, J.R. and Harker, J.H., eds). Pergamon Press, Oxford.

Cudney, B., Patel, S., Weisgraber, K., Newhouse, Y., and McPherson, A. (1994). Screening and optimization strategies for macromolecular crystal growth. *Acta Cryst.* **D50**, 414-423.

DeBolle, X., Vinals, C., Prozzi, D., Paquet, J., Leplac, R., Depiereux, E., Vandenhaute, J. and Feytmans, E. (1995). Identification of residues potentially involved in the interactions between subunits in yeast alcohol dehydrogenases. *Eur. J. Biochem.* **231**, 214-219.

Ducruix, A. and Giege, R. (1992). 'Phase diagrams' in Crystallisation of nucleic acids and protein (Ducruix, A and Giege, R., eds). Oxford University Press, New York.

Egan, R. and Sable, H. (1981). Transketolase kinetics. *J. Biol. Chem.* **256**, 4877-83.

Eklund, H., Nordstrom, B., Zeppezauer, E., Soderlund, G., Ohlsson I., Boiwe, T., Soderberg, B-O., Tapia, O., Branden, C-I. (1976). Three-dimensional structure of horse liver alcohol dehydrogenase at 2.4 Å resolution. *J. Mol. Biol.* **102**, 27-59.

Feher, G and Kam,Z. (1985). Nucleation and growth of protein crystals: General principles and assays. *Methods in Enzymology* **114**, 78.

Feigelson, R.S. (1988). The relevance of small molecule crystal growth and techniques to the growth of biological macromolecules. *J. Crystal Growth* **90**, 1-13.

Ganzhorn, A.J., Green, D.W., Hershey, A.D., Gould, R.M. and Plapp, B.V. (1987). Kinetic characterisation of yeast alcohol dehydrogenases. *J. Biol. Chem.* **262**, 3754-3761.

Gel filtration Principles and Methods. Pharmacia Biotech, 6 th Edition. RahmsiLund 9460, Sweden.

Gilliland, G. (1988). A biological macromolecule crystallization database - A basis for a crystallization strategy. *J. Cryst. Growth* **90**, 51-59.

Harris, E.L.V. (1995). 'Concentration of the extract' in Protein Purification Methods (Harris, E.L.V. and Angal, S., eds). Oxford University Press, New York.

Hashim, M.A. and Gupta, B.S. (1997). A study on the effect of operating parameters on the cross-flow microfiltration of yeast. *Bioseparation* **7**, 17-23.

Heinrich, P.C., Steffen, H., Janser, P. and Wiss, O. (1972). Studies on the reconstitution of apotransketolase with thiamine pyrophosphate and analogs of the coenzyme. *Eur. J. Biochem.* **30**, 533-541.

Hodgson, J. (1992). Controlling chirality in enzymatic synthesis. *Biotech.* **10**, 1093-1097.

Hon, C.C. and Reilly, P.J. (1979). Properties of β-Amylase immobilised to alkylamine porous silica. *Biotechnol. Bioeng.* **21**, 505-512.

Ion Exchange Chromatography Principles and Methods. Pharmacia Biotech. 18-1114-21, Edition AA.

Jacobsen, C., Garside, J., Hoare, M. (1998). Nucleation and growth of microbial lipase crystals from clarified concentrated fermentation broths. *Biotech. Bioeng.* **57**, 666-675.

Jancarik, J. and Kim, S. (1991). Sparse matrix sampling: a screening method for crystallization of proteins. *J. Appl. Cryst.* **24**, 409-411.

Jancarik, J. and Kim, S.H. (1991). Sparse matrix sampling: a screening method for crystallisation of proteins. *J. Appl. Cryst.* **24**, 409-411.

Khalaf, N., Govardhan, C., Lalonde, J., Persichetti, R., Wnag, Y. and Margolin, A. (1996). Cross-Linked Enzyme Crystals as highly active catalysts in organic solvents. *J. Am. Chem. Soc.* **118**, 5494-5495.

King, M.V. (1964). Standard preparations of ribonuclease crystals of modifications I and II. *Biochem. Biophy. Acta* **79**, 388-392.

Klibanov, A. M. (1997). Why are enzymes less active in organic solvents than in water? *TIBTECH* **15**, 97-101.

Jakoby, W. (1968). A technique for the crystallisation of proteins. *Anal. Biochem.* **26**, 295-298.

Kolmogorov, A.N. (1941). Dissipation of energy in the locally isotropic turbulence. *Comptes Rendus (Doklady) de l'Academie des Sciences de l'URSS* **32**, 16-18.

Kuimov, A., Knareva, N. and Kochetov, G. (1992). Morphological differences in crystals of multiple forms of yeast transketolase. *Biochem. Int.* **26,** 451-455.

Kunkel, W., Hadrich, H., Damaschun, H. and Damaschun, G. (1980). Alkoholdehydrogenase (ADH) in Hefezellen. III. Strukturuntersuchungen an zellularen ADH-Kristallen von Saccharomyces carlsbergensis mit Hilfe de Electronenmikroskopie und Rontgenkleinwinkelstreuung. *Mikroskopie (Wien)* **36**, 81-92.

Laane, C., Boenen, S., Hilhorst, R. and Veeger, C. (1987) ' Optimization of Biocatalysis in Organic media' in Biocatalysis in Organic media (Laane, C., Tramper, J. and Lilly, M.D, eds) Elsevier Science Publishers B.V., Amsterdam.

Lalonde, J. (1995). The preparation of homochiral drugs and peptides using Cross-Linked Enzyme Crystals. *CHIMICA OGGI* **13**, 33-37.

Lalonde, J. (1997). Enzyme catalysis: Cleaner, safer, energy efficient. *Chemical Engineering* **104**, 108-112.

Lalonde, J. (1997). Practical catalysis with enzyme crystals. *CHEMTECH.* **27**, 38-45.

Lalonde, J., Govardhan, C., Khalaf, N., Martinez, A., Visuri, K. and Margolin, A. (1995). Cross-linked crystals of *Candida rugosa* lipase: Highly efficient catalysts for the resolution of chiral esters. *J. Am. Chem. Soc.* **117**, 6845-6852.

Lee, T.S., Vaghjiani, J.D., Lye, G.J., and Turner, M.K. (1999). A rational approach to the batch production of cross-linked enzyme crystals (CLECs) for large-scale biocatalysis. *Enzyme Microb. Technol.*, in press.

Lee, T.S., Vaghjiani, J.D. and Turner, M.K. (1998). The stability of cross-linked enzymes for large-scale biocatalysis. ICHEME conference, Newcastle, England.

Levich, V.G. (1962). Physiochemical Hydrodynamics. Prentice-Hall, New York.

Levy, M.S., Ciccolini, A.S., Yim, S.S., Tsai, J.T., Titchener-Hooker, N., Shamlou, P.A. and Dunnills, P. (1998). The effects of material properties and fluid flow intensity on plasmid DNA recovery during cell lysis. *ISCRE* **15**, 1-17.

Levy, M.S., Collins, I.J., Yim, S.S., Ward, J.M., Titchener-Hooker, N., Shamlou, P.A. and Dunnill, P. (1998). Effect of shear on plasmid DNA in solution. *Bioproc. Eng.* **20**, 7-13.

Lilly, M.D. and Dunnill, P. (1976). Immobilised-enzyme reactors. Methods in Enzymology (Mosbach, K. ed). **XLIV**, 717-738.

Lindqvist, Y., Schneider, G., Ermler, U., and Sundstrom, M. (1992). Three-dimensional structure of transketolase, a thiamine diphosphate dependent enzyme, at 2.5 Å resolution. *EMBO J.* **11**, 2373.

Littlechild, J, Turner, N., Hobbs, G., Lilly, M., Rawas, A., and Watson, H. (1995). Crystallisation and preliminary X-ray crystallographic data with *Escherichia coli* transketolase. *Acta Cryst.* **D51**, 1074-1076.

Littlechild, J.A. (1991). Protein crystallisation: Magical or logical: Can we establish some general rules? *J. Phys. D: Appl. Phys.* **24**, 111-118.

Lowry, O.H., Rosebrough, N.J., Farr, A.L., and Randall, R.J. (1951) Protein measurement with the folin phenol reagent. *J. Biol. Chem.* **193**, 265-275.

Magonet, E., Hayen, P., Delforge, D., Delaive, E. and Remacle, J. (1992). Importance of the structural zinc atom for the stability of yeast alcohol dehydrogenase. *Biochem. J.* **287**, 361-365.

Maniatis, T., Sambrook, J. and Fritsch, E.F. (1989). Molecular Cloning: A Laboratory Manual. 2nd Edition, Volume **3**. Section 18.47.

Margolin, A. (1996). Novel crystalline catalysts. *TIBTECH* **14**, 223-230.

Mauson, A.J. (1993). Crossflow microfiltration of cell suspensions. *Australasian Biotechnology* **3**, 348-351.

McPherson, A. (1990). Current approaches to macromolecular crystallisation. *Eur. J. Biochem.* **189**, 1-23.

McPherson, A. (1995). Increasing the size of microcrystals by fine sampling of pH limits. *J. Appl. Cryst.* **28**, 362-365.

McPherson, A. (1990). Current approaches to macromolecular crystallisation. *Eur. J. Biochem.* **189**, 1-23.

Metzner, A.B. and Otto, R.E. (1957). Agitation of non-Newtonian fluids. *American Institute of Chemical Engineers Journal* **3**, 3-10.

Mullin, J.W., Crystallization. 3rd Edition, *Butterworth-Heinemann*, 1993, 148-150.
Nakanishi, K. and Tadokoro, T. (1987). The Specific resistance of cakes of microorganisms. *Chem. Eng. Comm.* **62**, 187-201.

Navia, M.A. and St. Clair, N.L. (1992). Use of cross-linked crystals as a novel form of enzyme immobilisation. US Patent Classification C12N11/00, C12P21/102.

Navia, M.A., St. Clair, N.L. and Griffith, J.P. (1993). ' Cross-Linked Enzyme Crystals (CLECs^{TM}) as immobilised enzyme particles' in Stability and stabilisation of enzymes' (Van den Tweel, W.J.J., Harder, A. and Buiteclear, R.M. eds.) Elsevier Science Publishers, 63-72.

Nilsson, U., Lindqvist, Y., Kluger, R. and Schneider, G. (1993). Crystal structure of transketolase in complex with thiamine thiazolone diphosphate, an analogue of the reaction intermediate, at 2.3 Å resolution. *FEBS* **326**, 145-148.

Ottens, E.P. and deJong, E. (1973). A model for secondary nucleation in a stirred vessel cooling crystalliser. *Ind. Engng. Chem. Fundam.* **12** , 179-184.

Paz, M.A., Blumenfeld, O.O., Rojkind, M., Henson, E., Furfine, C. and Gallop, P.M. (1965). Determination of carbonyl compounds with N-methyl benzothiazolone hydrazone. *Archives of Biochemistry and Biophysics* **109**, 548-559.

Persichetti, R., St.Clair,N., Griffith, J.P., Navia, M.A., and Margolin, A.L. (1995). Cross-Linked Enzyme Crystals (CLECs) of thermolysin in the synthesis of peptides. *J. Am. Chem. Soc.* **117**, 2732.
Persichetti, R.A., Lalonde, J., Govardhan, C.P., Khalaf, N.K. and Margolin, A. (1996). Candida Rugosa lipase: Enantioselectivity enhancements in organic solvents. *Tetrahedron Letters* **37**, 6507-6510.

Piszkiewicz, D. (1977). ' Multiple Substrate reactions' in Kinetics of chemical and enzyme-catalyzed reactions. Oxford University Press, New York.

Ramaswamy, S., Kratzer, D.A., Hershey, A.D., Rogers, P.H. Arnone, A., Eklund, H., and Plapp, B.V. (1994). Crystallisation and preliminary crystallographic studies of *Saccharomyces cerevisiae* Alcohol Dehydrogenase I. *J. Mol. Biol.* **235**, 777-779.

Ries-Kaut, M. and Ducruix, A (1992) ' Phase diagrams' in Crystallisation of nucleic acids and proteins (Ducruix, A. and Giege, R., eds) Oxford University Press, New York.

Ries-Kautt, M., and Ducruix, A. (1992) 'The physical chemistry of protein crystallisation' in Crystallisation of nucleic acids and proteins (Ducruix, A and Giege, R, eds) Oxford University Press, New York.

Roda, A, Girotti, S., Ghini, S. and Carrea, G. (1988). Continuous-flow assays with nylon tube-immobilised bioluminescent enzymes. *Methods in Enzymology* **137**, 161-171.

Rosevear, A. (1993) ' Immobilised biocatalysts' in Molecular biology and biotechnology (Walker, J.M. and Gingold,E.B., eds). The Royal Society of Chemistry. Cambridge, UK.

Rubin, B., Jamison, P. and Harrison, D. (1991). Lipases: Structure, mechanism and genetic engineering (Alberghins, L., Schmid, R.D., and Verger, R., eds.). VCH Verlagsgesellschaft MbH, Weinham, Germany, 63-66.

Schlichting, H. (1979). Boundary Layer Theory. 7th edition. McGraw-Hill, New York.

Shamlou, P.A. and Titchener-Hooker, N. (1993). 'Turbulent aggregation and breakup of particles in liquids in stirred vessels' in Processing of Solid-Liquid Suspensions. 1st Edition. Butterworth-Heinemann Ltd, Oxford.

Shamlou, P.A., Jones, A. G. and Djamarani, K. (1990). Hydrodynamics of secondary nucleation in suspension crystallisation. *Chem. Eng. Sci.* **45**, 1405-1416.

Sluyterman, L.A. and Graaf, J.M. (1969). The activity of papain in the crystalline state. *Biochim. Biophys. Acta* **171**, 277-228.

Sobolov, S.B., Bartoszko-Malik, A., Oeschger, T. and Montelbans, M. (1994). Cross-linked enzyme crystals of Fructose Diphosphate Aldolase: Development as a biocatalyst for synthesis. *Tetrahedron Letters* **35**, 7751-7754.

Sprender, G.A., Schorken, U., Sprenger, G., and Sahm, H. (1995). Transketolase A of *Escherichia coli* K12 purification and properties of the enzyme from recombinant strains. *European Journal of Biochemistry* **230**, 525.

St. Clair, N.L. and Navia, M.A. (1992). Cross-linked enzyme crystals as robust biocatalysts. *J. Am. Chem. Soc.* **114**, 7314-7316.

Stroh, W. (1998). Industrial Enzymes Market. *Genetic Engineering News*, 11-38.

Stura, E.A. and Wilson, I.A. (1992). 'Seeding techniques' in Crystallisation of nucleic acids and proteins (Ducruix, A and Giege, R, eds) Oxford University Press, New York.

Stura, E.A., Satterthwait, A.C., Calvo, J.C., Kaslow, D.C., and Wilson, I.A. (1994). Reverse Screening. *Acta Cryst.* **D50**, 448-455.

Synowiec, P., Jones, A.G., and Shamlou, P.A. (1993). Crystal break-up in dilute turbulently agitated suspension. *Chem. Eng. Sci.* **48**, 3485-3495.

Tischer, W. and Kasche, V. (1999). Immobilised enzymes: Crystals or carriers? *TIBTECH* **17**, 326-335.

Turner, M.K. (1999) 'Perspectives in Biotransformations' in Biotechnology (Rehm, H.-J. and Reed, G., eds). London, UK.

Visuri, K., Pastinen, O., Xiaoyan, W., Makinen, K., Leisola, M. (1999). Stability of native and cross-linked crystalline glucose isomerase. *Biotech. Bioeng.* ***64***, 377-380.

Working Party on immobilised biocatalysts within the European Federation of Biotechnology. (1983). Guidelines for the characterisation of immobilised biocatalysts. *Enzyme Microb. Technol.* **5**, 304-307.

Wang, C.Y. (1992). Slow rotation of a disc in a fluid-filled casing. *Acta Mechanica* **94**, 97-103.

Wang, Y., Yakovlevsky, K. and Margolin, A. (1996). An efficient synthesis of chiral amino acid and peptide alkylamides via CLEC-subtilisin catalysed coupling and *insitu* resolution. *Tetrahedron Letters* **37**, 5317-5320.

Wang, Y., Yakovlevsky, K., Khalaf, N., Zhang, B. and Margolin, A. (1996). Cross-linked crystals of subtilisin. *Ann. N. Y. Acad. Sci.* **799**, 777-783.

Weber, P. (1991). Crystallisation methods. *Advances in Protein Chemistry* **41**, 20-23.

Wolthuis R. and Dichiaria, V.C. (1997). 'Conventional Filtration' in Handbook of downstream processing (E.Goldberg ed). Hackie Academic and Professional, London, 20-47.

Woodley, J.M. and Titchener-Hooker, N.J. (1996). The use of windows of operation as a bioprocess design tool. *Bioproc. Eng.* **14**, 263-268.

Xu, K. and Klibanov, A. (1996). pH control of the catalytic activity of Cross-Linked Enzyme Crystals in organic solvents. *J. Am. Chem. Soc.* **118**, 9815-9819.

Zelinski, T. and Waldmann, H. (1997). Cross-linked enzyme crystals (CLECs): Efficient and stable biocatalysts for preparative organic chemistry. *Angew. Chem. Int. Ed. Engl.* **36**, 722-724.